Conference on

ENVIRONMENTAL EFFECTS ON ANTENNA PERFORMANCE

Proceedings, Vol. II

Edited by James R. Wait

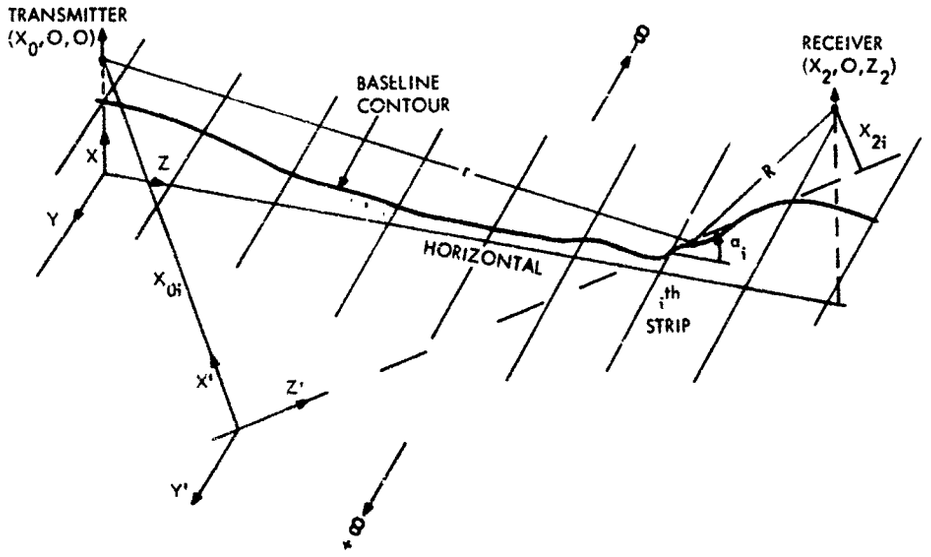

Sponsors:

ITS/ESSA/DoC
AFCRL/DoD
CIRES/ESSA/CU
GAP/IEEE

Boulder, Colorado
July 14-18, 1969

FOREWORD

This volume contains concise versions of the papers presented at the Conference on Environmental Effects on Antenna Performance which did not appear in Vol. I of the Proceedings. The papers presented here were reproduced from the manuscripts supplied by the authors. Editing on the submitted material was relatively light, although many of the manuscripts required at least some revision. As editor, I should like to thank the members of the advisory board for their assistance and, in particular, I am grateful to the conference secretary, Mrs. Eileen Brackett, for her diligence in assembling the papers and readying the material for the printer.

Volume I which was issued earlier is available from the Clearinghouse for Federal Scientific and Technical Information, Sills Building, 5285 Port Royal Road, Springfield, Virginia 22151. When ordering specify that the accession number is PB-183 715. Additional copies of this Vol. II are also available from the CFSTI for $3.00 and the accession number is AD 692 879..

James R. Wait

PROCEEDINGS - VOL. II

TABLE OF CONTENTS

Table of Contents (continued):

CONFERENCE ON ENVIRONMENTAL EFFECTS ON ANTENNA PERFORMANCE

Boulder, Colorado — 1969 July 14-18

General Information

Location: Radio Building, Department of Commerce Boulder Laboratories, 325 Broadway

Sponsors: Institute for Telecommunication Sciences (Environmental Science Services Administration, Research Laboratories)
Coöperative Institute for Research in the Environmental Sciences
Air Force Cambridge Research Laboratories
Department of Electrical Engineering (University of Colorado)
Denver-Boulder Chapter of the I.E.E.E. Group on Antennas and Propagation

Chairman: James R. Wait Secretary: Mrs. Eileen Brackett

Advisory Board: P. Blacksmith, R. C. Kirby, R. V. Row, R. Cohen, M. T. Ma, C. J. Sletten, H. V. Cottony, S. W. Maley, W. J. Surtees, W. Flock, R. J. Papa, W. F. Utlaut

Officers of Denver-Boulder IEEE/GAP Chapter:
R. Cohen, President
R. D. Hunsucker, Vice-President
D. C. Chang, Secretary

Registration Facilities: R. D. Hunsucker and D. C. Chang

Auditorium and Projection Facilites: H. V. Cottony and R. H. Ott

Cover Design: Courtesy of First National Bank, Boulder

Parking: A visitors' parking lot is located south of the Radio Building

Banquet: A reception, dinner and talks are being sponsored in connection with this conference by the Denver-Boulder IEEE Group on Antennas and Propagation. This banquet is being held at the University of Colorado Faculty Club, 972 Broadway, on Wednesday evening, July 16, with the reception commencing at 18h 30m. Tickets (at $4.25 per person) are available at the registration desk.

Dr. Morrel P. Bachynski, Director of Research at RCA, Montreal, will speak on "Plasma Experiments vs. Plasma Theory." The abstract for his talk follows:

The experimentalist often considers that plasma theory is too idealized to permit comparison with experiment. Meanwhile, the theoretician contends that plasma experiments are too uncontrolled to be amenable to theoretical interpretation. Using examples taken from theory and laboratory experiments related to electromagnetic waves in plasmas, this talk will consider:

a) theory which has been known for many years but only recent laboratory experiments have been suitable for comparison

b) experimental results which have been explained a number of years after the measurements

c) theory for which the experiments have yet to be done

d) experimental results for which the theory is yet undeveloped

e) experimental conclusions which theory has proven to be incorrect

f) theoretical results which experiment has proven to be incorrect

A parallel talk will be presented by Gertrude Wait, Ph.D. candidate and research associate in sociology at the University of Colorado, on "Unrest in Young America."

Registration:
Radio Building Lobby, Sunday, July 13, 15h 00m to 21h 00m
Monday, July 14, 07h 30m to 12h 00m

Proceedings: Concise versions of most of the papers presented at the Conference on Environmental Effects on Antenna Performance are being published in two volumes. Volume I of the Proceedings is currently available, and Volume II will become available in early August. Both volumes are obtainable at $3.00 each from the Clearinghouse for Federal Scientific and Technical Information, Sills Building, 5285 Port Royal Road, Springfield, Virginia 22151. Please refer to publication PB 183 715 for Volume I.

Lunch: Restaurants within walking distance are:
Cafeteria in Radio Building basement
Pizza Oven, 2620 Baseline Road
International House of Pancakes, 2450 Baseline Road
Mister Taco, 2720 Baseline Road

Coffee: There will be morning and afternoon coffee breaks at about 10h 30m and 15h 30m, with refreshments available in the Radio Building Cafeteria, located in the basement.

Travel Information and Assistance:
Boulder Travel Agency — 443-0380, 443-2700
Flatirons Travel Agency — 447-0372
National State Bank Travel Agency — 442-0351
Thrifty Travel Agency — 444-4722
Travel Center of Boulder — 442-2340
University Hill Travel Center — 443-2021

Bus Information (service to Denver airport):
(see bus schedule on page 7)

DETAILED SESSION PROGRAMS

Monday, July 14th — 08h 30m

Introductory Remarks: C. J. Sletten, Chief, Microwave Physics Laboratory, AFCRL; and R. C. Kirby, Director, ITS/ESSA

Session I — ELECTROMAGNETIC THEORY — Chairman, Professor J. R. Wait (ESSA Research Laboratories and CIRES)

I-1 Complex rays and the local properties of radiation in lossy media; H. L. Bertoni, L. B. Felsen and A. Hessel (Polytechnic Institute of Brooklyn, Brooklyn, N.Y.)

I-2 Transient dipole over a dielectric half-space; D. A. Hill (Ohio State University, Columbus)

I-3 The propagation constant of a small-diameter insulated helix; F. P. Ziolkowski (Raytheon Company, Norwood, Mass.)

I-4 An alternative method for deriving Fock's principle of the local field in the penumbra; R. H. Ott (ITS/ESSA)

I-5 Boundary value problems in radially inhomogeneous media; J. D. Fikioris (University of Toledo, Toledo, Ohio)

I-6 Radiation from a parallel-plate waveguide into an inhomogeneously filled space; R. J. Kostelnicek and R. Mittra (University of Illinois, Urbana)

Monday, July 14th — 13h 30m

Session II — BOUNDARY VALUE PROBLEMS — Chairman, Professor L. B. Felsen (Polytechnic Institute of Brooklyn, Brooklyn, N.Y.)

II-1 Prolate spheroidal and linear antennas in lossy media; R. J. Lytle (Lawrence Radiation Lab., Univ. of California, Livermore)

II-2 Metallic and dielectric antennas in conducting media; Giorgio Franceschetti, O. Bucci, E. Corti and G. Latmiral (University of Naples, and Istituto Universitario Navale, Naples, Italy)

II-3 Radiation from a semi-infinite dielectric-coated spherically tipped perfectly conducting cone; R. Chatterjee (Indian Institute of Science, Bangalore, India)

II-4 Electromagnetic coupling of horizontal loops over a stratified ground; Herbert Kurss (ESSA and Adelphi University, Garden City, N.Y.)

II-5 Quasi-static fields of subsurface horizontal electric antennas; P. R. Bannister (U.S. Navy Underwater Sound Laboratory, New London, Connecticut)

II-6 Magnetic field excited by a long horizontal wire antenna near the earth's surface; D.B. Large and L. Ball (Westinghouse Electric Corporation, Boulder, Colorado)

II-7 Numerical analysis of aircraft antennas; E. K. Miller, J. B. Morton, G. M. Pjerrou and B. J. Maxum (MBAssociates, San Ramon, California)

Tuesday, July 15th — 08h 30m

Session III — INFLUENCE OF HOMOGENEOUS HALF SPACE — Chairman, Professor M. Kharadly (University of British Columbia)

III-1 Finite tubular antenna above a conducting half-space; D. C. Chang (University of Colorado, Boulder)

III-2 EM propagation over a constant impedance plane; R. J. King (University of Wisconsin, Madison)

III-3 On the surface impedance concept; R. J. King (University of Wisconsin, Madison)

III-4 The impedance of a finite horizontal antenna above ground; W. J. Surtees (Defence Research Board, Ottawa, Canada)

III-5 Impedance of a finite-length insulated dipole in dissipative media; C. K. H. Tsao and J. T. de Bettencourt (Raytheon Company, Norwood, Mass.)

III-6 Distributed shunt admittance of horizontal dipole over lossy ground; C. K. H. Tsao (Raytheon Co., Norwood, Mass.)

III-7 The linear antenna in a piecewise homogeneous environment; D. V. Otto (Ohio State University, Columbus)

III-8 Characteristics of the ground wave attenuation function for highly inductive surfaces; D. B. Ross (Communications Research Centre, Ottawa, Canada)

III-9 Impedance of a Hertzian dipole over a conducting half-space; J. R. Wait (ESSA Research Laboratories, Boulder, Colo.)

Tuesday, July 15th — 13h 30m

Session IV — GROUND SCREEN EFFECTS — Chairman, Dr. W. F. Utlaut (ESSA)

IV-1 Radial wire ground systems for vertical monopole antennas; S. W. Maley (University of Colorado, Boulder)

IV-2 Effect of the ground screen on the field radiated from a monopole; W. J. Surtees (ITS/ESSA)

IV-3 Numerical studies of the effects of non-planar local terrain and ground screens; R. V. Row and D. M. Cunnold (Sylvania, Waltham, Mass.)

IV-4 Radiation of a monopole antenna on the base of a conical structure; G. A. Thiele, M. Travieso-Diaz (Ohio State University, Columbus); H. S. Jones (Harry Diamond Laboratories, Washington, D. C.)

IV-5 Current distribution on a finite length dipole in the presence of ground screens; V. R. Arens, U. R. Embry and D. L. Motte (Sylvania, Mountain View, California)

IV-6 Reflection of waves of arbitrary polarization from a rectangular mesh ground screen; G. A. Otteni (HMES-General Electric Co., Syracuse, N. Y.)

IV-7 Some design considerations for HF antenna ground screens; T. Kaliszewski (General Electric Company, Syracuse, N.Y.)

IV-8 Measured patterns of HF antennas and correlation with surrounding terrain; D. R. McCoy and R. D. Wengenroth (General Electric Co., HMES, Syracuse, N. Y.); J. J. Simons (RADC, Griffiss AFB, Rome, N. Y.)

Wednesday, July 16th — 08h 30m

Session V — ANTENNAS IN PLASMA — A — Chairman, Dr. J. Galejs (Sylvania, Waltham, Mass.)

V-1 Radiation by a VHF dipole-type antenna imbedded in its plasma sheath; R. V. DeVore and R. Caldecott (Ohio State University, Columbus)

V-2 Current distribution and input admittance of a cylindrical antenna in a gyrotropic medium; H. S. Lu and K. K. Mei (University of California, Berkeley)

V-3 Numerical solution of dipole radiation in a compressible plasma with a vacuum sheath surrounding the antenna; S. H. Lin and K. K. Mei (University of California, Berkeley)

V-4 Plane wave synthesis of plasma coated aperture admittance and radiation pattern; H. Hodara (Tetra Tech., Inc., Pasadena, California) and D. Damlamayan (California Institute of Technology, Pasadena)

V-5 Effects of electron acoustic waves on a dipole RF-magnetoplasma probe; H. Oya (NASA-Goddard Space Flight Center, Greenbelt, Md.)

V-6 Radiation characteristics of a slotted ground plane into a two-fluid compressible plasma; K. R. Cook (Colorado State University, Fort Collins) and R. B. Buchanan (Sylvania, Mtn. View, Calif.)

V-7 Studies of VLF radiation patterns of a dipole immersed in a lossy magnetoplasma; D. P. GiaRusso and J. E. Bergeson (Boeing Scientific Research Laboratories, Seattle, Washington)

V-8 Some features of electroacoustic waves excited by linear antennas in hot plasma; V. L. Talekar (Malaviya Regional Engineering College, Jaipur, India)

V-9 Linear antenna in anisotropic medium; P. Meyer (C. N. E. T., Issy-les-Moulineaux, France)

Wednesday, July 16th — 13h 30m

Session VI — ANTENNAS IN PLASMA — B — Chairman, Professor R. E. Collin (Case Western Reserve University, Cleveland, Ohio)

VI-1 Boundary and transition problems for antennas in warm plasmas; J. P. Lafon (Observatoire de Paris, Meudon, France)

VI-2 Studies of antenna-induced ionization problems; W. C. Taylor, J. B. Chown and T. Morita (Stanford Research Institute, Menlo Park, California)

VI-3 Behavior of strong field electromagnetic waves in anisotropic plasmas; M. P. Bachynski and B. W. Gibbs (RCA Research Laboratories, Montreal, Canada)

VI-4 The Trailblazer II reentry antenna test program; J. L. Poirier, W. Rotman, D. Hayes and J. Lennon (AFCRL, Bedford, Mass.)

VI-5 Single and multislot antennas in an inhomogeneous reentry plasma environment; K. E. Golden and G. E. Stewart (Aerospace Corporation, Los Angeles, California)

VI-6 Ionospheric antenna impedance probe; E. K. Miller (MBAssociates, San Ramon, Calif.), H. F. Schulte and J. W. Kuiper (High Altitude Engineering Laboratory, Univ. of Michigan, Ann Arbor)

VI-7 How to determine ELF/VLF transmitting antenna performance in the ionosphere; J. D. Leiphart (Naval Research Laboratory, Washington, D. C.)

VI-8 On the transient response of an antenna and the time decrease of Alouette spikes; P. Graff (CNET, Issy-les-Moulineaux, France)

Wednesday, July 16th — 18h 30m

EEAP/GAP reception and banquet: University of Colorado Faculty Club, 972 Broadway. Speakers: Dr. M. P. Bachynski and Mrs. Gertrude Wait.

Thursday, July 17th — 08h 30m

Session VII — RELATED ENVIRONMENTAL ASPECTS — Chairman, C. J. Sletten (AFCRL, Bedford, Mass.)

VII-1 Dipole radiation in the lunar environment; R. J. Phillips (Jet Propulsion lab., California Institute of Technology, Pasadena)

VII-2 VLF transmitting antennas using fast wave dipoles; E. W. Seeley (Naval Weapons Center Corona Laboratories, Corona, Calif.)

VII-3 Ground-wave propagation across strips and islands on a flat earth; R. J. King (Univ. of Wisconsin, Madison) and W. I. Tsukamoto (University of Colorado, Boulder)

VII-4 Some considerations on ground-wave propagation across coastlines and islands; R. K. Rosich (ITS/ESSA)

VII-5 VLF ground-based measurements over stratified Antarctic media; G. E. Webber and I. C. Peden (University of Washington, Seattle)

VII-6 Effective ground conductivity measurements at radio frequencies using small loop antennas; W. L. Taylor (ITS, ESSA)

VII-7 Phase measurements of electromagnetic field components; P. Cornille (University of California, Berkeley, and University of Lille, France)

Thursday, July 17th — 13h 30m

Session VIII — Round table discussion on: DESIGN TECHNIQUES FOR PATTERN CONTROL BY GROUND SCREENS — Moderator, Dr. R. V. Row (Sylvania, Waltham, Mass.)

Friday, July 18th — 08h 30m

Session IX — Informal Papers

IX-1 Radiation from an elevated vertical dipole above an extended ground screen; W. T. Patton (RCA, Moorestown, N. J.)

IX-2 Near field solutions for a vertical Hertzian dipole over a finitely conducting earth; D. C. Chang (University of Colorado); and J. R. Wait (ESSA)

IX-3 Pulse propagation into the ground; W. L. Curtis (Boeing Co., Seattle, Washington)

IX-4 Performance of valley spanning VLF antennas based on electromagnetic modelling; A. N. Smith and E. J. Jackson (Westinghouse Electric Corp., Boulder)

IX-5 Surface wave contributions in the backscattering from large, high-density dielectric spheres; M. A. Plonus and H. Inada (Northwestern University, Evanston, Illinois)

IX-6 Microwave transmission measurement through radiantly heated antenna windows; J. F. Fox, E. C. Lind and D. Q. Durant (McDonnell Douglas Astronautics Co., St Louis, Missouri)

IX-7 Optimum frequency for a VLF telecommunication system using buried antennas; R. Gabillard, J. Fontaine and P. Degauque (University of Lille, France)

IX-8 Propagation between parallel impedance surfaces; R. B. Dybdal (Aerospace Corporation, Los Angeles, California)

IX-9 Impedance of a dipole in a large laboratory magneto-plasma; S. Y. K. Tam (RCA Ltd., Montreal, Canada)

IX-10 Integral equation approach to the radiation from a vertical monopole over an inhomogeneous ground plane; J. R. Wait and K. P. Spies (ESSA).

IX-11 Microwave (4.75 GHz) surface impedance measurements of a 1° dielectric wedge on a perfect conductor; R. J. King and C. Hustig (University of Wisconsin, Madison)

NOTES: i) Prof. R. E. Collin was replaced by Prof. K. G. Balmain for Chairman of Session VI.

ii) The paper by J. P. Lafon, in Session VI, was not presented and no manuscript was received for the Proceedings.

iii) The paper by D. V. Otto, in Session III, was read by title only. The paper appears in Vol. I.

iv) Session IX was chaired by Prof. S. W. Maley.

v) The paper by H. Hodara and D. Damlamayan, in Session V, was not presented.

PROLATE SPHEROIDAL AND LINEAR ANTENNAS IN LOSSY MEDIA*

R. J. Lytle
Lawrence Radiation Laboratory, University of California
Livermore, California

Abstract. The short circuit current and charge distributions and the complex effective length for a prolate spheroidal receiving antenna, in a complex medium, have been determined for an arbitrary angle of incidence. In addition, the power decay as a function of ξ has been evaluated for a variety of situations for a prolate spheroidal transmitting antenna.

The boundary value problem depicted in Figure 1 has been solved by utilizing the method of separation of variables.

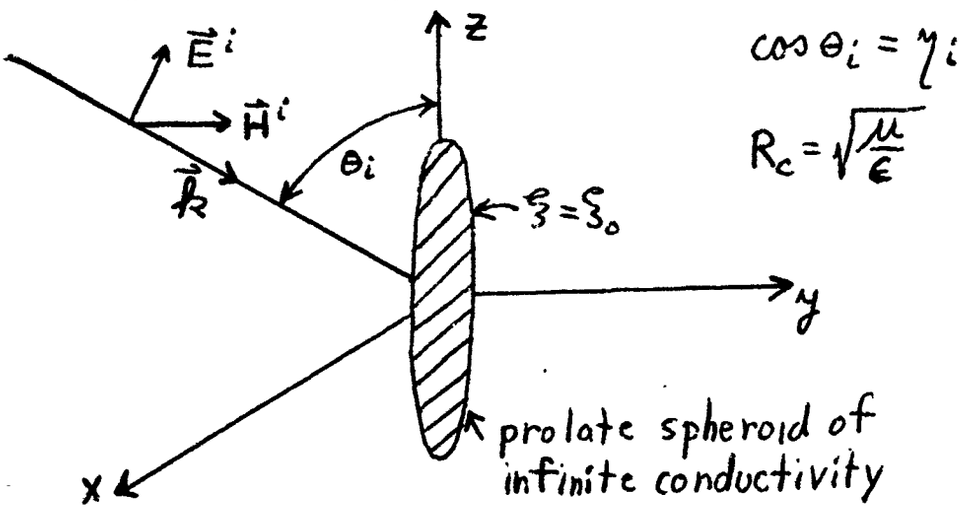

Figure 1

For an incident wave of the form

$$(1)\quad \vec{E}^i = E_o e^{j\vec{k}\cdot\vec{r}}(-\cos\theta_i \vec{a}_x + \sin\theta_i \vec{a}_z)$$

$$(2)\quad \vec{H}^i = \frac{E_o}{R_c} e^{j\vec{k}\cdot\vec{r}} \vec{a}_y$$

it can be shown that

$$(3)\quad E_\eta = E_\eta^{\,i} + E_\eta^{\,s} = -\frac{j E_o}{k\sqrt{(\xi^2-\eta^2)(\xi^2-1)}} \sum_{m,n} S_{mn}^{(1)}(c,\eta)\bullet$$

*Work performed under the auspices of the U. S. Atomic Energy Commission.

$$\Big\{\Big[(\xi^2-1)\frac{\partial R_{mn}^{(1)}(c,\xi)}{\partial\xi}\cos\phi\cos m\phi + m\xi\, R_{mn}^{(1)}(c,\xi)\sin\phi\sin m\phi\Big]A_{mn} +$$

$$\beta_{mn}\Big[(\xi^2-1)\frac{\partial R_{mn}^{(4)}(c,\xi)}{\partial\xi}\cos\phi\cos m\phi + m\xi\, R_{mn}^{(4)}(c,\xi)\sin\phi\sin m\phi\Big] -$$

$$\alpha_{mn}\Big[(\xi^2-1)\frac{\partial R_{mn}^{(4)}(c,\xi)}{\partial\xi}\sin\phi\sin m\phi + m\xi\, R_{mn}^{(4)}(c,\xi)\cos\phi\cos m\phi\Big]\Big\},$$

where β_{mn} and α_{mn} are the expansion coefficients for the scattered field, and A_{mn} is $4\,j^n\,S_{mn}^{(1)}(c,\eta_i)/N_{mn}(c)$.

As $E_\eta = 0$ at $\xi = \xi_o$, by multiplying (3) by $S_{lt}^{(1)}(c,\eta)$ and integrating the results from -1 to +1 in η and from 0 to 2π in ϕ, and evaluating the result at $\xi = \xi_o$, one can obtain for $E_o = k$

$$(4)\quad \alpha_{lt}-\beta_{lt} = \frac{4(j)^t S_{lt}^{(1)}(c,\eta_i)}{N_{lt}(c)}\cdot\frac{\Big[\sqrt{\xi_o^2-1}\,\frac{\partial R_{lt}^{(1)}(c,\xi_o)}{\partial\xi} + \frac{\xi_o}{\sqrt{\xi_o^2-1}}R_{lt}^{(1)}(c,\xi_o)\Big]}{\Big[\sqrt{\xi_o^2-1}\,\frac{\partial R_{lt}^{(4)}(c,\xi_o)}{\partial\xi} + \frac{\xi_o}{\sqrt{\xi_o^2-1}}R_{lt}^{(4)}(c,\xi_o)\Big]}.$$

By utilizing this result, one can show that the current distribution $I(\eta)$ for the short circuited receiving antenna is

$$(5)\quad I^{sc}(\eta) = \frac{-j4\pi E_o}{kR_c}\sqrt{(\xi_o^2-1)(1-\eta^2)}\cdot$$

$$\sum_n \frac{(j)^n S_{ln}^{(1)}(c,\eta_i)\, S_{ln}^{(1)}(c,\eta)}{N_{ln}(c)\Big[\xi_o R_{ln}^{(4)}(c,\xi_o) + (\xi_o^2-1)\frac{\partial R_{ln}^{(4)}(c,\xi_o)}{\partial\xi}\Big]}$$

The short circuit charge distribution $Q^{sc}(\eta)$ can be determined via use of the continuity equation and equation (5).

By appropriately coupling the above results with previously obtained results (Lytle and Schultz,1968) for the current distribution $I^{tr}(\eta)$, charge distribution $Q^{tr}(\eta)$, and input impedance Z_o of a prolate spheroidal transmitting antenna, one can obtain such quantities as the complex effective length and the current and charge distributions of a loaded receiving antenna.

Another quantity of interest is the rate of decay in the complex medium of the power generated by a transmitting antenna. This has been determined by evaluating the power passing through a series of confocal prolate spheroids surrounding the transmitting antenna.

Examples of results obtained for some of the above quantities follow.

R. J. Lytle and F. V. Schultz (1968), Linear Antennas in Plasma Media, Purdue University, School of Electrical Engineering, TR-EE 68-10.

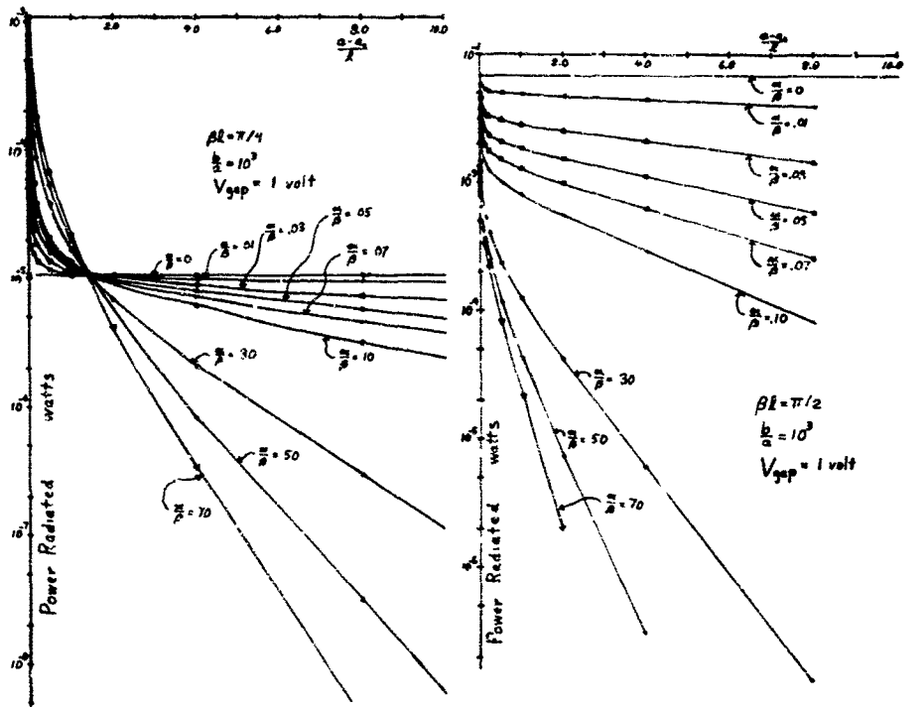

Radiated Power Dependence Upon Phase Length and Loss ("a" is the semiminor axis of a confocal spheroid surrounding a transmitting antenna with a semiminor axis "a_o")

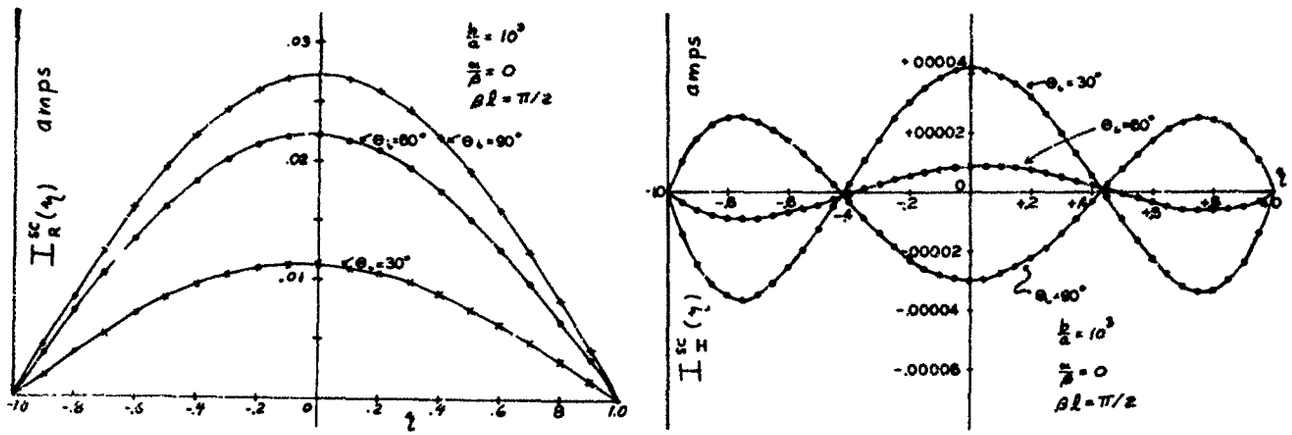

Short Circuit Current Dependence Upon Angle of Incidence (E_o = k volts/meter) and Transmitter Current for $\alpha/\beta = .5$ (V_{gap} = 1 volt)

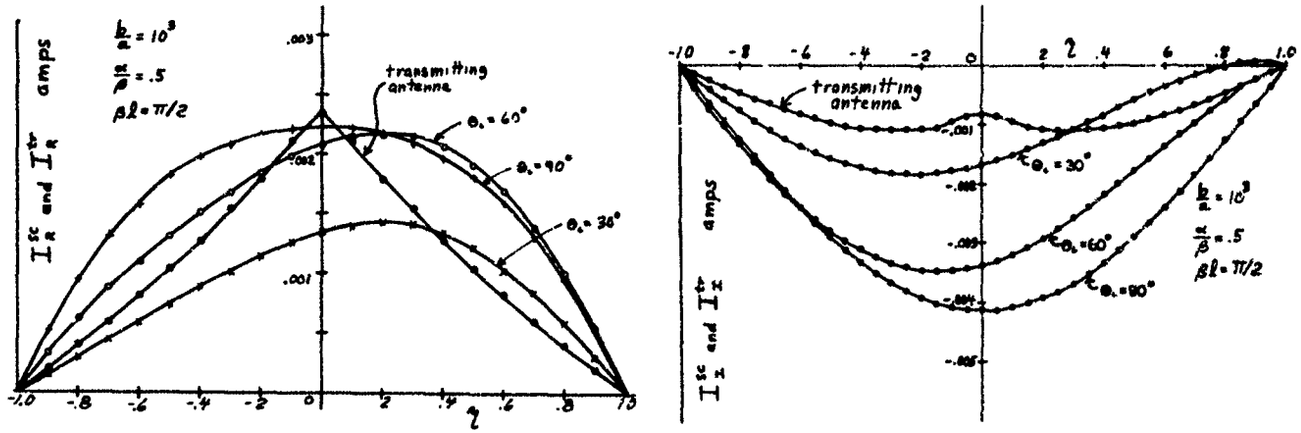

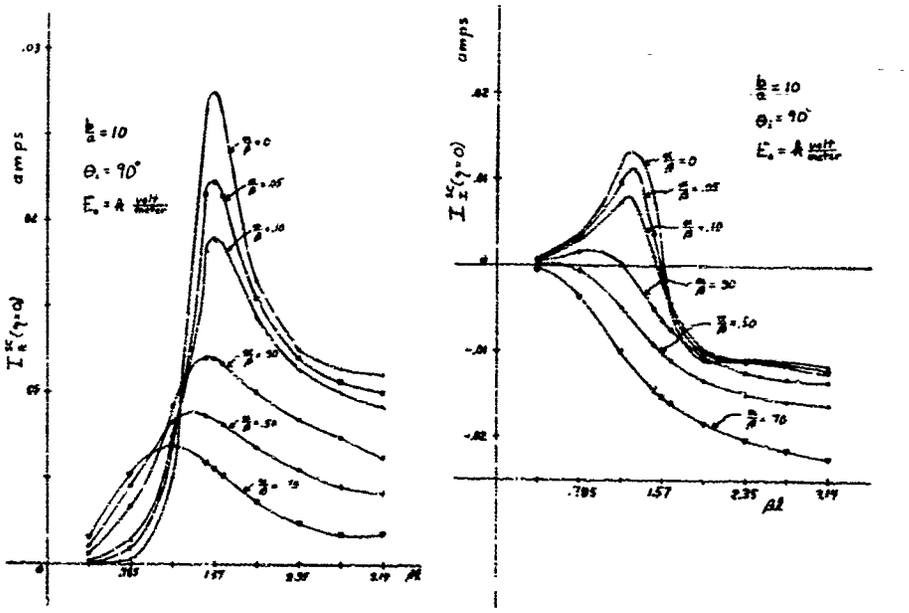

Short Circuit Current Dependence Upon Phase Length and Loss

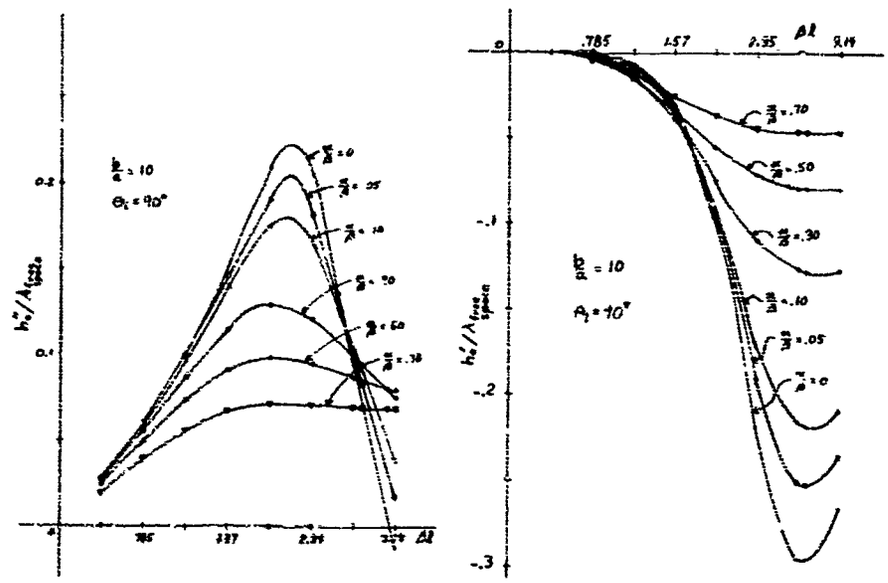

Normalized Complex Effective Length Dependence Upon Phase Length and Loss

NUMERICAL STUDIES OF THE EFFECTS OF NON-PLANAR LOCAL TERRAIN AND GROUND SCREENS

by

R. V. Row and D. M. Cunnold*

Sylvania Electronic Systems, Waltham, Mass.

ABSTRACT

Numerical integration of the vector form of Green's theorem for electromagnetic fields has been used to evaluate the coupling between a pair of vertical dipoles over a two-dimensional non-planar electrically non-homogeneous ground. Antennas with arbitrary free-space radiation patterns can be accommodated. The results of this method are compared with previous computation for planar ground and ground screen using the compensation theorem approach. Agreement is good except at angles below a few degrees. New results on the effects of a finite ground screen system in proximity to a sloping beach and a flat sea with varying tide levels are given and compared to some HF band measurements.

- - - - - - - - - - - -

In an earlier paper [Cunnold, Row, Arnold, 1968] the writers described a method of determining approximately the coupling between two horizontal electric (dipole) antennas over a piecewise homogeneous non-planar two-dimensional ground.

The method if based upon numerical integration of Green's vector theorem for electromagnetic fields

$$E = -\frac{1}{4\pi}\int_s [-iw\mu(n\times H)\phi + (n\times E)\times\nabla\phi + (n\cdot E)\nabla\phi]\,ds \quad (1)$$

where $\phi = \frac{e^{-ikR}}{R}$ is the scalar free-space Green's function

* Dr. Cunnold is a consultant to Sylvania

and the required field components nxH, nxE and n·E are approximated at each point of the surface in the sense of classical optics, but using appropriate Fresnel reflection coefficients at each point of the surface. Agreement with a limited set of experimental measurements was seen to be excellent. Liepa [1968] has applied a similar technique to determine the field from a horizontal line current source illuminating a hemi-cylindrical boss on an infinite conducting plane, a problem for which an exact analytic solution is available. He found excellent agreement between the exact and approximate field distributions.

The approach used by Cunnold et al [1968] has been extended to vertically oriented dipole antennas over two-dimensional ground, as shown in Figure 1. As in the earlier work, the ground surface is approximated by a series of connected planar strips of infinite extent in the y direction. The computer program evaluates the normalized transfer impedance

$$\frac{Z_t}{R_{rad}} = \frac{Z_\ell^t}{R_{rad}} + \sum_i \frac{Z_i^t}{R_{rad}} \qquad (2)$$

where R_{rad} is the radiation resistance of an elementary dipole, Z_d^t is the transfer impedance between the antennas in the absence of the ground, and Z_i^t is the ground scattered contribution from the i-th strip.

For a short electric dipole of length $d\ell$

$$Z_t = E_x d\ell$$

Equation (1) is used to evaluate E_x so that after a stationary phase integration in the y' coordinate only the z' integration need be done numerically.

The field components, $H_{y'}$, $E_{x'}$, $E_{z'}$ and E_x^{inc} are calculated on the basis of Norton's [1937] far-field expressions.

Comparison with Known Results

Provided the Norton ground wave terms are included in the field expressions and the lower antenna of the pair is taken as the receiver, excellent agreement is obtained between the strip method and Norton's results for dipoles over a homogeneous flat ground. Wait [1967] has examined the situation of an elevated electric dipole over a circular ground screen on a flat earth. Agreement with Wait's results is excellent except at angles below 5°, where the non-stationary nature of Eq. (1) will exhibit errors in the final result through errors in approximating the true fields $n \times H$, $n \times E$ and $n \cdot E$ to a greater degree than the stationary formulation used by Wait.

Effects of Proximity to the Sea

An antenna installed close to the sea is in an environment which changes with tide level. Figure 2 shows a profile for which extensive computations have been made at frequencies of 5, 10, 20 and 35 MHz and screen lengths of 150, 500 and 750 feet. The receiving antenna is 1 foot above the screen, representing a monopole. Figure 3 shows the effect of increasing the screen length from 150 feet to 500 feet to 750 feet under low tide conditions. A significant improvement in gain is realized in going from a 150-foot to 500-foot screen, with the maximum improvement occurring at a progressively lower angle as the frequency is increased. A lesser additional improvement in gain is realized by extending the screen over the down sloping section of beach to the edge of the sea. Figure 4 shows the effects of a 10-foot increase in tide level with a 150-foot screen. The maximum change (increase) in gain is about 1 dB and shows up at the highest frequency. Additional computational results not presented here show that changes in gain caused by tide level are somewhat smaller for the greater ground screen lengths.

The computations shown in Figures 3 and 4 were repeated for a receiving antenna with a $\cos^{\frac{3}{2}} \theta$ pattern. Apart from a general reduction in power gain at angles above about 10°, the results are in substantial agreement with those shown in these which, of course, pertain to a dipole.

Comparison with Observation of Tide Level Changes

Extensive flight test pattern measurements [Simons et al 1968] have been made on an HF band log-periodic monopole element installed on a low profile beach installation at Keflavik Naval Station, Iceland. The contour lines are more or less parallel over the 260° to 340° seaward sector and hence constitute a reasonable approximation to a two-dimensional ground over this sector. The most interesting of these data for our purposes (shown in Figure 7) are the 30-MHz measurements taken on October 29, 1967, at an azimuth of 260° (which extends over the sea). One set of these data pertain to low tide and the other to high tide (water 8-feet higher). Figure 5 shows the actual profile (solid curve) along the 260° azimuth, where the datum level is transferred from mean low water (low tide) to the 14-foot contour for purposes of entering the baseline elevation data into the computer program. The lightly dashed straight line is the sloping beach profile approximation which simplifies the labor of entering profile data into the computer. The strip method program was run for both these profiles; the former (actual profile) case being designated strip-by-strip format in Figure 6. In the computations the ground screen (No. 10 AWG wire with 12-inch spacing) extended from -55 feet to +80 feet. It is evident from Figure 6 that the results obtained with the sloping beach format are in excellent agreement with the strip-by-strip input, especially for the low tide case. The additional set of curves, shown with light dash and double dots in Figure 6, refer to the gain of a pair of vertical dipoles 6 feet and 14 feet above an infinite flat sea, respectively. These latter curves show that in general it is not possible to predict the influence of changes in sea level by such a simple model. There is a striking resemblance between the detailed shape of the predicted curves as shown in Figure 6 and the measurements including a crossover at about 14° in both measurements and predictions. The maximum increase in gain in going from low tide to high tide is 2.1 dB at an angle of 10° in the predictions, and 3.6 dB at 8.5°

in the measurements. It should be noted that at angles below 1.5° the high tide measurements show a relative field strength that is about 1.4 dB greater than at low tide. The opinion is offered that these two relative field strength (gain) curves should be coincident at all angles below 1.5°, as is the case for dipoles at low heights over an infinite sea shown in the dash-double-dot curves of Figure 6. The dash-double-dot curve in Figure 7 represents a uniform downward shift of 1.4 dB for the high tide experimental data. When this is done the maximum "observed" increase in gain in going from low tide to high tide is 2.4 dB at 9°, which compares even more favorably with the strip method predictions in Figure 6. Of course the "observed" crossover point is now shifted down to 12.5° compared to about 14° in the predictions.

It is concluded that the strip method does very well in predicting the detailed shape of the radiation pattern at angles above 1.5° or 2° in this one instance of a low-profile beach installation. The fact that the measurements were made using the LP element on the beach whereas the predictions are for a short vertical dipole should not change the conclusions substantially, as evidenced by the discussion in the preceding section.

ACKNOWLEDGMENTS

The work reported here was supported in part by the Rome Air Development Center, U.S. Air Force Systems Command, and the Advanced Research Projects Agency, Department of Defense, Mr. Carmen Malagisi, RADC, kindly provided the pattern measurement data on the Keflavik LP monopole.

REFERENCES

1. Cunnold, D. M., R. V. Row and C. E. Arnold, "Analytical and Experimental Studies of Coupling Between Antennas over a Two-Dimensional Ground Surface of Known Controu," IEEE Trans. on Antennas and Propagation, Vol. AP-16, pp. 291-298; May 1968.

2. Liepa, V. V., "Numerical Approach for Predicting Radiation Patterns of HF-VHF Antennas over Irregular Terrain." IEEE Trans. on Antennas and Propagation, Vol. AP-16, pp. 273-274; March 1968.

3. Norton, K. A., "The Propagation of Radio Waves over the Surface of the Earth and in the Upper Atmosphere, Part II," Proc. IRE, Vol. 25, pp. 1203-1236; 1937.

4. Wait, J. R., "On the Theory of Radiation from a Raised Electric Dipole over an Inhomogeneous Ground Plane," Radio Science, Vol. 2, pp. 997-1004; 1967.

5. Simons, J. J., F. C. Wilson and R. A. Schneible, "HF Antenna Gain Pattern Measurements: Expanded LITTLE IDA Program," Tech. Report RADC-TR-68-248, Rome Air Development Center, U.S. Air Force Systems Command, Griffiss Air Force Base, Rome, N. Y.; September 1968.

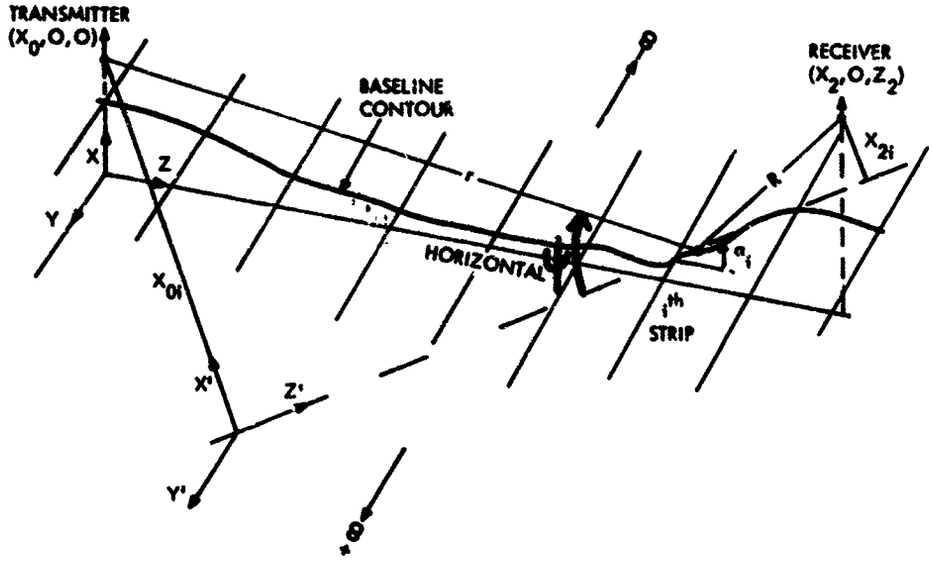

Figure 1. Coordinate Systems for Computing Transfer Impedance

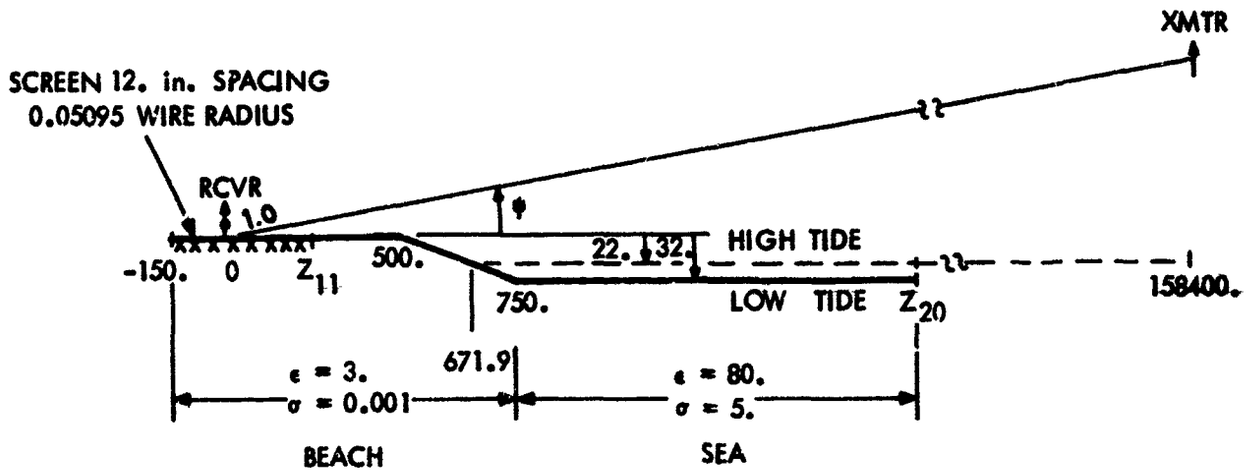

Figure 2. Geometry of Merrimac Light Coast Guard Station Sloping Beach Profile

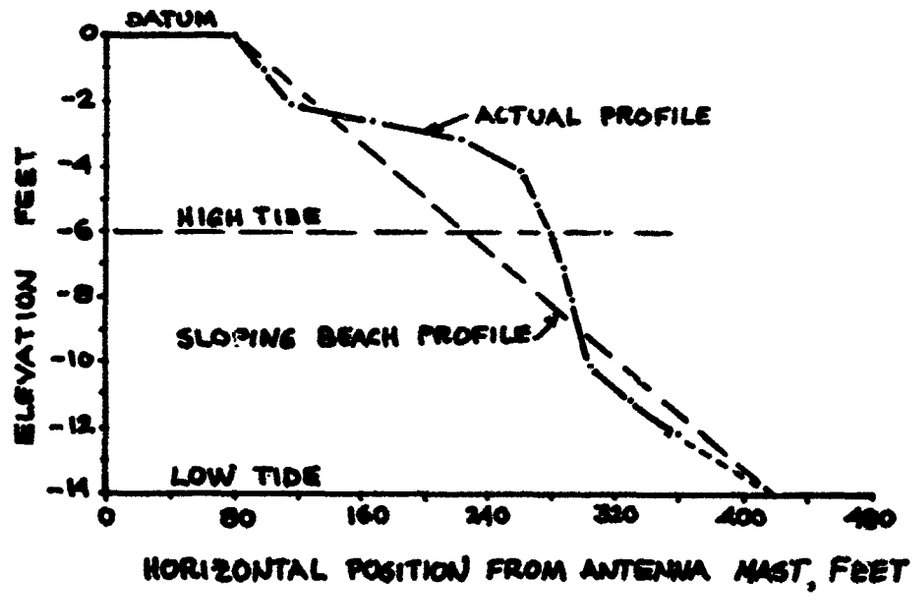

Figure 5. Elevation Profile along 260° Boresight Azimuth for Keflavik Naval Station

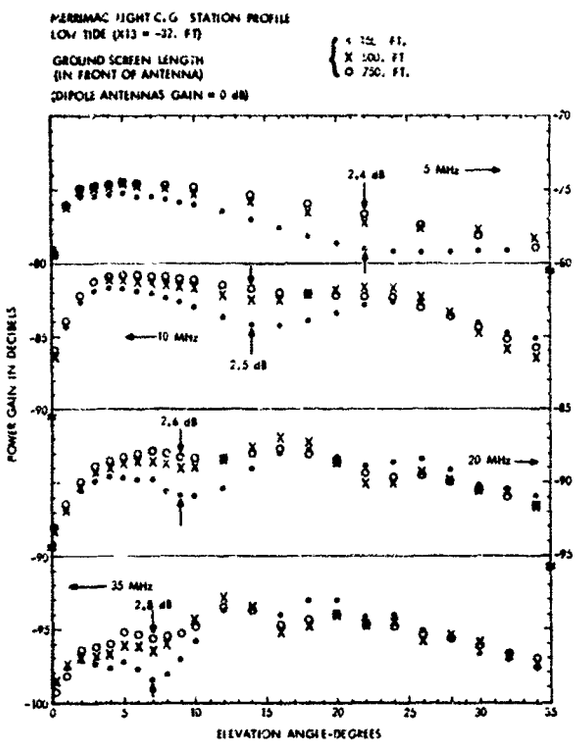

Figure 3. Power Gain for Vertical Dipoles at Four Frequencies for Three Sizes of Ground Screen—Merrimac Light Coast Guard Station Profile at Low Tide

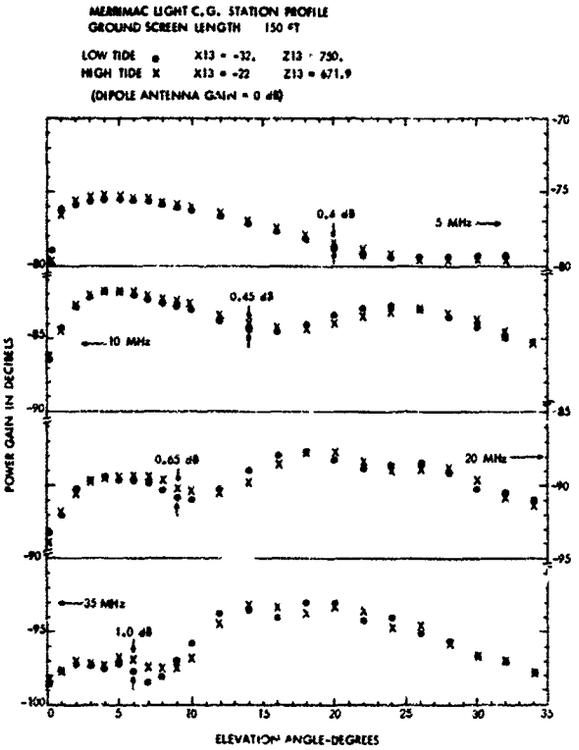

Figure 4. Power Gain for Vertical Dipoles at Four Frequencies for a 150-Foot Ground Screen—Merrimac Light Coast Guard Station Profile at Low Tide and High Tide

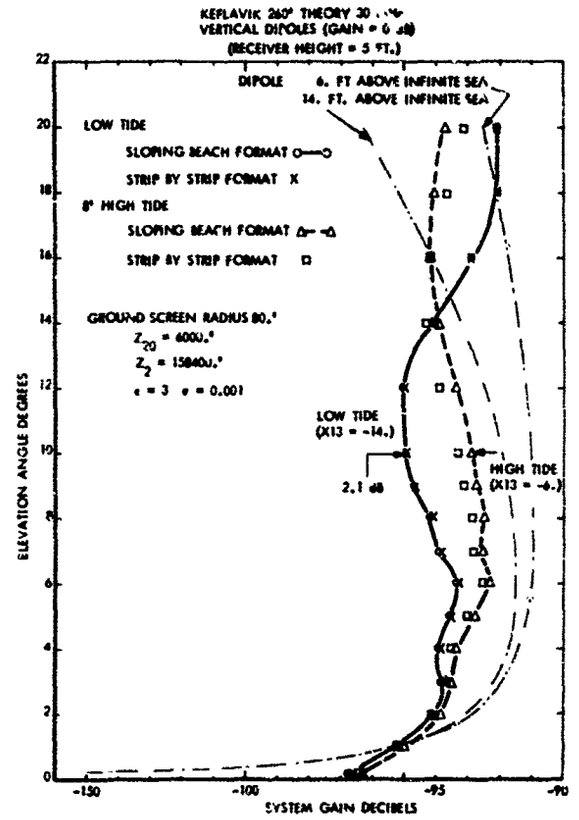

Figure 6. Predicted Power Gain for a Pair of Vertical Dipoles at 30 MHz Over Keflavik Naval Station 260° Profile

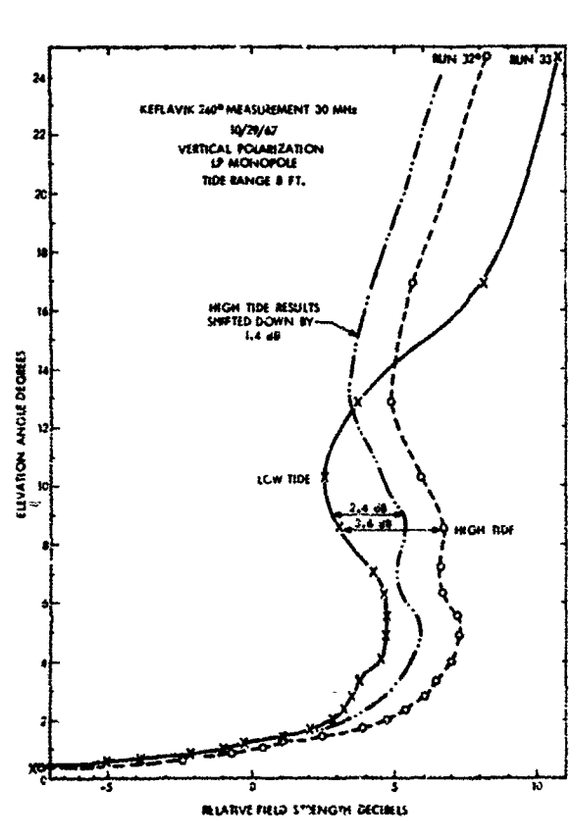

Figure 7. Measured Relative Field Strength on 260° Azimuth for an LF Monopole Antenna at Keflavik Naval Station Showing Tide Effect on October 29, 1967

THE CURRENT DISTRIBUTION ON A FINITE LENGTH DIPOLE IN THE PRESENCE OF GROUND SCREENS

Virgil R. Arens, U. R. Embry, and D. L. Motte

Sylvania Electronic Systems, Western Division
Post Office Box 205
Mountain View, California 94040

ABSTRACT

Some of the mathematical and numerical techniques using digital computers which will lead to determining the current distribution on a finite length dipole in the presence of radial ground screen are presented. Computed results for the input impedance for non-resonant vertical dipoles near the interface for various ground conductivities and dielectric constants are given. The input impedance for a non-resonant dipole in the presence of a planar array of radial wires of various lengths is shown.

1. INTRODUCTION

On a number of occasions investigators (Wait, 1967) have had to make assumptions with respect to the current distribution on finite length dipoles above and near variously shaped ground screens. It is our goal to develop a set of techniques that will allow one to calculate, using digital computers, the current distribution under these conditions.

The methods under investigation are the method of moments (Harrington, 1968), Hallen's integral equation (Hallen, 1938; Mei, 1965), and the integral equation approach (Tanner and Andreasen, 1967). All three of these approaches make use of the integral of free space Green's function.

2. Green's Function

In our study of dipoles, we believe that we have developed some useful methods in evaluating the integral of the Green's function.

In the first method one can simply perform a numerical integration of the function. Perhaps one should not use the word "simply", though, because the integration for the diagonal terms of the matrix pose some extremely difficult numerical problems.

For these terms the observation point lies on the surface of the integration segment so that the integrand comes within δ of a pole, where δ is the radius of the wire. To get an idea of the difficulty this introduces, the approximated numerical value for the integral has not become stable after using up to 64 points of Gaussian quadrature (corresponding to a polynomial of degree 127) and up to 9000 points using the trapezoid rule.

In the second method one rewrites the equations in cylindrical coordinates. This considerably simplifies the work because ρ and z components can be integrated separately after a local rotation and translation to give a two dimensional problem and then dotted with a direction vector at the observation segment.

The third method makes use of spline functions and has the potential of allowing us to develop a program free of all numerical integrations. This is accomplished by a piece-wise approximation of e^{-jkR} in cubic polynomials over one cycle. When the resulting polynomials in the variable kR are placed under the integral it is found that the terms of the resulting integrand are all integrable in closed form. The particular functions one uses are called cubic splines, an excellent account of which is found in Handscomb (1966).

As indicated earlier, when the observation point lies on the segment of the cylinder that is to be integrated, a singularity occurs in the expression for the electric field. In point of fact in the derivation of the equation an interchange of differentiation and integration was made which is not necessarily valid for these segments. Fortunately, VanBladel (1961) investigated this case some years ago and had defined a principal value of the integral for the diagonal terms.

3. Evaluation of the Integral of the Green's Function

The evaluation of the integral of the Green's function as was indicated earlier can at times be evaluated by using only numerical techniques, or a MacLaurin series expansion. Some authors have in the past tried more difficult methods that involve, for example, Hankel or Bessel functions. Now note that:

$$\int_a^b \frac{e^{-jkR}}{R}\,dx = \int_a^b \frac{e^{-jkR}-1}{R}\,dx + \int_a^b \frac{dx}{R} = \int_a^b \frac{e^{-jkR}-1}{R}\,dx + \ln\left[\frac{b+\sqrt{b^2+\rho^2}}{a+\sqrt{a^2+\rho^2}}\right] \quad (1)$$

With this simple change, the integral in the final equation can now be accurately evaluated by as few as two or three points of Gaussian quadrature for all values of R and accuracy of 5 significant digits, since the integrand is finite for R equal to zero. Here, then, is a simple and accurate numerical technique for evaluating the freespace Green's function, which we have not seen elsewhere in the literature. It illustrates very nicely the fact that it is not always expedient to begin a numerical evaluation of a function by expanding it in a power series.

4. Antennas Over A Finite Conducting Ground

In considering antennas over ground, it is easy to see that the free-space Green's function is no longer valid. Here one needs to match a set of boundary conditions at the interface between the half spaces. A Green's function which must meet these conditions is called a modified Green's function. Banos (1966) gives the properly modified Green's functions that are valid nearly everywhere in the upper half space.

The total Green's function is the sum of the free space Green's function for the image of the source segment and a correction term to account for the fact that the ground has finite conductivity. Banos deals primarily with the evaluation of this correction term. If one considers a dipole just above the ground, then one finds that none of the expressions given by Banos are valid. For this region we are developing an adaptive numerical integration technique.

5. Ground Screens

Ground screens play two roles in high frequency antennas. The first role is used in association with monopoles and the ground screen then is commonly called a counterpoise. Here one is interested in distributing current into the earth in a least loss manner to give an antenna with a high efficiency. The second role, which is used with both monopoles and dipoles, is the use of ground screens to modify or change the far field pattern of antennas.

The method of obtaining the current distribution in the presence of ground screens can be obtained in at least two ways. The desired method is dependent on the number of wires in the ground screen. Consider for a moment, the simplest of all counterpoises, a limited number of radial wires buried in the earth used in

conjunction with a monopole. In this system the counterpoise is considered a part of the antenna. The impedance matrix which defines the antenna includes terms representing the mutual impedance between segments of the antenna and the buried wires.

When the number of wires in the ground is large, the size of the matrix may become too large to consider the buried wires as part of the radiating system. When the size of the ground screen is sufficiently large one can take the expressions for surface impedance given by Wait (1956, 1958) and Larsen (1962), and determine an equivalent dielectric constant and earth conductivity and substitute these in Bano's equations to determine the modified Green's function.

If the ground screen is not large or the edge of the screen is near the antenna it is conceivable that one could determine a different modified Green's function. However, in view of the fact that one is attempting to determine the mutual impedance between two Hertzian dipoles due to the presence of ground screens.

6. Reducing the Number of Equations

Use of the symmetries of a system reduces the work involved in solving problems connected with the system. In simple structures, the symmetry corditions may be clear, and intuitive ideas are adequate to take advantage of them. In a more complicated system, intuition may become vague and a systematic method is needed to examine the effects of the various symmetry conditions. We have developed a two step procedure that considers all symmetry conditions when setting up the calculation of the current at specified points where the current will be determined. Symmetry conditions may show that some of these points will have equal currents; hence, assign only one variable and gather the coefficients to form a single term in each equation. (This is equivalent to adding columns of the equation matrix) This leads to an overdetermined system, with more equations than unknowns. The second step is to determine which equations are redundant and remove them; thus obtaining smaller sets of equations to be solved.

As an example, consider a monopole with radial ground wires spaced ten degrees apart. If one specifies that the current will be found at five points on each wire, the result is a set of 185 equations in the 185 unknown currents. If the symmetry of the ground screen is invoked, the current distribution in any wire must be the same as any other, so five unknowns suffice for the ground screen current values. The set now involves ten equations in ten unknowns.

7. Results

The current distributions and input impedance were computed for a center-fed-non-resonant dipole. The dipole length was 15 meters, the diameter was 0.006 meters and the frequency was 10 mHz. For compactness, only imput impedance plots are shown. For most cases, the current distribution obtained was not sinusoidal.

Figure 1 shows the input impedance of the dipole in free space, and with the tip 0.01 meter above the surface, in a vertical position, over various types of ground. The value for the perfect conductor was checked by computing the impedance for each of two collinear antennas fed in phase.

Figure 2 shows the effect on the input impedance when a radial array of wires is placed near one end of the dipole. Values are shown for various lengths of 4-wire and 36-wire arrays. The values for 9-wire and 18-wire arrays show similar patterns. As might be expected, many short wires have more effect than a few short wires. As the wires in the array approach a length of half a wave-length, the arrays with few wires cause a greater change than the arrays with many wires.

Placing a vertical dipole over smooth homogenous ground appears to increase the input resistance. Placing the dipole over an array of short radial wires increases the reactance, with a small change in the resistance. The combined effects are expected to cause the input impedance to approach that of the dipole over a perfect reflecting surface. If the array contains many wires, the length should be about 0.15 to 0.2 wave-length; with few wires, the length should be greater, to about 0.25 wave length.

9. Conclusion

The digital computer programs that are being developed will, when complete, allow one to evaluate the properties of any dipole antenna in any orientation between horizontal and vertical over a ground screen.

The approaches are being developed with the idea in mind that other antennas such as the log periodic or rhombic are more important than dipoles; the work on dipoles is a means to develop the techniques.

Besides the advantage of speed, economy, and flexibility relative to experimental methods, the methods outlined here will provide answers with a precision and detail unobtainable by flight testing full scale high frequency antennas. The knowledge of the

current distribution and input impedance provides insight to the antenna's operation and enhances the engineer's design tools.

REFERENCES

Wait, J.R. (1967), Canadian Journal of Physics, Vol 45, p. 3091, Sep 1967.

Harrington, R. F. (1968), Field Computation by Moment Methods, MacMillian Co, New York, 1968.

Hallen, E. (1938), "Theoretical Investigation into the Transmitting and Receiving Qualities of Antennas," Nova Acta, Royal Soc. Sciences, (Uppsala), Vol 11, pp 1-44, Nov 1938.

Mei, K. K. (1965), "On the Integral Equation of Thin Wire Antennas," IEEE Transactions on Antennas and Propagation, Vol AP-13, pp 374-378 (May 1965).

Tanner, R. and Andreasen, M. (1967), "Numerical Solution of Electromagnetic Problems," IEEE Spectrum, Vol 4, No. 9, pp 53-61, Sept. 1967.

Silver, S. (1949), Microwave Antenna Theory and Design, McGraw-Hill Book Company, 1949.

Van Bladel, J. (1961), "Some Remarks on Green's Dyadic for Infinite Space, IEEE Transactions on Antennas and Propagation, Vol AP-9, Nov 1961, pp 563-566.

Handscomb, D. C. (1966), Methods of Numerical Approximation, Pergamon Press, p 163, 1966.

Banos, A. (1966), "Dipole Radiation in the Presence of a Conducting Half-Space, Pergamon Press, 1966.

Wait, J.R. (1956), "On the Theroy of Reflection from a Wire Grid Parallel to an Interface Between Homogeneous Media I," Applied Science Research, Vol B6, p259, 1956.

Wait, J. R. (1958), "On the Theory of Reflection from a Wire Grid Parallel to an Interface Between Homogeneous Media II," Applied Science Research, Vol B7, p 355, 1958.

Larsen, T. (1962), "Numerical Investigations of the Equivalent Impedance of a Wire Grid Parrallel to the Interface Between Two Media," NBS Jcurnal of Research, Section D, Radio Propagation, Vol. 66 D, No. 1, p 8, 1962.

Wait, J. R, "The Theory of an Antenna Over an Inhomogeneous Ground Plane," Electromagnetic Theory and Antennas, (Ed. E. C. Jordan), Pergamon Press, Oxford, pp. 1079-1098; 1963. A

Wait, J. R. and L. C. Walters, "Influence of a Sector Ground Screen on the Field of a Vertical Antenna, NBS Monograph 60, April 1963. B

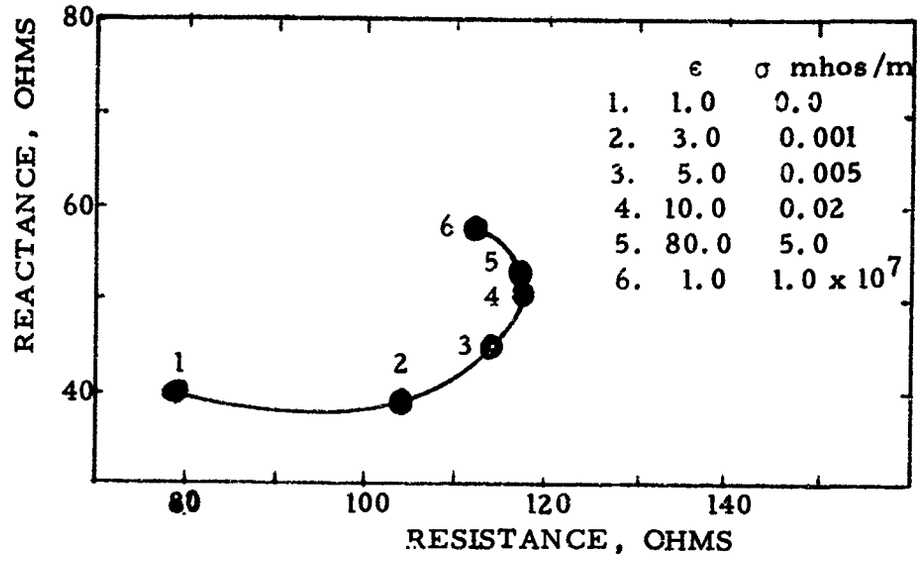

Fig. 1. Input Impedance of a Half-Wave Dipole Over Ground.

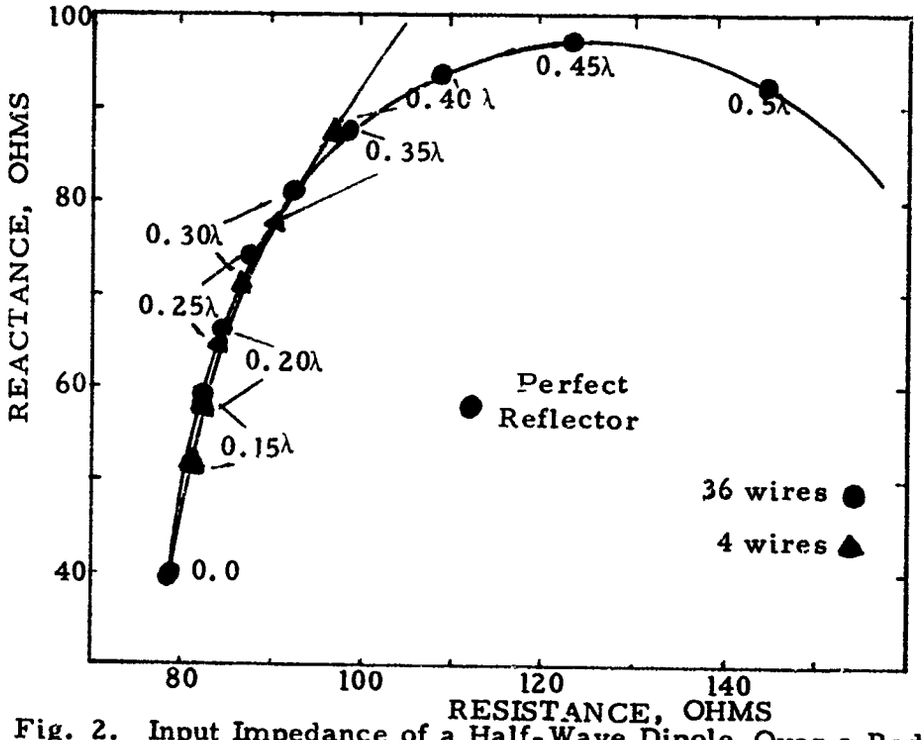

Fig. 2. Input Impedance of a Half-Wave Dipole Over a Radial Array of Wires of Varying Length.

MEASURED PATTERNS OF HF ANTENNAS AND CORRELATION WITH SURROUNDING TERRAIN

D. R. McCoy, R. D. Wengenroth
General Electric Company, HMES, Syracuse, N. Y.
and
J. J. Simons, RADC, Griffiss Air Force Base, Rome, N. Y.

A large number of fullscale radiation patterns have been measured on several HF antennas with various siting conditions. From the data it can be demonstrated conclusively that siting plays a major role in the radiation characteristics, as expected. A study of the data reveals ways of modeling the earth so as to adequately predict the influence of various parameters on antenna coverage. Thus, these data provide a firm reference with which various theories can be verified. Only two examples from the many available are presented in this paper.

1. Introduction

It has been well established by theory that antenna surroundings will modify the far-field radiation patterns of an antenna system – that in fact, the antenna is composed of the actual radiators and any territory many miles away which may be illuminated by the system. In the high frequency range, where the wavelengths are quite large and the antenna beam widths in general relatively broad, this phenomena becomes extensive. This paper presents some results of a measurement program on such a system, demonstrating the effect. Only a brief sampling of the data is presented here. A more complete presentation is made elsewhere.[2,3] It also discusses techniques whereby predictions may be made of the impact of surroundings on such a proposed installation.

2. Discussion

The full-scale patterns were measured using a KC-135 aircraft, instrumented with a receiving antenna on the tail boom, and a set of four receivers multiplexed inside. Four transmitters operating at different frequencies were time-multiplexed into the antenna on the ground, allowing for four patterns to be measured on each pass over the antenna. The aircraft was flown at a constant altitude (nominally 30,000 ft.) and the range and signal strength were recorded in the air. Flight path was controlled by ground radar and the navigator out to a maximum range of approximately 250 nautical miles. The data was then scaled, calibration data applied and the elevation angle and signal strength calculated and plotted, yielding relative data which in most cases was reproducible to within 1 dB.

These full-scale patterns of HF antennas installed with various siting conditions have been made jointly by General Electric Company and the RADC test center The installations range from a site atop a mountain overlooking the ocean in Greenland to a sea shore site in Iceland, with the ground screen end touching the ocean water at high tide. Most of the results discussed here are of two identical sets of log periodic elements, one looking north and the other south over land in upper New York State. Of particular interest is the series of patterns obtained at boresight (188°) and at plus and minus 10° (198°, 178°) of boresight looking south. The antenna is on a hill overlooking the Mohawk valley. From the elevation of 1760 feet above sea level the land drops off rapidly to 7-900 feet (a slope of approximately 6°) into the valley 10 to 20 miles away. In the 198° direction the terrain is broken up with several hills so that there is no flat land. This pattern (not shown) does not display the rapid lobing at the higher angles. The profile shown in figure 1 demonstrates the condition on boresight (188°). The radiation pattern for this direction is shown in figure 2. The identical model of antenna looking to the north from the same hill exhibits entirely different radiation characteristics, as demonstrated in figure 3. In this direction the initial slope is about 6° but the elevation levels off at about 1400 to 1500 feet in a short distance and stays constant to the Adirondack Mountain region 30-40 miles away. This contouring is shown in figure 4.

A consideration of the specular reflection from a combination of the slope in close and the relatively flat terrain further out leads to a rapidly varying pattern at low angles and a wide minimum at slightly higher elevation angles. It therefore appears from an observation of measured data that there is a third effect at the lower angles, in which the flat plane ripple is suppressed. This is probably due to the energy being blocked by the slight roll immediately in front of the antenna. There were minor differences in the lobing structure, particularly to the south, when snow was on the ground. Several values of ground constants were considered in calculating the above mentioned patterns. Proper choice of ground constants ($K = 30$ and $\sigma = .001$) seemed to give a good fit to the measured data, with the reservations of suppression of rapid lobing at the lower angles.

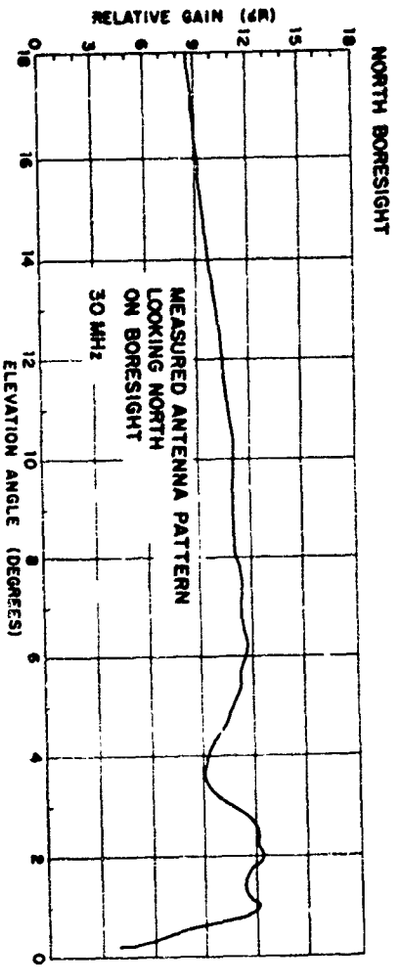

Figure 4

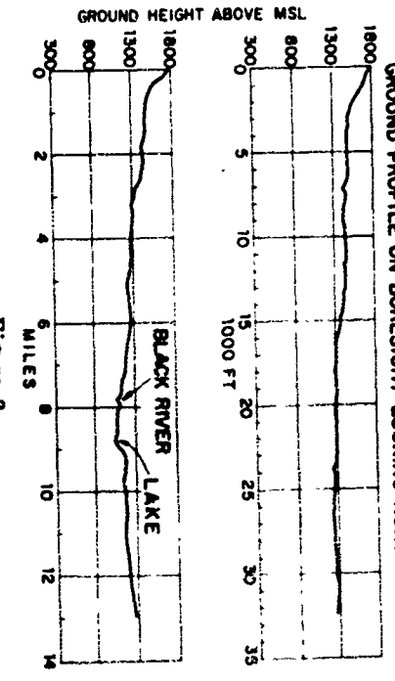

Figure 3

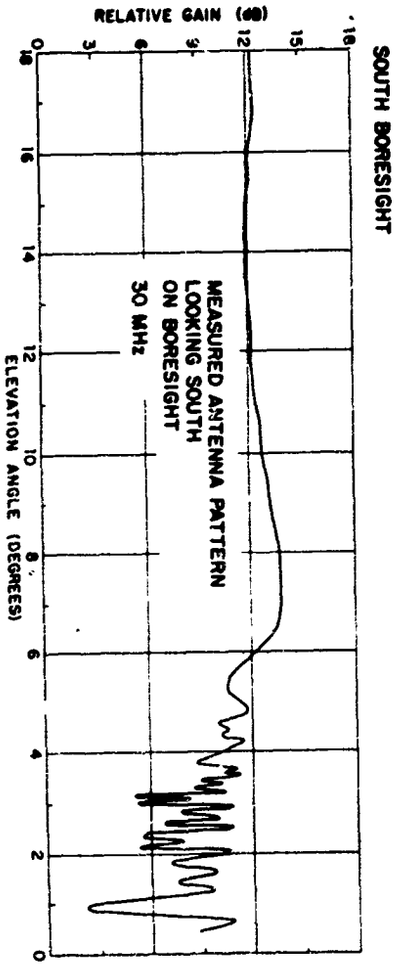

Figure 2

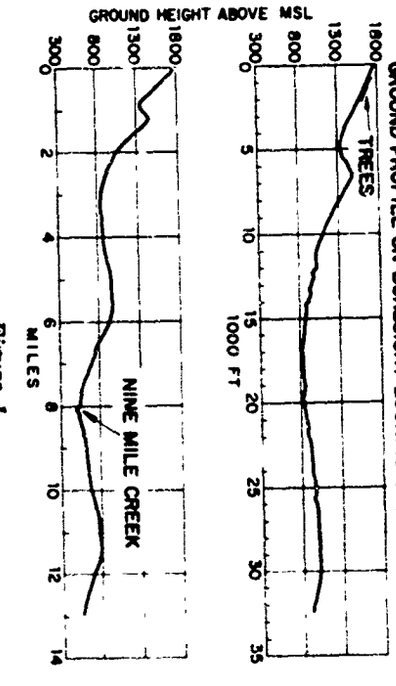

Figure 1

Figure 5 shows the measured patterns at the Keflavik (Iceland) site. The antenna is located on the shore line with the ground plane extending to the water. In this case there was a noticeable effect of the tidal variations, which were greater than 13 feet. A calculation of the expected patterns for the low and high tide conditions provides an excellent prediction of the effect as can be seen from figure 6. This same antenna, when set on a 2560 foot hill overlooking the snow, rock, hills etc. and finally the ocean 17 miles away, at Thule, Greenland, displayed violent lobing, even though the earth dropped off sharply in front of the antenna to an elevation of approximately 1500 feet above sea level.

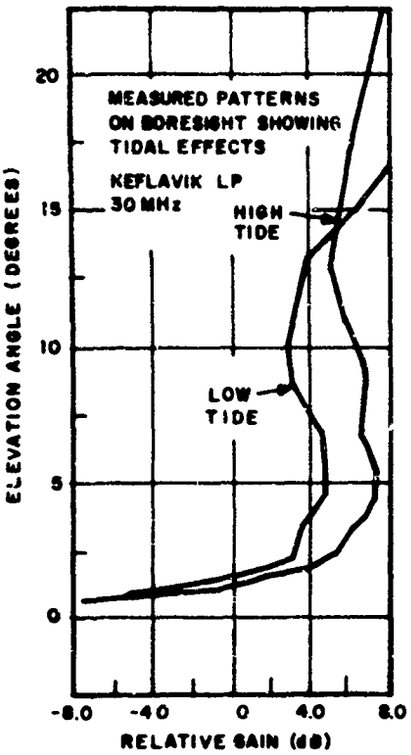

Figure 5

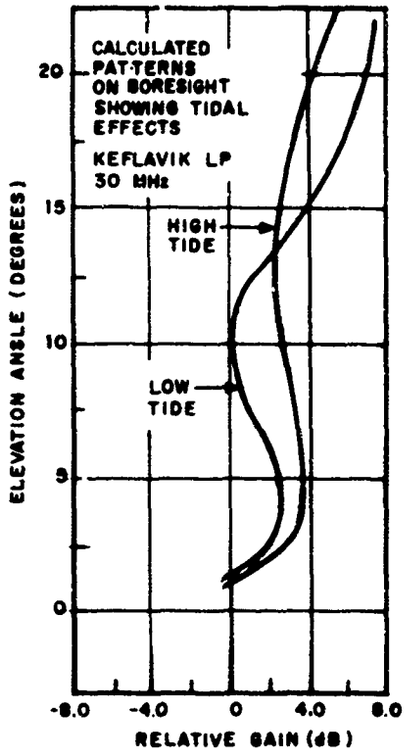

Figure 6

A technique of modeling the land in front of an antenna with a series of flat planes and knife edges has been developed.(1) This program estimates the worst case limit for the particular geometry assumed. A result of using this program to analyze the Thule antenna is shown in figure 7. In this case the very rough terrain was assumed to be approximated by two knife-edge points and intervening flat planes. As can be seen, the low angle coverage prediction is quite good. It is obvious that an added effect occurs in the 2.5° to 4.5° region, causing a wide lobe of high amplitude and phasing with the more regular pattern. Perhaps a superposition of these data with returns from additional specular points would be in order to further refine this result.

In the case of the data presented above for the Starr Hill site in New York State, there are no significant sharp obstructions in the path to the north and the program does not apply; however, it has been used with fair success on the south-looking antenna.(2) The program utility can be enhanced by more accurate modeling and perhaps by replacing the knife edge diffraction with hemicylinders and allowing for extended specular reflection planes. This is being studied at the present time.

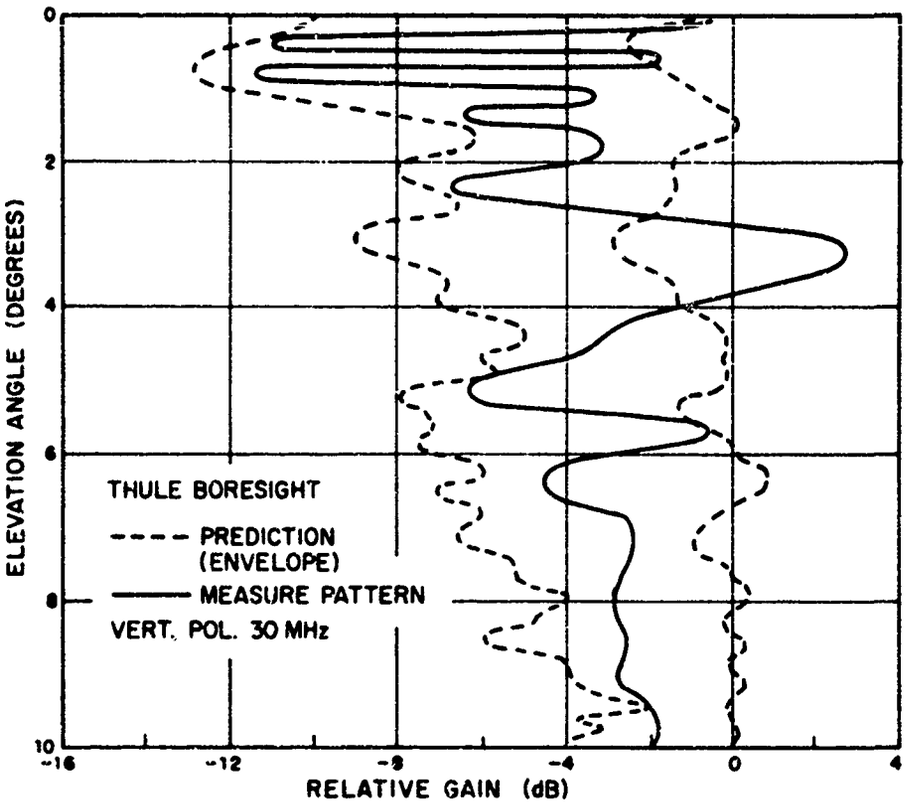

Figure 7

3. Conclusions

From the observed data it is completely demonstrated that siting plays a major part in determining the radiation characteristics of an antenna working in at the HF frequency range. It is also evident that, by carefully studying the terrain condition and contour for several miles in front of the antenna, a good prediction of the performance can be made.

4. References

(1) The Effect of the Surroundings on HF Antenna Patterns (U), R. D. Wengenroth and G. F. Farrell, Jr., General Electric Company, Syracuse, N.Y., ARPA OHD Symposium, NBS, Boulder, Colorado, June 1966.

(2) H. F. Antenna Pattern Measurement Results from ESO, D. R. McCoy, G.E., J. J. Simons, RADC, Griffiss AFB, N. Y. Nerem Convention, Oct. 1968.

(3) RADC-TR-68-248, H. F. Antenna Gain Pattern Measurements: Expanded Little ida Program (U), by Simons, Joseph J., Wilson, Frederick C. and Schneibel, Richard A., September, 1968, Unclassified.

Acknowledgment

The authors wish to express their appreciation to Dr. G. A. Otteni for his assistance in the preparation of this paper.

"The unpublished literature cited above is available on request from the authors (Ed.)."

RADIATION BY A VHF DIPOLE-TYPE ANTENNA IMBEDDED IN ITS PLASMA SHEATH*

R.V. DeVore and R. Caldecott

ElectroScience Laboratory
Department of Electrical Engineering
The Ohio State University
Columbus, Ohio 43212
2 June 1969

ABSTRACT

This paper describes the performance of a VHF dipole antenna located at the tip of an otherwise pointed reentry nosecone. Transmission and reflection measurements made during a recent flight experiment are presented and compared with calculations made for an appropriate theoretical model.

INTRODUCTION

The performance of a thin (k_0a = .092) VHF dipole-type antenna located at the tip of a 9° nose cone during an almost vertical reentry at a relatively constant velocity of 16.8 kft/sec is described. The reentry period reported covers a time span of eight seconds with an altitude range of 230 to 100 kft.

The antenna as shown in Fig. 1 is an asymmetrical dipole with the cylindrical quarter-wave stub acting as one arm and the payload skin as the other arm. It is balun-fed, the outer conductor of the cable being connected to the cone and the center conductor to the cylinder. A quarter-wave choke section was introduced behind the conical arm, hopefully to decouple the aft portion of the conical payload. That this was not fully achieved is evident from the free-space radiation pattern of Fig. 2. Note the "notch" at broadside which is primarily attributable to the excitation of the afterbody.

---

*The work reported in this abstract was supported in part by Contract F33615-67-C-1643 between Air Force Avionics Laboratory, Air Force Systems Command, Wright-Patterson Air Force Base, Ohio and The Ohio State University Research Foundation.

THE FLIGHT DATA

The altitude, velocity and angular coordinates of the trajectory were obtained by four tracking radars, 2750 to 5500 MHz. The X-band telemetry signals were recorded by three receiving stations. The VHF transmission was received by four slightly separated CP antennas and provided separate VHF-AGC records.

The telemetered signals of an on-board gyro and accelerometer together with known initial reentry conditions and the precession frequency provided angle-of-attack data so that the aspect angle (the angle between the cone axis and receiver direction) could be computed. The precession rate was verified by the cyclic variation of the VHF transmission level due to the "notch" in the pattern.

During the flight the impedance of the antenna was measured with a four-probe reflectometer and telemetry recorded as shown in Fig. 3. Except for one short time interval, preliminary to maximum signal attenuation, the modulus of the reflection coefficient was relatively constant. In addition the antenna was operated in a receiving mode, a radiometer being used to record the effective noise temperature of the plasma at the antenna terminals. This data is presented in Fig. 4 where the "average" noise temperature is approximately 35000K. Outside of the time period shown the antenna receiver was saturated by VHF interference, so at the time the VHF transmission was undergoing maximum attenuation the plasma noise and interfering signal contribution could not be resolved.

In Fig. 5 the VHF transmitted signal which was recovered from the calibrated AGC records of three different receivers is presented. The solid curve connects the average received values. A maximum signal attenuation of 17 dB is observed at 193 kft.

THE ANALYTICAL MODEL OF THE ANTENNA

We approximate the flight situation with a gap-excited finite dipole in an infinite, uniform plasma column. The far-zone result is similar to that for the Hertzian dipole in the infinite column, with the exception of the current-plasma interaction. Using the result of Ting[1] et al. The ratio of the power with and without plasma radiated in the direction θ is given by

$$P = \frac{\left(\frac{4}{\pi k_o b \sin\theta}\right)^2 \left|\frac{J_0(k_o a\sqrt{\varepsilon_p - \cos^2\theta})}{J_0(ka\sin\theta)}\right|^2 \left|\int_{-L}^{L} I(x)\varepsilon^{-ik_o\cos\theta x}\,dx\right|^2}{\left|\frac{\varepsilon_p \sin\theta}{\sqrt{\varepsilon_p-\cos^2\theta}} J_1(k_o b\sqrt{\varepsilon_p-\cos^2\theta})H_0^{(1)}(k_o b\sin\theta) - J_0(k_o b\sqrt{\varepsilon_p-\cos^2\theta})H_1^{(1)}(k_o b\sin\theta)\right|^2} \quad (1)$$

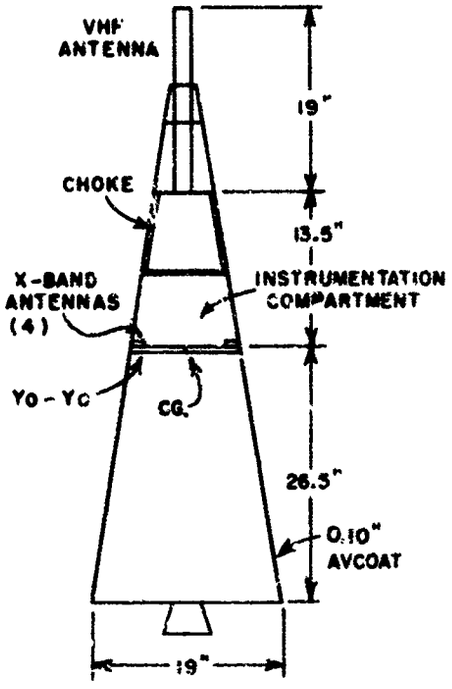

Fig. 1. THE ANTENNA AND PAYLOAD.

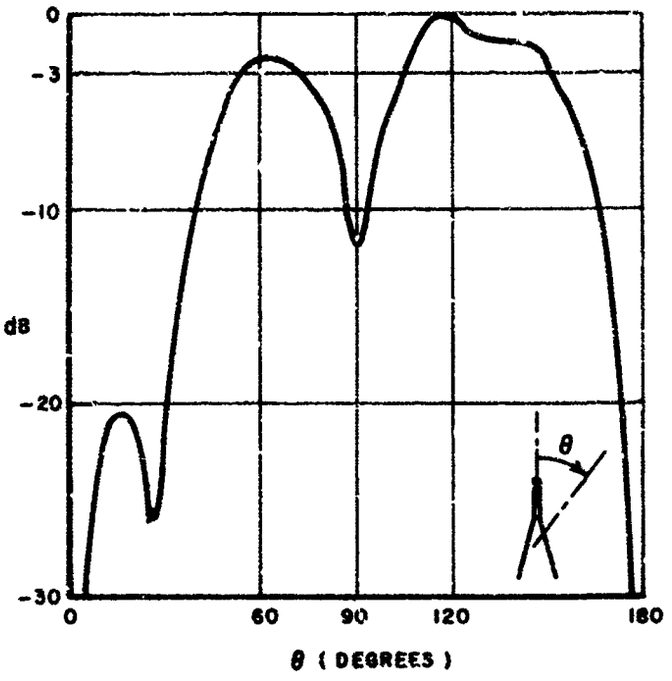

Fig. 2. E-PLANE RADIATION PATTERN OF ANTENNA (f = 231.4 MHz).

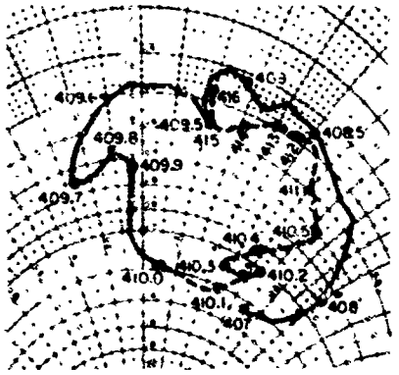

Fig. 3. ANTENNA IMPEDANCE DURING REENTRY.

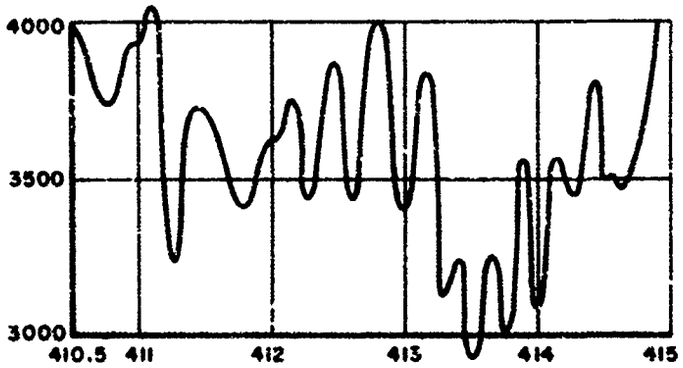

Fig. 4. EFFECTIVE PLASMA NOISE TEMPERATURE AT ANTENNA TERMINALS.

where

$$(2) \qquad \epsilon_p = 1 - \frac{(\omega_p/\omega)^2}{1 + i\,\nu/\omega}$$

2L is the dipole length (approximately $\lambda/2$), a is the antenna radius and b is the radius of the plasma column. The other symbols and functions are the usual.

THE INVISCID FLOW FIELDS

Some estimate of the parameter ω_p which characterizes the cold plasma must now be found. The simplified stream-tube method of Seiff and Whiting,[2] which assumes

(1) isentropic flow along streamlines, (2) flow parallel to vehicle axis and (3) the shape of the pressure distribution normal to the body is predictable (by first-order blast wave theory). In our trajectory, conditions (1) and (3) are probably valid but (2) is never satisfied. The angle of attack is small, so we hesitatingly ignore the crossflow. We also assume an equilibrium flow for all altitudes, which is not exactly the case.

Using the profiles calculated from the inviscid flow, we find a monotonically increasing attenuation from 230 to 100 kft. (A traveling wave form of current is assumed on the antenna.) Referring to the flight data of Fig. 5 we see this is not the case.

THE VISCOUS BOUNDARY LAYER

Maximum attenuation at 193 kft. indicates a shock-boundary layer interaction. Due to the question as to the nature of the flow and the great boundary layer thickness at this altitude, a quantitative calculation is subject to question. Nevertheless, we proceed with the phenomenological approach to the laminar thermal boundary as given by Schlichting[3] since some estimate of its effect is preferable to none.

The quantity that controls the thermal boundary layer overshoot is the Eckert number. We assume a constant temperature (300°K) cylinder. The inviscid flow calculations indicate that the kinetic temperature at the surface remains approximately constant at 3000°K throughout the trajectory. Since the velocity is constant then the Eckert number is primarily dependent on the specific heat, which for air is a rapidly varying function of density in the 2500-5000°K range.[4] To effect our calculations we assume that the specific heat of the boundary layer is specified by the inviscid flow body streamline. (A rather severe approximation due to the variation of c_p through the boundary layer.)

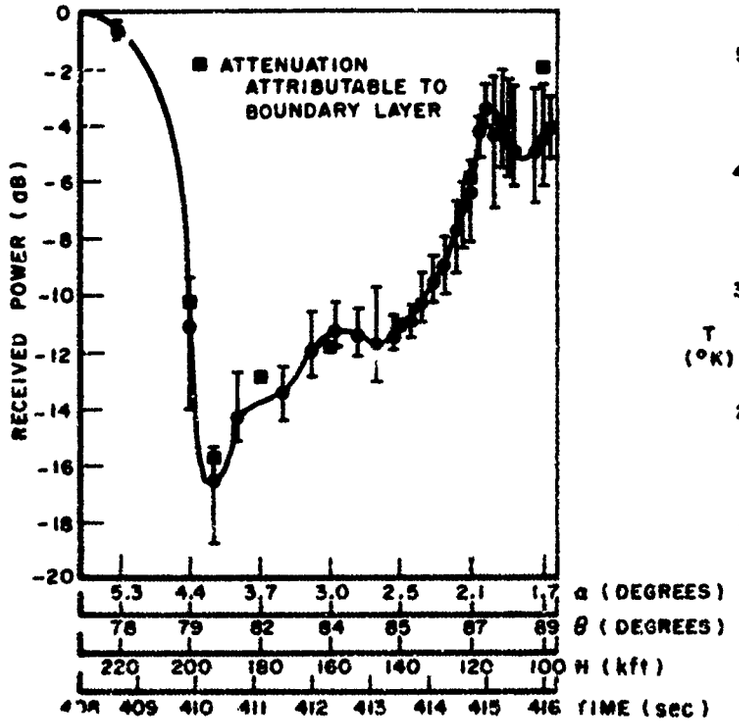

Fig. 5 VHF ANTENNA TRANSMISSION AS RECORDED BY THREE DIFFERENT GROUND RECEIVERS (REENTRY VELOCITY ≈ 16.8 kft/sec)

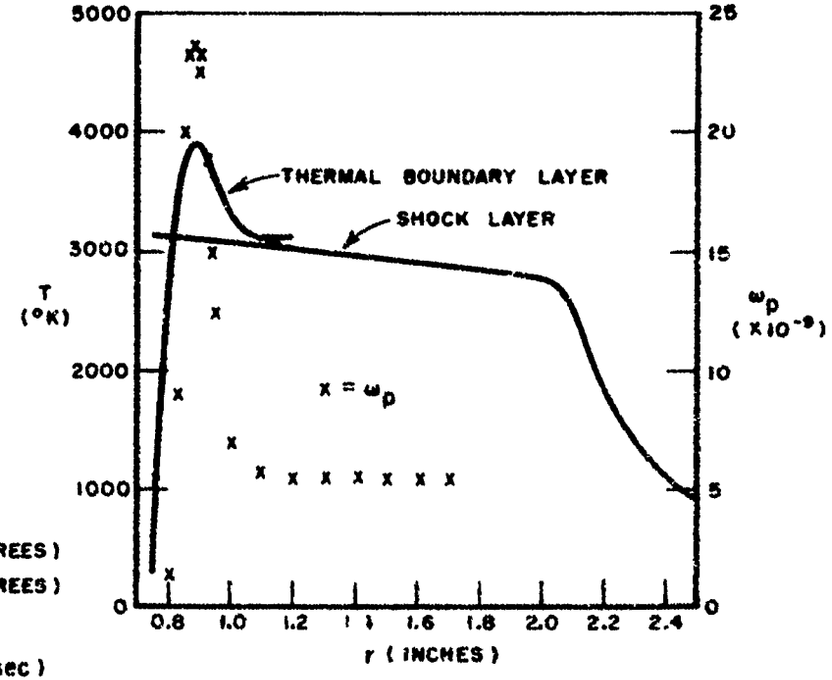

Fig. 6. RADIAL TEMPERATURE AND ω_p PROFILES AT 140 kft, 2 INCHES FROM CYLINDER FACE.

Using the matching point scheme of Evans and Huber,[5] the joined boundary layer - inviscid solution at 140 kft., shown in Fig. 6, is representative of the results obtained at other stations along the cylinder and altitudes. Also shown in Fig. 6 is the ω_p profile obtained from equilibrium conditions.

DISCUSSION

From other work based on plane wave theory it was found that thin symmetrical inhomogeneous layers could be represented quite well by equivalent uniform layers. It was observed that the equivalent thickness was well approximated by the distance between the two points where $\omega_p \approx .7\ \omega_{p_{max}}$.

With the ν and ω_p found from the boundary layer results and the equivalent plasma radius determined as just indicated, Eqs. (1) and (2) were evaluated for eight different altitude points. The attenuation due to the boundary layer is shown in Fig. 5. To effect better agreement with experiment, one must add the attenuation due to the shock layer ranging from 0.2 dB at 200 kft. to 4.1 dB at 120 kft. A more exact result would be given by a modification of Eq. (1) to include two coaxial layers.

In conclusion, it was found that the VHF transmission by a dipole-type antenna imbedded in an electrically thin axisymmetric plasma sheath is explained by the viscous boundary layer. Although the flow is quite complicated, a constant temperature cylinder is assumed, and the dipole is unbalanced, it is believed that the flight data and analysis tend to show that the antenna currents are somewhat isolated from the plasma by the cool leading edge of the boundary layer and the presence of a dielectric ablative coating over a significant portion of the antenna. This conclusion is consistent with three experimental observations:

1. Only as the greatest attenuation occurred did the antenna resonate.

2. There was no significant pattern change as evidenced by the ubiquitous notch.

3. The driving point impedance (Fig. 3) does not indicate tight coupling.

REFERENCES

1. C.Y. Ting, B.R. Rao and W.A. Saxton, "Theoretical and Experimental Study of a Finite Cylindrical Antenna in a Plasma Column," IEEE Trans. Ant. Prop. AP-16 246 (1968).

2. A. Seiff and E.E. Whiting, "Calculation of Flow Fields from Bow-wave Profiles for the Downstream Region of Blunt-Nosed Circular Cylinders in Axial Hypersonic Flight," NASA TN D-1147 (1961). Also,

   J.E. Terry and C.S. James, "A Parametric Study of Hypersonic Flow Fields about Blunt Nosed Cylinders at Zero Angle of Attack," NASA TN D-2342 (1964).

3. H. Schlichting, Boundary-Layer Theory, McGraw-Hill, Chap. XII (1968).

4. A.S. Predvoditelev et al., "Charts of Thermodynamic Functions of Air for Temperatures 1000 to 12,000°K and Pressures .001 to 1000 atm.," Associated Technical Services, Inc., Glen Ridge, N.J. (1962).

5. J.S. Evans and P.W, Huber, "Calculated Radio Attenuation Due to Plasma Sheath on Hypersonic Blunt-Nosed Cone," NASA TN D-2043 (1963).

EFFECTS OF ELECTRON ACOUSTIC WAVES ON A CYLINDRICAL DIPOLE TYPE RF MAGNETO-PLASMA PROBE

By

Hiroshi Oya*
Laboratory for Space Sciences
Goddard Space Flight Center
Greenbelt, Maryland

ABSTRACT

The effect of electron acoustic wave generation has been investigated for a short cylindrical dipole antenna in an anisotropic (magneto-active) warm plasma, considering the collisions between electrons and heavy particles. Calculations have been carried out for a homogeneous plasma using the hydrodynamic approximation and the quasi static approximation. It is obtained that the resistance due to electron acoustic wave increases steeply near the upper hybrid resonance frequency. The theory developed in this paper can explain the experimental results around the above frequency range in terms of emission of electron acoustic waves and electron collisions.

INTRODUCTORY REMARKS

The impedance of an antenna immersed in a warm plasma has been investigated extensively in the recent decade. Considerable progress has been made in the case of the warm isotropic plasma (a bibliography will be cited in a full version of this work). In the case of the magneto-active plasma, however, the theory to explain the electron acoustic wave effects on RF plasma probe experiments (Oya and Obayashi, 1966, 1967; Stone et al 1966), which has been carried out in the ionospheric plasma, is not adequately developed.

THEORETICAL PROCEDURE

In this paper the problem is investigated from the standpoint of an RF probe. The short cylindrical dipole antenna impedance is calculated in a magnetoactive warm plasma; the EM field is neglected since the problem is restricted in a region where the electrostatic field is completely dominant. The existence of the ion sheath is also neglected since the frequency range of interest is near the electron plasma and upper hybrid resonance frequency.

*NAS-NRC Resident Research Associate

The macroscopic hydro-dynamic equation is used to descrive electron motions considering the electron collisions between heavy particles. Maxwell's equation, the equation of continuity and the equation of the state are used being transformed into Fourier space with respect to the three dimensional problems. All time functions are expressed by the factor $e^{j\omega t}$ where ω and t are the angular frequency and time respectively. In this case, whole set of basic equations is expressed in a comprehensive form by introducing a dielectric matrix which has elements expressed as functions of ω, wave vector $\vec{k}$, plasma frequency f_p. gyro-frequency f_H and temperature T.

The basic equation is solved to obtain the potential function ϕ as the first step of impedance calculations; in this case quasi static approximation is employed. One of important boundary condition to solve the differential equation is charge q_s, and current J_s distributions on the antenna. It is assumed that the particles in the plasma are completely reflected back through a contact region between the plasma and the RF probe, which, in Fourier transformed space, effectively gives $-jk\cdot\tilde{J}_s + jw\tilde{q}_s = 0$ on the antenna. Hence,once we find the charge function $\tilde{q}_s$, the problem can be solved by obtaining the inverse Fourier transformation. In this work, q_s is assumed to be distributed uniformly on a short cylindrical dipole whose axis is parallel to the DC magnetic field. This is equivalent to the model of Balmain [1965], which is used to obtain the impedance in the case of an isotropic plasma; and the same technique is also used to obtain the antenna impedance by using the e.m.f. method.

The impedance value is finally expressed by an integration in which an integrant is a complicated complex function. This integration is carried out numerically for the ionospheric plasma parameters.

RESULTS AND DISCUSSIONS

A numerical calculation of the impedance value is obtained for a short cylindrical dipole antenna whose elements have length L = 1m, and radius ρ_1 = 0.01m. In this result, the gyroresonance, the plasma resonance, and the upper hybrid resonance are indicated. The remarkable evidence of the electron thermal effect is the presence of the acoustic wave resistance which is enhanced near the upper hybrid resonance frequency and, also, in a frequency range below the gyroresonance frequency. In a frequency range higher than $\sqrt{2\ f_p^2 + f_H^2}$, the electron acoustic wave cannot exist since the wave length becomes smaller than the Debye shielding length; thus the acoustic resistance is not present.

In practice, we cannot neglect the existence of an ion sheath surrounding the RF probe, except for the case of sheath collaps condition which can be artificially produced by applying a high DC voltage to the probe. In the frequency range in which $|Z(\omega)| >> |1/C_s\omega|$ where C_s is the so called sheath impedance, however, the effect of sheath impedance is completely negligible [Oya, 1967]. Thus we can confirm that above the sheath resonance frequency the ion sheath effect is not serious, and around the plasma, and upper hybrid resonance frequency the ion sheath effect is completely negligible.

A microscopic approach to electron acoustic waves in an anisotropic warm plasma was considered by Bernstein [1958]. Bernstein's relation is developed for a case near the upper hybrid resonance by Fejer and Calvert [1964]. The dispersion equation is only slightly different from Fejer and Calvert's equation near the upper hybrid resonance frequency and indicate that the theoretical approach of this work in a frequency range around the upper hybrid resonance obtains results similar to the microscopic treatment of the plasma and is sufficient to discuss the quantitative nature of the upper hybrid resonance.

In Fig. 1, examples of impedance value using absolute value and phase angle are illustrated for plasma parameters of the ionosphere at altitude of 100 km(a), 500 km(b) and 1000 km(c). The phase variation indicates that near the upper hybrid resonance there is strong enhancement of the electron acoustic wave; the power dissipation of this acoustic waves affects the sharpness of the resonance. In the collision dominant regime (see a), however, the power dissipation is caused by the collisions. The sharpness of the resonance is investigated for the ionospheric plasma in altitude range of 100 km ~ 1000 km being compared with rocket observation result [Oya, 1967]. There is good agreement between the theoretical calculation and the experimental result.

CONCLUDING REMARKS

The theory is developed in an anisotropic warm plasma for a short cylindrical dipole RF probe immersed in an homogeneous ionospheric plasma. Near the plasma frequency and upper hybrid resonance frequency the results are completely useful and a complicated feature of the experimental result obtained in the ionosphere can be explained. This work may be a starting point for investigations of the electron acoustic wave effect in wider frequency ranges including the cyclotron harmonic effects and ion sheath effect.

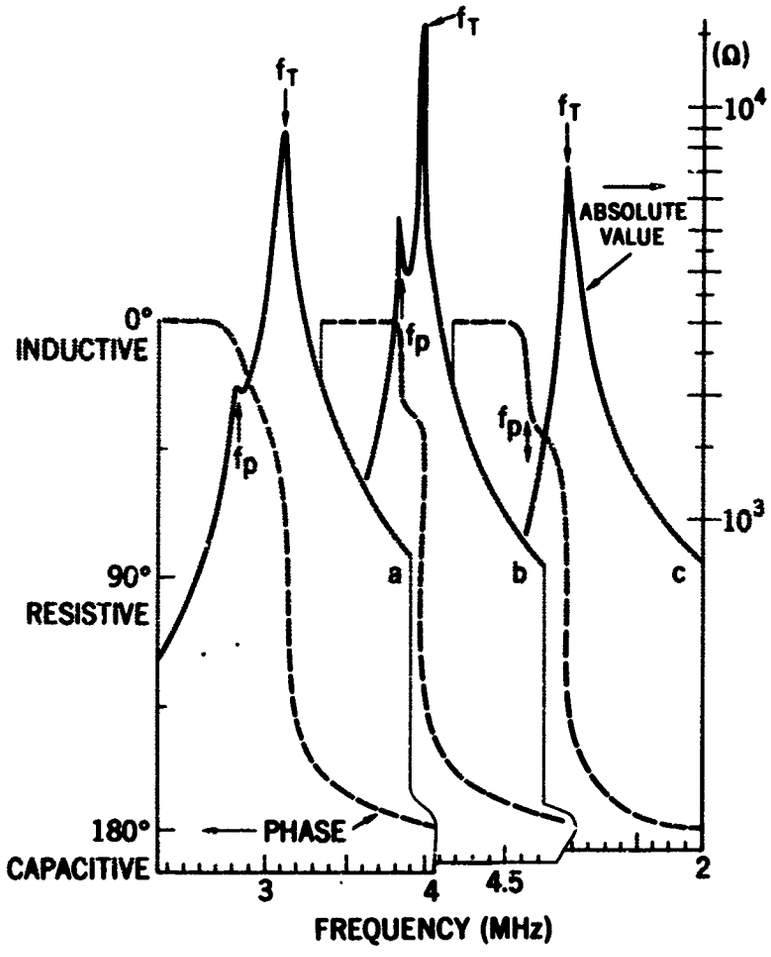

Fig. 1. Three examples of calculated impedance value around the upper hybrid resonance frequency, for the following cases:

	f_p(MHz)	f_H(MHz)	T(°K)	ν
a)	2.84	1.35	1000	10^5
b)	4.00	1.42	1300	10^2
c)	1.28	0.96	1400	1.0

5

REFERENCES

Balmain, K.G. (1965), impedance of a short dipole in a compressible plasma, Radio Science, J. Res. NBS 69D, No. 4, 559-566.

Bernstein, I.B. (1958), waves in a plasma in a magnetic field, Phys. Rev. 109, No. 1, 10-21.

Fejer, J. A. and W. Calvert (1964), resonance effects of electrostatic oscillations in the ionosphere, J. Geophys. Res. 69, No. 23, 5049-5062.

Oya, H. and T. Obayashi (1966), measurement of ionospheric electron density by a gyro-plasma probe: a rocket experiment by a new impedance probe, Rep. Ionos. Space Res. Japan 20, No. 2, 199-213.

Oya, H. and T. Obayashi (1967), rocket measurement of the ionospheric plasma by gyro-plasma probe, Rep. Ionos. Space Res. Japan 21, No. 1, 1-8.

Stone, R.G., J. K. Alexander and R.R. Weber (1966), measurement of antenna impedance in the ionosphere - II, Planet. Space Sci. 14, 631-639.

DETERMINATION OF ELF/VLF TRANSMITTING ANTENNA PERFORMANCE IN THE IONOSPHERE

J. Plumer Leiphart

Satellite Communication Branch
Communications Sciences Division
Naval Research Laboratory, Washington, D.C. 20390

An experiment is planned that will determine the effects of the magnetoionic medium on propagation between an ELF/VLF source in the ionosphere and a surface-based receiver. Proper implementation of this propagation experiment requires that instrumentation to measure the driving point impedance and efficiency of transmitting electric dipoles and loop antennas in the anisotropic ionosphere.

An ELF/VLF propagation experiment is being planned by the Navy to determine how energy emitted from a spacecraft in the ionosphere propagates through the ionosphere, couples across the air-ionosphere boundary, energizes the Earth-air-ionospheric cavity, and propagates to the surface of the Earth. A high power transmitter in an orbiting spacecraft will be the source of power. Receiving and analysis equipment at many geographic locations will determine signal strength, polarization and direction of arrival. Total time delay and frequency shift will be determined by comparison with telemetered replicas of the transmitted ELF/VLF signals.

However, losses and other characteristics of the propagation path cannot be determined from the received signals unless the characteristics of the emitted signals are known. Some information relative to the radiated signals can be deduced from measurements made on the transmitting antenna. These will be outlined in this paper. In addition, the antenna measurements will provide a base for future experimentation and guide the design of efficient couplers between the high power transmitting source and the terminals of an antenna immersed in the ionosphere.

In order to obtain a wide range of propagation path parameters and many "in-situ" conditions for measuring antenna performance, a polar orbit with an apogee of 2500 kilometers and a perigee of 350 kilometers is planned. Including diurnal variations, this will provide a range of electron densities from 10^6 electrons/meter^3 to

10^{13} electrons/meter^3. The predominate ion will change from H^+ to O^+ between the apogee and perigee. The other magnetoionic parameter affecting the antenna will be the strength of the Earth's magnetic field which will produce electron gyro frequencies of 350 kHz to 1500 kHz.

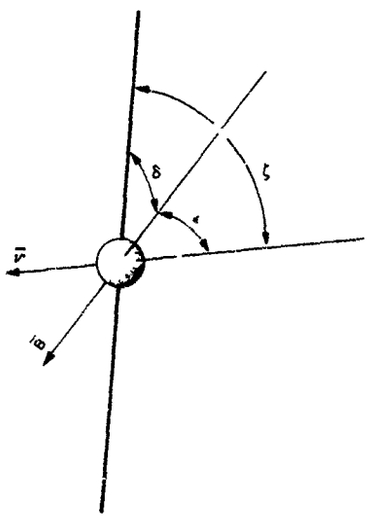

FIGURE 1. Angles determining sheath characteristics

It is anticipated that the ion sheath around the dipole elements will be the controlling parameter affecting the antenna reactance at low drive levels. This ion sheath will be perturbed by the $\bar{v} \times \bar{B}$ potentials induced in the antenna structure. The size and shape of the ion sheath will depend greatly upon the magnitude of $\bar{v}$ and $\bar{B}$ and the angles δ, ϵ, and ζ, shown in Figure 1, which uniquely define the orientation of the antenna relative to $\bar{B}$ and $\bar{v}$.

A recent analysis by Mr. Dennis Baker of the Naval Research Laboratory based on such a perturbated sheath confirms the antenna capacity measurements of the LOFTI II A spacecraft experiment which carried a simple dipole. The spinning antenna on LOFTI II A is depicted in Figure 2 as wheel spokes in the x-z plane. The spin axis $\bar{S}$ is along the y axis and the x-y plane contains the Earth magnetic vector $\bar{B}$. The spacecraft carried a two-axis magnetometer measuring components of the magnetic field parallel to the spin axis and along the antenna. When the antenna was in the direction of the x-axis, the magnitude of the component of the magnetic field parallel to the antenna is at a maximum. During the course of the experiment the angular displacement between the position for minimum capacity and the x-axis varied. Among other results of

VLF Ground Based Measurements over Stratified Antarctic Media

G. E. Webber and I. C. Peden
Electrical Engineering Department
University of Washington, Seattle, Wn. 98105

ABSTRACT

The near-field phase and amplitude broadside to a long horizontal dipole near Byrd Station, Antarctica, are measured at 12.8 khz. The resulting data, together with an appropriate mathematical model suggest reasonable values of depth and bulk complex permittivity for the glacial ice, and a conductivity figure for the underlying earth.

INTRODUCTION

The phase and amplitude characteristics of the near field broadside to a long horizontal dipole at very low frequencies constitute a potential source of useful information about the nature of the underlying media [Biggs, 1968]. This study concerns Antarctic glacial terrain, and makes use of data collected recently in the Byrd Glacier area to draw tentative conclusions about the nature of the sub-surface media. The method suggests the depth of the ice shelf is in the neighborhood of 2250 meters, that the bulk relative complex dielectric constant of the ice may be approximated by the figure 6.0 - j14, and that the conductivity of the underlying earth approaches 0.10 mho per meters. All of these figures are shown to be reasonable in light of available data from other sources.

EXPERIMENT AND MATHEMATICAL MODEL

Two electric dipoles 21 and 8 miles long respectively, lie at right angles near the top of a thick ice shelf at an Antarctic site 12 miles from Byrd Station; they may be operated independently of each other in the 3-30 khz. frequency range. Although they are used primarily for polar ionospheric studies, the following auxiliary experiment was conducted during January 1969. With the 21 mile dipole excited at 12.8 khz. and the 8 mile dipole unexcited, a vehicle equipped with VLF receiving and telemetry instrumentation was driven away from the dipole center along a broadside path with respect to the axis of the 21 mile antenna. It sampled the vertical magnetic field over a total distance of 11 miles, approximately 3/4 wavelength, in the general direction of Byrd Station. The field amplitude was measured along this path at ground level; simultaneously, the signal was telemetered back to the station for phase comparison at the transmitter. These data are interpreted in terms of theoretical predictions to be described. Further comparison is made with findings recently

will be under control to provide for variation from low levels up to the power obtainable from a source capable of supplying better than 1 kilowatt into the antenna coupling unit. This power will be modulated to provide a constant envelope signal or various pulse combinations. This provides the experimenter with a wide range of parameters for propagation path experimentation, ionospheric excitation, and antenna performance determination.

The spacecraft will contain a broad spectrum of instrumentation to measure the parameters affecting the experiment; in particular, methods of measuring absolute spacecraft attitude, antenna orientation relative to the Earth's magnetic field, and devices for measuring electron density and ion constituency.

A prime factor to be known about antennas is the far-field pattern. For this purpose, the ground receiving system is quite limited. Actually, any practical measurement technique will be a compromise. However, other experimenters will have orbiting spacecraft containing receiving equipment which will provide some indication as to the far field in the ionosphere. Similarly, one or more spacecraft launched and separated from the transmitting spacecraft could provide information. A receiving rocket launched in a trajectory cutting through the radiated field would also provide field pattern information. In addition, a receiver in the spacecraft acting like a top-side sounder would establish confidence that the signal was radiated by receiving energy reflected or refracted back from discontinuities or inhomogenuities. Unfortunately, it is impractical to thoroughly scan the entire volume to determine the patterns, how they change with radial distances, and the relative power densities in the several propagating modes.

Most information relative to antenna performance will be obtained at the transmitting spacecraft.

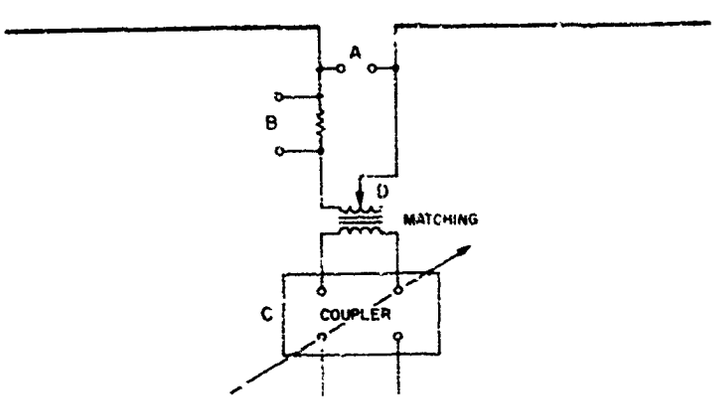

FIGURE 3. Impedance measurement points

First, the current into the antenna measured at B (shown in Figure 3) and the voltage measured at A across the antenna terminals, together with their relative phases, will be telemetered to Earth. This data will be correlated with the environmental data and experiment parameters.

Secondly (as shown in Figure 3), the antenna coupling unit and matching transformer will be servo-controlled to obtain maximum power transfer. The position of the transformer tap and the reactance position will be telemetered to monitor the performance of the servo system. This information, providing the range and bandwidth of the servo system is adequate to follow the changes, will confirm the results obtained by measurement of voltage, current, and phase.

It is anticipated that there will be non-linear effects observable by changing the level of the drive power. Harmonics and other frequencies, detectable on the ground or in the spacecraft receiver, will be generated and related to the antenna performance behavior. This non-linearity will be reflected in the waveforms of the antenna current and driving voltage. These waveforms will likely be telemetered to Earth but only for special tests since they require large bandwidths in the telemetry channels. In order to conserve telemetry bandwidth, these waveforms (as shown in Figure 4) will be processed by a harmonic analyzer on the spacecraft and the results relayed in digital form to the telemetry stations.

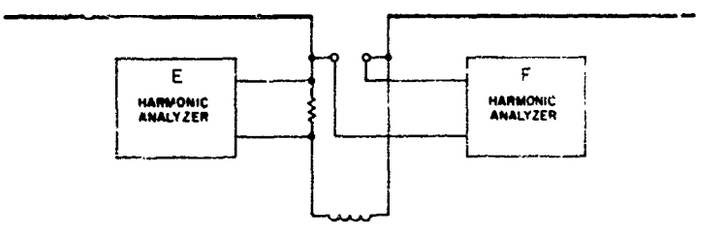

FIGURE 4. Method of determining non-linear characteristics

Potentials will probably be sufficiently large to cause the sheath to collapse at one end of the antenna as shown in Figure 5. Simple measurement of reactance across the antenna terminals A and B will not be sufficient to reveal this asymmetry. Measurement of the capacity between each of the antenna terminals and the body of the spacecraft, terminal C, will provide some information relating the capacity between the sheath and each of the dipole elements. Additional information relative to the sheath formation will be obtained by putting direct current biases between the antenna elements and the spacecraft and by an electron-gun on the spacecraft.

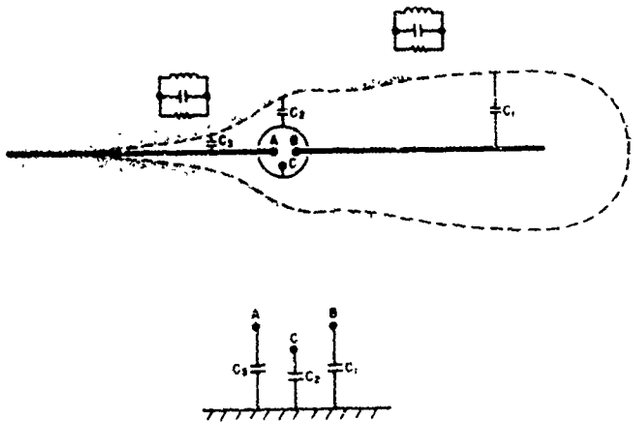

FIGURE 5.
Measurement of pulsating sheath

Figure 5 shows a static representation of the sheath. When the antenna is used for transmission, the driving potential across the antenna terminals and along the antenna may equal or exceed the $\bar{v} \times \bar{B}$ potentials. In any case, there will be a sheath which oscillates from one end of the dipole to the opposite end of the dipole at the driving frequency. Measurements at the driving frequency will not reveal the full dynamic nature of the sheath. In order to study this pulsating sheath, these capacities will be measured at frequencies of the order of ten to a hundred times that of the driving frequency. The representation of the circuit by three capacitors in the lower part of Figure 5 is grossly simplified, since the capacity is distributed and the ionosphere bounding the sheath is not an electrical short but has a complex impedance as diagrammatically indicated in the upper part of the figure. In order to determine some characteristics of the antenna-sheath-plasma circuit, these impedances will be measured at several frequencies and a sheath impedance derived from the data.

This experiment is still in the formulation stages and should be of great interest to those interested in the effect of plasma and anisotropic media on antennas. Any comments to make this a more definitive and productive experiment would be appreciated.

VLF Ground Based Measurements over Stratified Antarctic Media

G. E. Webber and I. C. Peden
Electrical Engineering Department
University of Washington, Seattle, Wn. 98105

ABSTRACT

The near-field phase and amplitude broadside to a long horizontal dipole near Byrd Station, Antarctica, are measured at 12.8 khz. The resulting data, together with an appropriate mathematical model suggest reasonable values of depth and bulk complex permittivity for the glacial ice, and a conductivity figure for the underlying earth.

INTRODUCTION

The phase and amplitude characteristics of the near field broadside to a long horizontal dipole at very low frequencies constitute a potential source of useful information about the nature of the underlying media [Biggs, 1968]. This study concerns Antarctic glacial terrain, and makes use of data collected recently in the Byrd Glacier area to draw tentative conclusions about the nature of the sub-surface media. The method suggests the depth of the ice shelf is in the neighborhood of 2250 meters, that the bulk relative complex dielectric constant of the ice may be approximated by the figure 6.0 - j14, and that the conductivity of the underlying earth approaches 0.10 mho per meters. All of these figures are shown to be reasonable in light of available data from other sources.

EXPERIMENT AND MATHEMATICAL MODEL

Two electric dipoles 21 and 8 miles long respectively, lie at right angles near the top of a thick ice shelf at an Antarctic site 12 miles from Byrd Station; they may be operated independently of each other in the 3-30 khz. frequency range. Although they are used primarily for polar ionospheric studies, the following auxiliary experiment was conducted during January 1969. With the 21 mile dipole excited at 12.8 khz. and the 8 mile dipole unexcited, a vehicle equipped with VLF receiving and telemetry instrumentation was driven away from the dipole center along a broadside path with respect to the axis of the 21 mile antenna. It sampled the vertical magnetic field over a total distance of 11 miles, approximately 3/4 wavelength, in the general direction of Byrd Station. The field amplitude was measured along this path at ground level; simultaneously, the signal was telemetered back to the station for phase comparison at the transmitter. These data are interpreted in terms of theoretical predictions to be described. Further comparison is made with findings recently

obtained by the U.S. Army Cold Regions Research Laboratories regarding the underlying ice structure in connection with a six inch core drilled through the glacier at Byrd.

The relevant mathematical model is illustrated in Figure 1; it comprises a homogeneous, isotropic, lossy dielectric ice layer covering a semi-infinite region of imperfectly conducting earth. The ice layer lies below a semi-infinite region whose properties are those of free space; plane boundaries are assumed throughout. Assuming a horizontal line source at the air-ice interface, expressions may be derived for the horizontal electric field at this boundary in terms of distance from the source. These are well known, and have been presented before [Wait, 1962; Collin, 1960; Biggs and Swarm, 1965]. The vertical magnetic field is of course simply related to these expressions through Maxwell's equations. Digital computer techniques are used to obtain accurate solutions; they are cast in a general form to permit application to a variety of natural media, of which ice and underlying earth represent a special case.

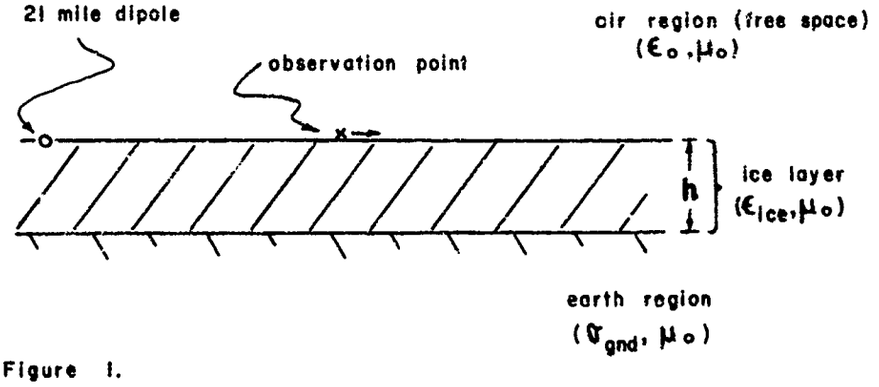

Figure 1.

It is shown that two basic modes are the primary contributors to the total field at the interface, namely a component representing propagation in the ice layer and one propagating along the interface itself. An additional weak lateral wave contribution results from propagation just below the earth-ice interface. A brief mathematical discussion summarizes their origins in terms of an integral evaluation in the complex plane. Predictions are made regarding the phase and amplitude of the electric field at the air-ice interface in terms of a range of possible complex dielectric constants and layer depths. The best fit to the experimental data is found to occur for the combination of parameters indicated above. Figures 2 and 3 illustrate the agreement obtained under these conditions.

Figure 2

PHASE LAG vs DISTANCE

(H_z)

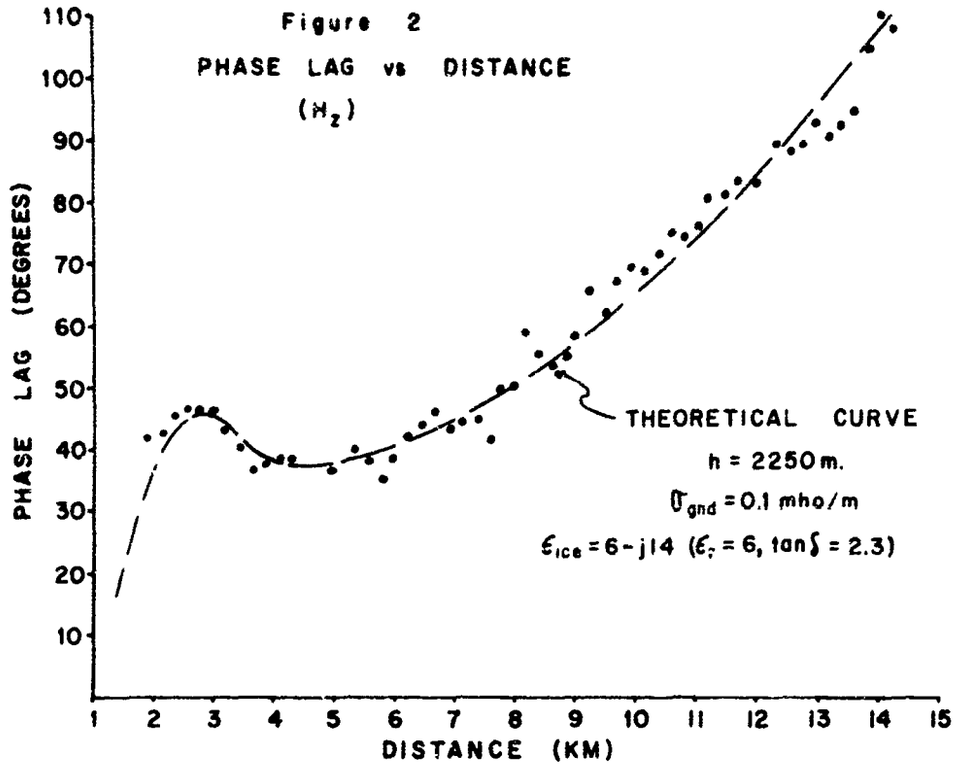

Figure 3 — ATTENUATION vs. DISTANCE

(H_z)

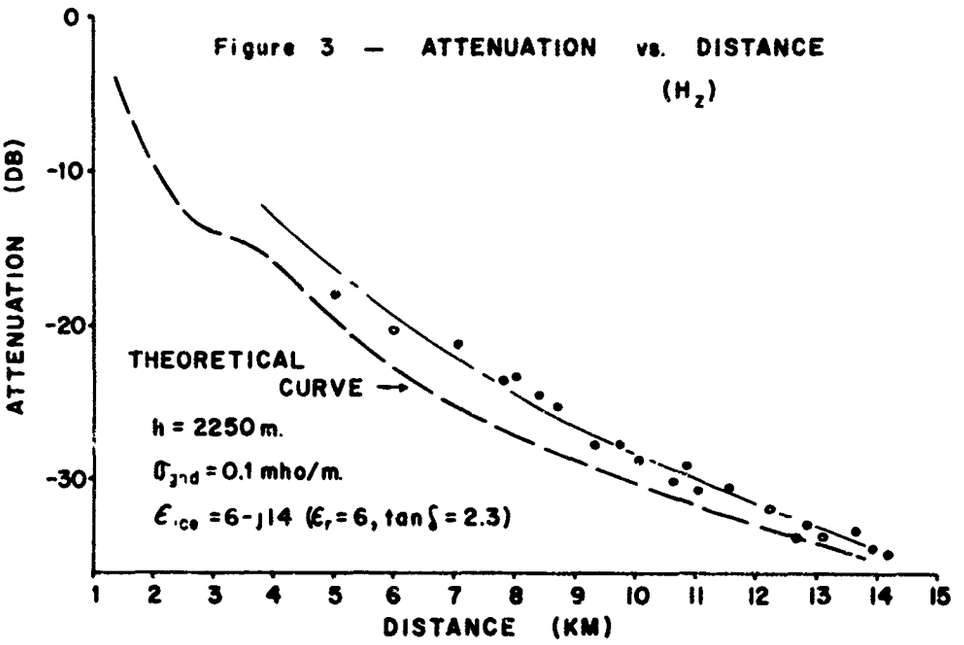

DISCUSSION AND CONCLUSIONS

The vertical thickness of the glacier at Byrd Station has been measured directly by drilling to the bottom [Gow, Ueda and Garfield, 1968]; the resulting depth was 2164 meters, which compares well with our value of 2250 meters. Other investigations have yielded depth figures varying up to 2570 meters in the neighborhood of Old Byrd Station [Thiel, Bentley, Ostenso, and Behrendt; 1959], where the ice-rock interface is believed to be quite irregular along a path roughly parallel to, and only a few miles from the path traveled by our vehicle.

A conductivity of 0.1 mho per meter is slightly high for the underlying rock, but not unreasonable for the mixture of granite, ice and water found at the bottom of the drill hole by Gow, Ueda and Garfield. Furthermore, our method is relatively insensitive to the assumed conductivity of the underlying medium, so long as this is greater than 0.001 mho per meter.

No experimental data are available regarding the complex permittivity of the ice as a function of depth at the drill site or elsewhere in the Byrd Glacier area, although the density and complex dielectric constant of the surface snow have been measured at several different temperatures at 10 khz. [Rogers, 1967]; $\varepsilon^* = \varepsilon_o(2.7 - j2.7)$ at - 30° C, with a density of approximately 0.4 gm/cc is a typical figure; the complex permittivity decreases with temperature, and increases with pressure packing until impermeable ice results at a depth of approximately 65 meters [Hatherton, 1965]. Assuming that this parameter is essentially independent of pressure over the entire vertical depth of the glacier, and primarily dependent on temperature and the presence of impurities, it is possible to infer some bounds on the expected average figure. Simple straight-line approximations to the temperature profile measured in the drill hole [Gow, et. al.] yield an average temperature near -20° C. This temperature, in turn, suggests a lower bound of 3 - j6.7 for the complex permittivity in terms of the figure for pure ice at 12.8 khz. at this temperature [Watt and Maxwell, 1960]. Impurities in the glacial ice can be expected to increase the dielectric and loss factors. A step toward accounting for their presence is made by assuming them to be comparable to or less than those of the Athabasca Glacier in Alberta, Canada, for which Watt and Maxwell give some data. Their figure of 14 -j21, measured in the surface ice at 0° C, is taken as an upper bound since it is known that the quantity of interest decreases at lower temperatures. Moreover, the greater isolation of the Byrd Glacier from civilization suggests a lower impurity level relative to that at the Athabasca Glacier. On these grounds, our value of 6 - j14 ($\varepsilon_r = 6$, $\tan \delta = 2.33$) appears justified.

It is concluded that the measurement of the phase and amplitude of the VLF ground wave can provide information about the nature of glacial ice and the sub-surface land boundary. It may be viewed as a valuable adjunct to other methods currently in use to study these characteristics of the Antarctic terrain.

Acknowledgement: The authors wish to thank Mr. J. C. Rogers and Mr. A. Chandler of the University of Washington Electrical Engineering Department for helpful discussions and for assistance with the in-site measurements at the U.W. Longwire Antenna site. This work was supported by the National Science Foundation under grant No. GA-1610.

REFERENCES

Biggs, A.W. (May 1968), Geophysical Exploration in polar areas with very low frequency phase variations, IEEE Trans. Ant. & Prop. Vol. AP-16, No. 3, 364-365.

Wait, J.R. (1962), Electromagnetic Waves in Stratified Media, MacMillan Book Company, New York.

Collin, R.E. (1960), Field Theory of Guided Waves, McGraw-Hill Book Company, New York.

Biggs, A.W. and Swarm, H.M. (1965), Analytical Study of the Radiation Fields from an electric dipole in stratified and inhomogeneous Antarctic terrain, Technical Report No. 98, Dept. of E.E., Univ. of Wn.

Gow, A.J., Ueda, H.T., and Garfield, D.E. (6 Sept. 1968), Antarctic ice sheet: preliminary results of first core hole to bedrock, Sci. 161, 1011-1013.

Rogers, J.C., private communication

Hatherton, T. (1965), Antarctica, A.H. and A.W. Reed Publishers of New Zealand Books, Wellington, Auckland N.Z.

Thiel, E., Bentley, C.R., Ostenso, N.A., and Behrendt, J.C., (July 1959), Oversnow traverse programs, Byrd and Ellsworth Stations, Antarctica, 1957-58; seismology, gravity, and magnetism, IGY Glac. Rpt. Series No. 2, IGY World Data Center A, Glaciology, Am. Geog. Soc. Sec. II, 5-8.

Watt, A.D. and Maxwell, E.L., (1960), Measured electrical properties of snow and glacial ice, J. Res. NBS 64D (Radio Prop.) No. 4, 357-63.

Tai, C. T. (1951), The effect of a grounded slab on radiation from a line source, J. Appl. Phys., 22, 405.

RADIATION FROM AN ELEVATED VERTICAL DIPOLE ABOVE AN EXTENDED GROUND SCREEN

W. T. PATTON

RCA, MOORESTOWN, NEW JERSEY

A good inductive ground screen used to provide low angle space wave radiation from a vertical dipole can support the Sommerfeld surface wave since the phase angle of the effective surface impedance can exceed 45 degrees and may approach 90 degrees for a very good screen. The Sommerfeld attenuation functior is important to accurate calculation of ground screen effects for screens of large extent.

The ability of an antenna system to establish long range links via the ionosphere is determined by the characteristics of the space wave radiation pattern at low elevation angles. For a short vertical dipole over a homogeneous earth, the pattern is given by

$$G_1 = \cos\psi \frac{e^{jkh\sin\psi} + R_{v_1} e^{-jkh\sin\psi}}{2} \quad \text{where} \quad R_{v_1} = \frac{\sin\psi - \frac{Z_1(\psi)}{\mathcal{Z}}}{\sin\psi + \frac{Z_1(\psi)}{\mathcal{Z}}} \tag{1}$$

(2)

is the Fresnel reflection coefficient for vertical polarization. $\frac{Z_1(\psi)}{\mathcal{Z}}$

$$\frac{Z_1(\psi)}{\mathcal{Z}} = \frac{1}{n}\left(1 - \frac{\cos^2\psi}{n^2}\right)^{1/2}, \quad n = \left(\varepsilon_r - j\frac{\sigma}{\omega\varepsilon_o}\right)^{1/2} \tag{3}$$

is the surface impedance of a finitely conducting earth. The space wave radiation pattern (1) of a vertical dipole generally shows sharp attenuation for elevation angles below 10 to 15 degrees.

Two methods of improving low angle radiation are 1) increasing vertical directivity by elevating the dipole and 2) providing a ground screen under the antenna of sufficiently large extent to be effective at low elevation angles. Ground screens longer than 100 wavelengths are required to control the pattern at angles about 5 degrees elevation. Following Wait (1967) with the Sommerfeld attenuation function included as in Wait (1963) the space wave radiation pattern of the composite system is given approximately by

$$G_3 = G_1 + \frac{Z_2 - Z_1}{\mathcal{Z}} \cdot \frac{1+R_{v_1}}{2} \int_0^{ka} \frac{X^2}{H^2+X^2} e^{-j\sqrt{X^2+H^2}} J_1(X\cos\psi)\, W(X,Z_2)\, dX \tag{4}$$

The Sommerfeld attenuation function is (5)

$$W(X,Z_2) = 1 - j\sqrt{\pi p}\, e^{-w}\, \mathrm{erfc}(j\sqrt{w}), \quad w = \left(1 + \frac{H}{X}\frac{\mathcal{Z}}{Z_2}\right)^2 P, \quad P = -j\frac{X}{2}\left(\frac{Z_2}{\mathcal{Z}}\right)^2$$

and Z_2 is the composite surface impedance formed by the parallel combination of the surface impedance of the earth (equation 3) and the impedance of the ground screen. If the ground screen is composed of parallel wires or a wire grid, its impedance is given approximately by

$$\frac{Z_s}{\eta} \approx j \frac{d_w}{\lambda} \ln\left(\frac{d_w}{2\pi c_w}\right) \qquad (6)$$

where d_w is the grid spacing and c_w is the wire radius. The grid impedance is inductive and, to be effective in improving low angle radiation, must be much smaller than surface impedance of the ground. Thus the composite surface impedance determining the behavior of the Sommerfeld attenuation function will be inductive with a phase angle approaching 90 degrees. The magnitude and phase of this function shown in Figures 1 and 2 show the effect of the Sommerfeld surface wave as noticed by Wait (1957) for highly inductive ground systems (phase angle over 45 degrees). It is manifest by the attenuation function exceeding unit magnitude and undergoing rapid phase variation.

Satisfactory results can be obtained from equation (4) by setting W equal to one only when the magnitude of the numeric distance P in equation (5) is much less than one. This may often be the case for antenna systems where good radiation below elevation angles of about 10 to 15 degrees is not of primary concern. However, for good performance at lower elevation angles, an extended ground screen must be used and, in the interest of economy, the largest wire spacing consistent with good performance is desirable. In this case, the Sommerfeld attenuation function must be included in equation (4).

The effect of grid spacing on the elevation pattern can be determined initially by considering the composite ground system to be of infinite extent. The patterns shown in Figure 3 are for this case. The interesting result is that for large grid spacings, the radiation pattern of the elevated dipole is poorer than that over unaided ground. The reason for this can be seen when equation (1) is approximated for very small elevation angles

$$G_2 \approx \frac{\cos\psi \sin\psi}{\sin\psi + \frac{Z_2}{\eta}} \left(1 + jkh \frac{Z_2}{\eta}\right) \qquad (7)$$

where the subscript 2 denotes the impedance of the earth as augmented by the wire grid. Since Z_2 is highly inductive, G_2 is reduced as the dipole height h is increased and obtains a minimum at a height depending upon the magnitude and phase of Z_2. The pattern of a finite extended ground screen will tend to be better than those shown in Figure 3 at the lower elevation angles due to diffraction from the end of the screen.

The Sommerfeld attenuation constant should be included in calculations leading to the design and evaluation of economical ground systems for low angle radiation. Elevating the dipole above the ground screen can in some cases result in poorer performance than might be had with a monopole on the ground.

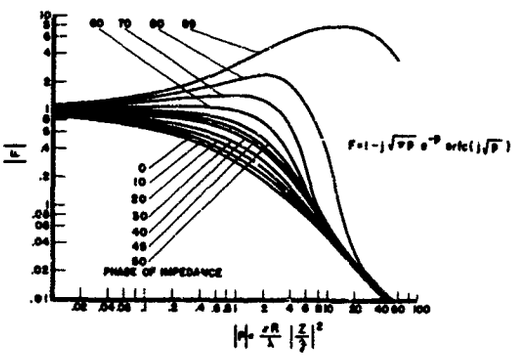

Magnitude of Sommerfeld's
Attenuation Function

Figure 1

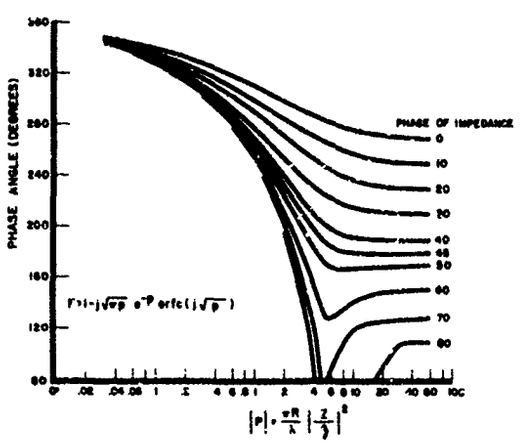

Phase of Sommerfeld's
Attenuation Function

Figure 2

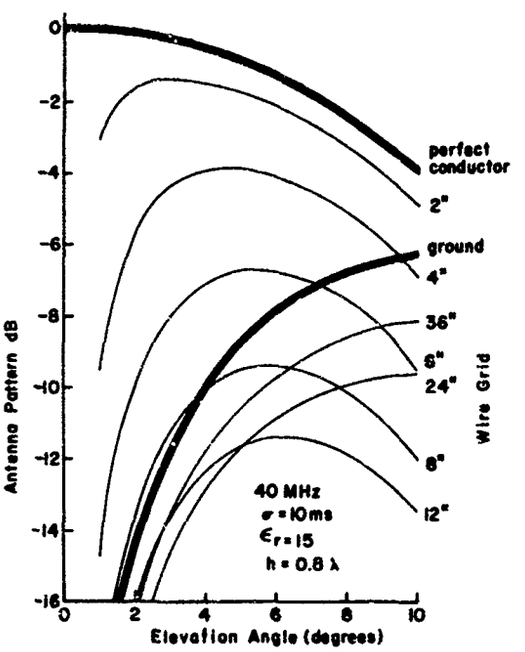

Radiation From An Elevated Dipole
Above A Composite Ground System

Figure 3

References

Wait, J. R. (1967) Radio Science, Vol. 2 (New Series) No. 9, 997-1004.

Wait, J. R. (1963), Electromagnetic Theory and Antennas, Part 2
(Ed. by E. C. Jordan) Pergamon Press, Macmillan, New York, 1079-1097.

Wait, J. R. (1957), J. Research NBS, 59, No. 6, 365-377.

NEAR FIELD SOLUTIONS FOR A VERTICAL HERTZIAN DIPOLE OVER A FINITELY CONDUCTING EARTH

David C. Chang, University of Colorado
James R. Wait, ESSA Research Laboratories, Boulder, Colorado 80302

Various approximations to the exact formal integral representation are considered. A new approximate form is obtained which appears to be valid even when the dipole is near a poorly conducting earth. Numerical comparisons with the exact integral formula verify some of the conjectures.

1. INTRODUCTION

The complete electromagnetic field of a vertical Hertzian electric dipole of current moment $I_o\, ds$, located at a distance z_o above a homogeneous half-space of conductivity σ and dielectric constant ϵ can be determined from a Hertz vector $\vec{\Pi}$ which has only a z component [Baños, 1966]. The formal exact solution for the time-harmonic problem is expressible in the form

$$\vec{E} = \nabla \times \nabla \times \Pi_z \vec{a}_z \; ; \quad \vec{H} = (\sigma - i\omega\epsilon) \nabla \times \Pi_z \vec{a}_z \; ; \tag{1}$$

$$\Pi_z(\rho, z) = \left(-\frac{i\zeta_o I_o\, ds}{4\pi}\right) K(z, z_o; \rho) \; ; \quad K = K^{(p)} + K^{(s)} \; , \tag{2}$$

where the primary influence is

$$K^{(p)}(z, z_o; \rho) = \frac{e^{i k_o [(z-z_o)^2 + \rho^2]^{\frac{1}{2}}}}{k_o [(z-z_o)^2 + \rho^2]^{\frac{1}{2}}} \; , \tag{3}$$

and the secondary influence is

$$K^{(s)}(z, z_o; \rho) = i \int_o^\infty R(a)\, e^{i k_o (z+z_o)[1-a^2]^{\frac{1}{2}}} J_o(k_c \rho a) \frac{a\, da}{[1-a^2]^{\frac{1}{2}}} \; ; \tag{4}$$

$$R(a) = [n^2(1-a^2)^{\frac{1}{2}} - (n^2 - a^2)^{\frac{1}{2}}] / [n^2(1-a^2)^{\frac{1}{2}} + (n^2 - a^2)^{\frac{1}{2}}] \; . \tag{5}$$

Here, $n = [(\sigma - i\omega\epsilon)/(-i\omega\epsilon_c)]^{\frac{1}{2}}$ is the (complex) refractive index of the earth; $\zeta_o = 120\pi$, the characteristic impedance of the free-space; k_o, the free-space wave number and $\vec{a}_z$ is the unit vector along the z direction. In (1)-(5), the time-dependence $e^{-i\omega t}$ is

assumed. Since the secondary influence $K^{(s)}$, in (4), is expressed only in terms of an integration in the Fourier-transform plane α, various asymptotic solutions have been developed for different ranges of observation [Baños, 1966]. Specifically, the knowledge of the field near the vertical axis (i.e., $\rho \simeq 0$) is important in the determination of the self-impedance of the source dipole using the e.m.f. method [Wait, 1962] as well as in the finding of a better approximate solution for the current of a finite linear antenna using the integral equation approach [Chang and Wait, 1969]. In the past, approximate formulas which give the expression in closed forms have been developed for cases when the source dipole is located far away from the earth ($k_o(z + z_o) \geq 10$) [Jasik, 1961], and when the earth is highly conductive [Wait, 1962; Lavrov and Knyazev, 1965]. However, in a more general situation, the source and the observation point are near the ground which, itself, may not be highly conductive. In this case, the available formulas fail to give an adequate description of the physical problem. Motivation for a more general analysis has arisen in connection with the design of HF antennas for special applications and more recently in the remote sensing of the moon's surface.

2. APPROXIMATE SOLUTION NEAR THE VERTICAL AXIS

In the following derivation, we make the assumptions:

$$\rho \ll (z + z_o) \quad \text{and} \quad k_o \rho \ll 1 \,, \quad (6); \qquad |n|^2 \geq 10 \,. \qquad (7)$$

Branch cuts at $\alpha = \pm 1$ and $\alpha = \pm n$, in the expressions (4) and (5) are so chosen that $|\arg (\alpha^2 - n^2)^{\frac{1}{2}}| \leq \pi/2$ and $|\arg (\alpha^2 - 1)^{\frac{1}{2}}| \leq \pi/2$. We now let $z + z_o = d$ and split the integration path in (4) into two parts:

$$K^{(s)}(z, z_o; \rho) = i\left(\int_0^1 + \int_1^\infty\right) R(\alpha)\, e^{ik_o d(1-\alpha^2)^{\frac{1}{2}}}\, J_o(k_o \rho \alpha)\, \frac{\alpha\, d\alpha}{(1-\alpha^2)^{\frac{1}{2}}}$$

$$= i\int_0^1 [n^2\alpha - (n^2 - 1 + \alpha^2)^{\frac{1}{2}}]/[n^2\alpha - (n^2 - 1 + \alpha^2)^{\frac{1}{2}}]\, J_o(k_o \rho [1-\alpha^2]^{\frac{1}{2}}$$

$$\times\, e^{ik_o d\alpha}\, d\alpha + \int_0^\infty [i n^2 \alpha - (n^2 - 1 - \alpha^2)^{\frac{1}{2}}]/[i n^2 \alpha + (n^2 - 1 - \alpha^2)^{\frac{1}{2}}]$$

$$\times\, e^{ik_o d\alpha}\, J_o(k_o \rho [1 + \alpha^2]^{\frac{1}{2}})\, d\alpha \,. \qquad (8)$$

In deriving (8), a change of variables $(1 - \alpha^2)^{\frac{1}{2}} \to \alpha$ and $(\alpha^2 - 1)^{\frac{1}{2}} \to \alpha$ has been applied to the first and second integrals, respectively. In the first integration, $\alpha \leq 1$, we can approximate $(n^2 - 1 + \alpha^2)^{\frac{1}{2}}$ by n, when it is compared with $n^2\alpha$, based on (7). This

approximation apparently is better than $o\left(|n|^{-2}\right)$. On the other hand, the second integrand contributes significantly only when $a \leq 1/(k_o d)$ because of the exponential decay term in the integrand. Again, based upon (7), we can approximate $(n^2 - 1 - a^2)^{\frac{1}{2}}$ by n. Also, because of (6), the Bessel function $J_o(k_o \rho [1 \mp a^2]^{\frac{1}{2}})$ can be approximated by 1. To determine the error involved, we can estimate the remainder or "error" term:

$$\Omega(n, d) = \int_o^{\infty} \left[\frac{in^2 a - (n^2 - 1 - a^2)^{\frac{1}{2}}}{in^2 a + (n^2 - 1 - a^2)^{\frac{1}{2}}} - \frac{ina - 1}{ina + 1} \right] e^{-k_o a d} J_o(k_o \rho [1 + a^2]^{\frac{1}{2}}) da$$

$$\simeq \int_o^{1/k_o d} \left[\frac{in^2 a - (n^2 - 1 - a^2)^{\frac{1}{2}}}{in^2 a + (n^2 - 1 - a^2)^{\frac{1}{2}}} - \frac{ina - 1}{ina + 1} \right] da \quad .$$

It is not difficult to show that this is of the order of $1/|n|^4$ or $1/(|n|^3 k_o^2 d^2)$. Consequently, we can approximate (8) as

$$K^{(s)}(z, z_o; \rho) \cong K_c(z, z_o)$$

$$\cong i \int_o^1 [(na - 1)/(na + 1)] e^{iak_o d} da + \int_o^{\infty} [(ina - 1)/(ina + 1)] e^{-ak_o d} da .$$

This can be recombined to give

$$K_c(z, z_o) = i \int_o^{\infty} \{1 - 2/[n(1 - a^2)^{\frac{1}{2}} + 1]\} e^{ik_o d(1-a^2)^{\frac{1}{2}}} \frac{a\, da}{(1 - a^2)^{\frac{1}{2}}}$$

$$= K_{c_1}(z, z_o) + K_{c_2}(z, z_o) \quad , \qquad (9)$$

where

$$K_{c_1}(z, z_o) = i \int_o^{\infty} e^{ik_o d(1-a^2)^{\frac{1}{2}}} \frac{a\, da}{(1 - a^2)^{\frac{1}{2}}} = \frac{e^{ik_o(z+z_o)}}{k_o(z + z_o)} \quad , \qquad (10)$$

and

$$K_{c_2}(z, z_o) = -2i \int_o^{\infty} \{1/[n(1-a^2)^{\frac{1}{2}} + 1]\} e^{ik_o d(1-a^2)^{\frac{1}{2}}} \frac{a\, da}{(1 - a^2)^{\frac{1}{2}}}$$

$$= \frac{2i}{n} e^{-ik_o d/n} \int_{1+1/n}^{i\infty} e^{ik_o d a'} \frac{da'}{a'}$$

$$= \frac{2i}{n} e^{-ik_o d/n} E_1(-ik_o \bar{r}) \quad ; \quad \bar{r} = (z + z_o)(1 + 1/n) \quad . \qquad (11)$$

where E_1 is the exponential integral of the first order [Abramowitz and Stegun, 1964]. Substitution of (10) and (11) into (9) yields

$$K_c(z, z_o) = \frac{e^{ik_o(z+z_o)}}{k_o(z+z_o)} + \frac{i2}{n} e^{-ik_o d/n} E_1(-ik_o \bar{r}) \quad , \qquad (12)$$

where the complex distance $\bar{r}$ is defined in (11). It is interesting to note that when $|n| \gg 1$ and $k_o d/|n| \ll 1$, (12) becomes

$$K_c(z, z_o) \cong \frac{e^{ik_o(z+z_o)}}{k_o(z+z_o)} + \frac{i2}{n} E_1(-ik_o[z+z_o]) = K_L(z, z_o) \qquad (13)$$

which agrees with the approximate solution obtained by Wait [1962] and Lavrov and Knyazev [1965].

In the limiting case when $|n| \to \infty$, a perfectly conducting ground, only the first term in (12) remains which corresponds exactly to the contribution from an image source below the ground. On the other hand, if $k_o(z + z_o) \gg 1$, using the asymptotic expansion [Abramowitz and Stegun, 1964] of $E_1(x)$, we have

$$K_c(z, z_o) \cong \frac{e^{ik_o(z+z_o)}}{k_o(z+z_o)} - \frac{2}{n} \frac{e^{ik_o(z+z_o)}}{k_o(z+z_o)(1+1/n)}$$

$$\cong \left(\frac{n-1}{n+1}\right) \frac{e^{ik_o(z+z_o)}}{k_o(z+z_o)} = K_J(z, z') \quad , \qquad (14)$$

which agrees with the approximate solution used by Jasik [1961] and Berry and Chrisman [1966]. It corresponds to the reflected portion of a normally incident wave and is the first term of an asymptotic series representation intended for use at higher frequencies [Wait, 1962].

3. DISCUSSION

In order to discuss the various approximate solutions, the exact solution $K^{(s)}$, in (4), which is expressed only in terms of an integration in a complex transform plane α, is evaluated numerically and is compared with our approximate solution K_c in (12); the one used by Lavrov and Knyazev [1965], K_L in (13); and the one used by Jasik [1961] and Berry and Chrisman [1966], K_J in (14). The earth

ground is chosen to have a conductivity of 10^{-2} mho/m and a relative dielectric constant of 10. The operating frequency is set at 100 MHz, giving a refractive index of the earth $n = 3.175 + i\,0.28$ which is not particularly large. Both the amplitude and phase of these solutions are plotted against the normalized distance $k_o(z+z_o)$, i.e., the total distance of the source dipole and the observation point, in Figures 1 and 2. When the source and the observation point are close to the ground (i.e., $k_o(z + z_o) \leq 1.0$), both K_c and K_L agree reasonably well with the exact solution $K^{(s)}$, while K_J does not. Perhaps better than what we assume in the derivation, the error involved is less than 10% so long as $k_o(z + z_o) \geq 0.25$, or the total distance is longer than 0.04 of a free-space wavelength! Farther away from the ground (i.e., $k_o(z + z_o) \geq 1$), the error in K_c is almost negligible. In the same range, however, the error in the approximate solution K_L tends to be worse, while the one with K_J is better. This is due to the fact that the error in K_L is on the order of $1/|n^2|$.

For all practical purposes, K_c can be used adequately for a medium with arbitrary refractive index. If, on the other hand, $|n|$ is large compared with one, K_L is preferred, because of its simplicity for application to impedance calculations of low antennas over a well conducting earth [Wait, 1969].

4. REFERENCES

Abramowitz, M., and I. A. Stegun (1964), Handbook on Mathematical Functions, pp. 228-251, Dover Publications, New York.

Banos, A. (1966), Dipole Radiation in the Presence of a Conducting Half-Space, Pergamon Press, Oxford.

Berry, L. A., and M. E. Chrisman (Sept. 1966), Linear high frequency antennas over a finitely conducting spherical earth, ESSA Tech. Report No. IER8-ITSA8.

Chang, D. C., and J. R. Wait (1969), Theory of a finite, tubular, vertical dipole antenna above an infinite dissipative half-space (to be published).

Jasik, H. (ed.) (1961), Antenna Engineering Handbook, McGraw-Hill Book Co., New York.

Lavrov, E. A., and A. S. Knyazev (1965), Prizemnye i Podzemnyye Antenny, Sovetskoye Radio, Moscow.

Wait, J. R. (Sept.-Oct. 1962), Possible influence of the ionosphere on the impedance of a ground-based antenna, J. Research NBS, vol. 66D, No. 5, 563-569.

Wait, J. R. (1969), Impedance of a Hertzian dipole over a conducting half-space, Vol. I, pp. 89-94, Proceedings of the Conference on Environmental Effects on Antenna Performance (ed. J. R. Wait), Boulder, Colorado, July 14-18, 1969.

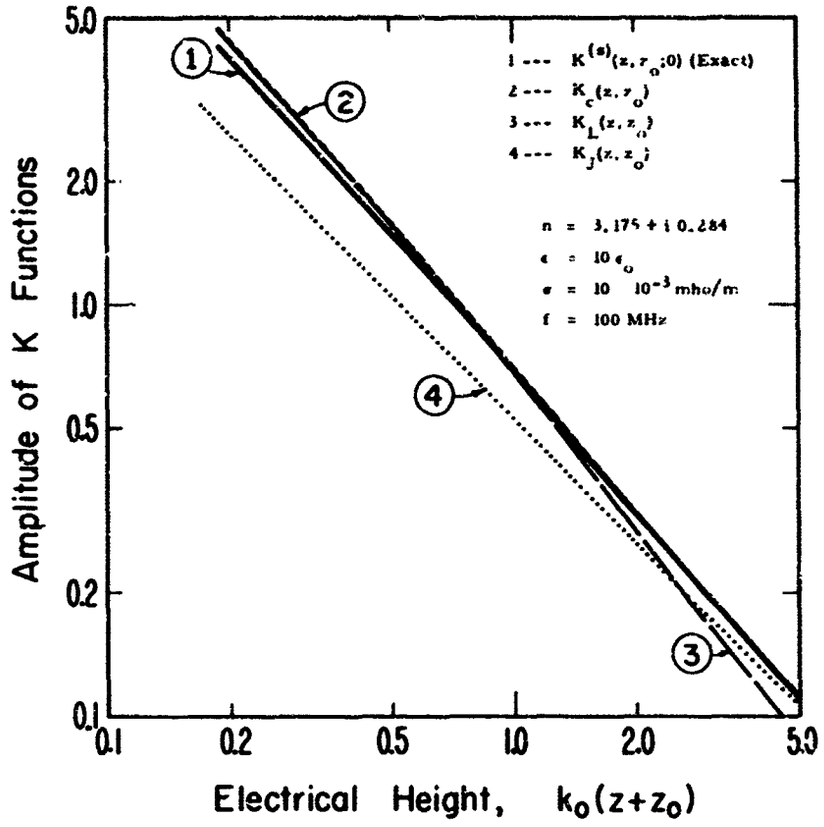

Fig. 1 -- Amplitude of K functions

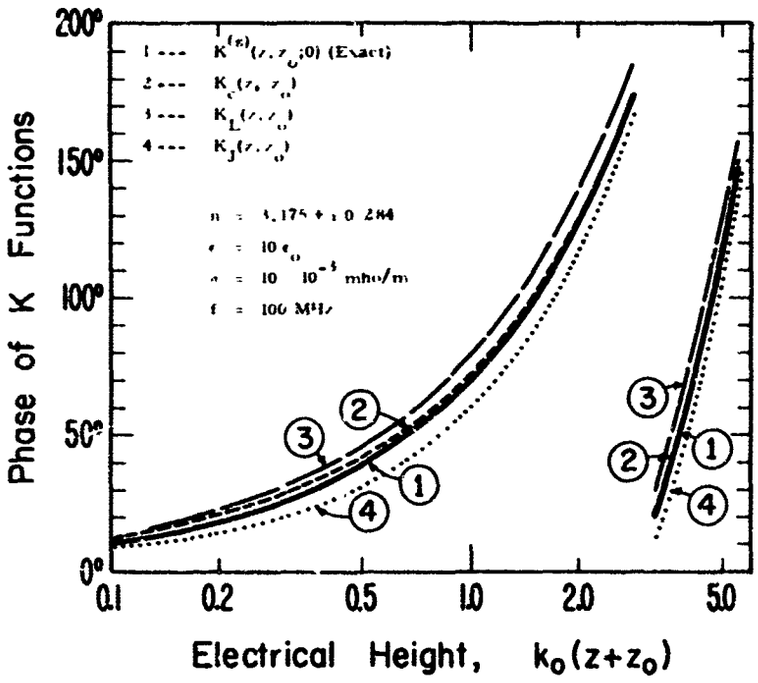

Fig. 2 -- Phase of K functions.

PULSE PROPAGATION INTO THE GROUND

by
Walter L. Curtis
The Boeing Company
Seattle, Wash. 98124

Abstract

The transmission of a delta function plane wave into a plane earth is determined. The complex dielectric properties of the ground are modeled using an empirical relationship that exhibits a typical variation of conductivity with frequency. Numerical results are presented for both high and low loss grounds as a function of depth.

Introduction

The subject of pulse propagation into the ground has continued to be of general interest because of the need to analyze the effects on electronic systems of high amplitude electromagnetic transients. Such transients might be produced by lightning or a nuclear burst. The purpose of this paper is to gain some insight into the shielding properties of the earth against pulses. Wait[1] has considered this problem in considerable detail and gives an excellent summary of previous work by others. More recently King and Harrison[2] investigated this problem using a Gaussian-shaped pulse. The problem considered here is that of a delta function plane wave normally incident on a plane earth. In this way, the resulting pulse at different depths will exhibit features due to the lossy earth which are not masked by frequency limitations of the source pulse. In addition, the results for any other incident pulse shape is just the convolution of the incident pulse and the result given here. Previous investigations by others have assumed the earth to have a conductivity that is constant for all frequencies. The present analysis uses a model for conductivity that more closely matches experimental measurements.

Analysis

The problem is solved by finding the steady state solution and then taking the inverse transform numerically on a computer to find the pulse shape at different depths in the ground. As shown in Figure 1, the transmitted wave is in the earth. It is assumed that the earth has a permeability of free space and a complex relative dielectric constant, $\bar{\epsilon}_g$, given by

$$\bar{\epsilon}_g = \epsilon_g - j\frac{\sigma}{\omega \epsilon_o}$$

where ϵ_g, is the usual relative dielectric constant which as a value around 8 to 25 depending on the moisture content, σ is the conductivity of the ground, ω is 2π times frequency, and is the permittivity of free space. Normally the conductivity is assumed constant with the frequency, but measurements on typical soil show considerable variation with frequency--especially at higher frequencies where it tends to be directly proportional to frequency. This is well known for low loss dielectrics where the loss tangent defined as $\sigma/\omega\epsilon_o\epsilon_g$ is usually assumed

independent of frequency. To account for this, the following model for $\bar{\epsilon}_g$ was used in this study:

$$\bar{\epsilon}_g = \epsilon_g - j\left(\frac{\sigma_g}{\omega \epsilon_o} + \epsilon_g L_g\right)$$

where σ_g is the usual low frequency conductivity and typically has values from .002 to .02 mhos per meter and L_g is the high frequency loss tangent. There is little information available on values of for different soils but measurements on a soil sample from the Seattle area show a value of 0.5. The above model is good for all practical purposes but is not too convenient when extended to the entire complex frequency domain. An alternative model that overcomes this and still has about the same variation with real frequencies is

$$\bar{\epsilon}_g \quad \epsilon_g - j\sqrt{\left(\frac{\sigma_g}{\omega \epsilon_o}\right)^2 + (\epsilon_g L_g)^2}$$

The steady state solution for the electric field in the earth, $E_t(\omega)$, in terms of the incident field, $E_i(\omega)$, is

$$E_t = T\, e^{-\gamma d} E_i$$

where T is the transmission coefficient of the earth-air interface, γ is the propagation constant of the earth and d is the depth. T and γ are well known and can be written in terms of the complex dielectric constant as

$$T = \frac{2}{1 + \sqrt{\bar{\epsilon}_g}}$$

and

$$\gamma = \frac{j\omega}{3\times10^8}\sqrt{\bar{\epsilon}_g}$$

Assuming the incident pulse in time is an unit amplitude delta function, then $E_i(w) = 1$. The field in the earth as a function of time and depth is then the inverse transform of E_t, i.e.,

$$e_t(t,d) = \frac{1}{2\pi}\int_{-\infty}^{\infty} E_t\, e^{j\omega t}\, d\omega = \frac{1}{\pi}\int_{-\infty}^{\infty} \frac{e^{-\gamma d + j\omega t}}{1 + \sqrt{\bar{\epsilon}_g}}\, d\omega$$

Results

The above transform has been evaluated numerically on a computer. The results for two different conductivities and several different depths are shown in Figures 2 and 3. Figure 2 shows the results for $\sigma_g = .002$, $\epsilon_g = 10$ and $L_g = .5$ which is representative of a moist low loss soil found in the Seattle area. At all depths, the pulse is characterized by a positive high amplitude narrow pulse followed by a low amplitude slowly decaying negative tail. The peak of the pulse shows a delay corresponding to that expected for a wave propagating to the same depth in loss less dielectric. It should also be noted that the positive pulse appears almost symmetrical about its peak. Figure 3 shows the results for only a change in the low frequency conductivity, i.e., $\sigma_g = .02$, $\epsilon_g = 10$ and $L_g = .5$. This is representative of a soil with about the same moisture content as before, but with a greater amount of ionizing material present. It is not known how L_g might change so it was left fixed for this example. The same pulse characteristics are observed but with much lower amplitude. At depths less than

2 meters, the positive pulse is still quite symmetrical and has a time delay the same as before. However, at greater depths the pulse becomes skewed and its peak occurs at a greater time delay. For example, at a depth of 10 meters the peak occurs at about 250 nanoseconds instead of 100 as before. In addition, the peak amplitude decays much more rapidly with depth than it did with the lower conductivity.

Conclusions

The impulse response for propagation into the ground has been found and typical examples shown. These results show the limiting values of pulse width and rise time for any source. For example, at a depth of 1 meter the maximum rise time and minimum pulse width will be on the order of a few nanoseconds while at 10 meters depth it will be on the order of 50 to 100 nanoseconds. The results for any other incident pulse shape can be found by convolution with the results presented here.

References

1) J. R. Wait, Appl. Sci. Rev., B8, pp 21?-254, (1960)
2) R. W. P. King, and C. W. Harrison, Jr., J. Appl. Phy., V.39, No. 9, pp 4444-4452, (1968)

FIGURE 1: PULSE PROPAGATION INTO THE GROUND

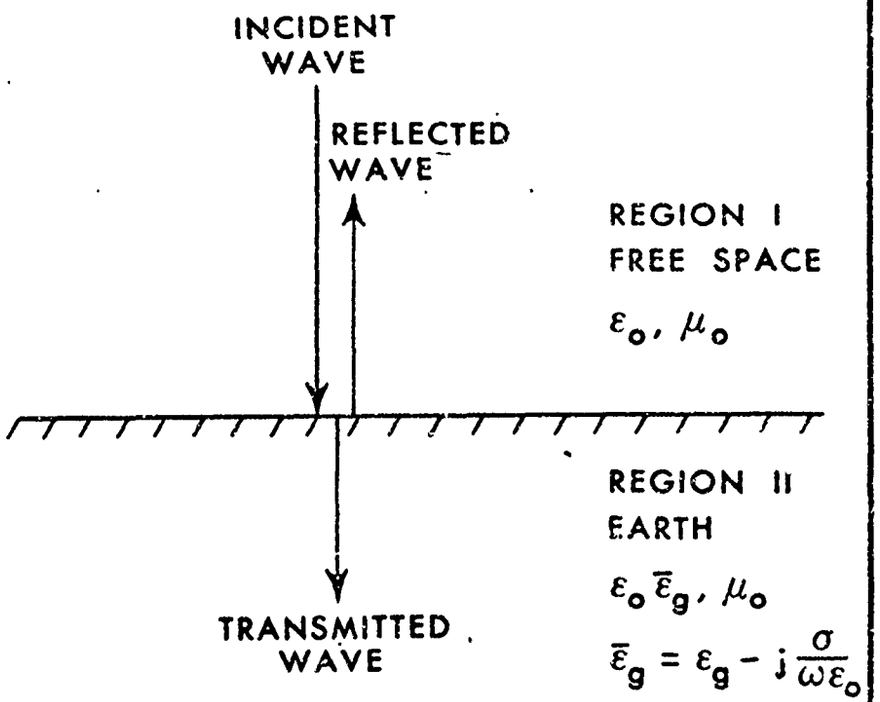

● STEADY-STATE SOLUTION

$$E_t = T\, e^{-\gamma d} E_i$$

WHERE $T = \dfrac{2}{1 + \sqrt{\bar{\varepsilon}_g}}$

$$\gamma = j\frac{\omega}{c}\sqrt{\bar{\varepsilon}_g}$$

$$\bar{\varepsilon}_g = \varepsilon_g - j\left(\frac{\sigma_g}{\omega\varepsilon_o} + \varepsilon_g L_g\right)$$

ε_g = RELATIVE DIELECTRIC CONSTANT OF THE GROUND

σ_g = CONDUCTIVITY OF THE GROUND

L_g = HIGH FREQUENCY LOSS TANGENT OF THE GROUND

● PULSE SOLUTION

$$E_i = 1$$

$$e_t(t, d) = \frac{1}{2\pi}\int_{-\infty}^{\infty} E_t\, e^{j\omega t}\, dw$$

$$= \frac{1}{2\pi}\int_{-\infty}^{\infty} \frac{2\, e^{-\gamma d + j\omega t}}{1 + \sqrt{\bar{\varepsilon}_g}}\, dw$$

FIGURE 2: DELTA FUNCTION RESPONSE OF LOSSY EARTH AS A FUNCTION OF DEPTH

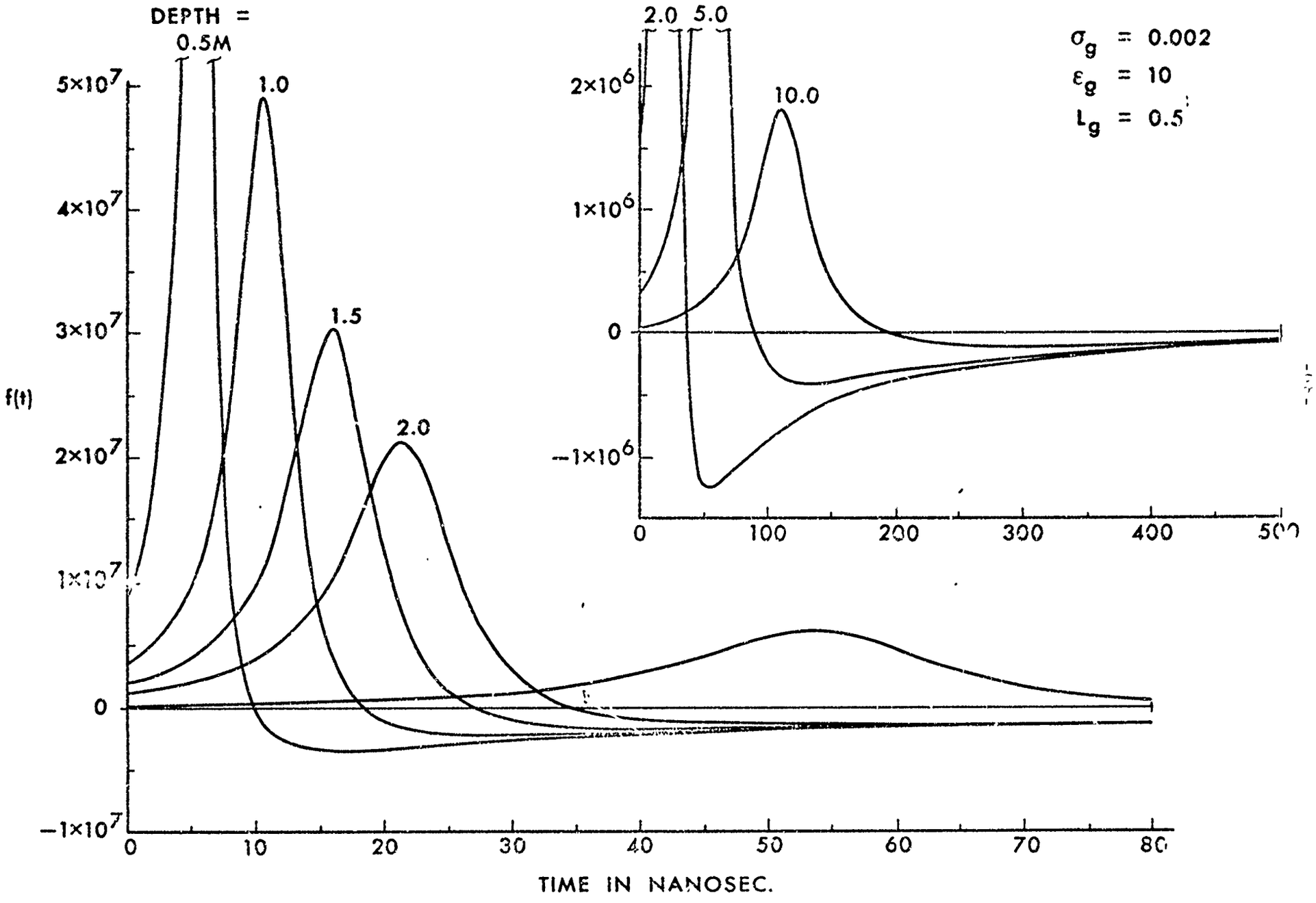

FIGURE 3: DELTA FUNCTION RESPONSE OF LOSSY EARTH AS A FUNCTION OF DEPTH

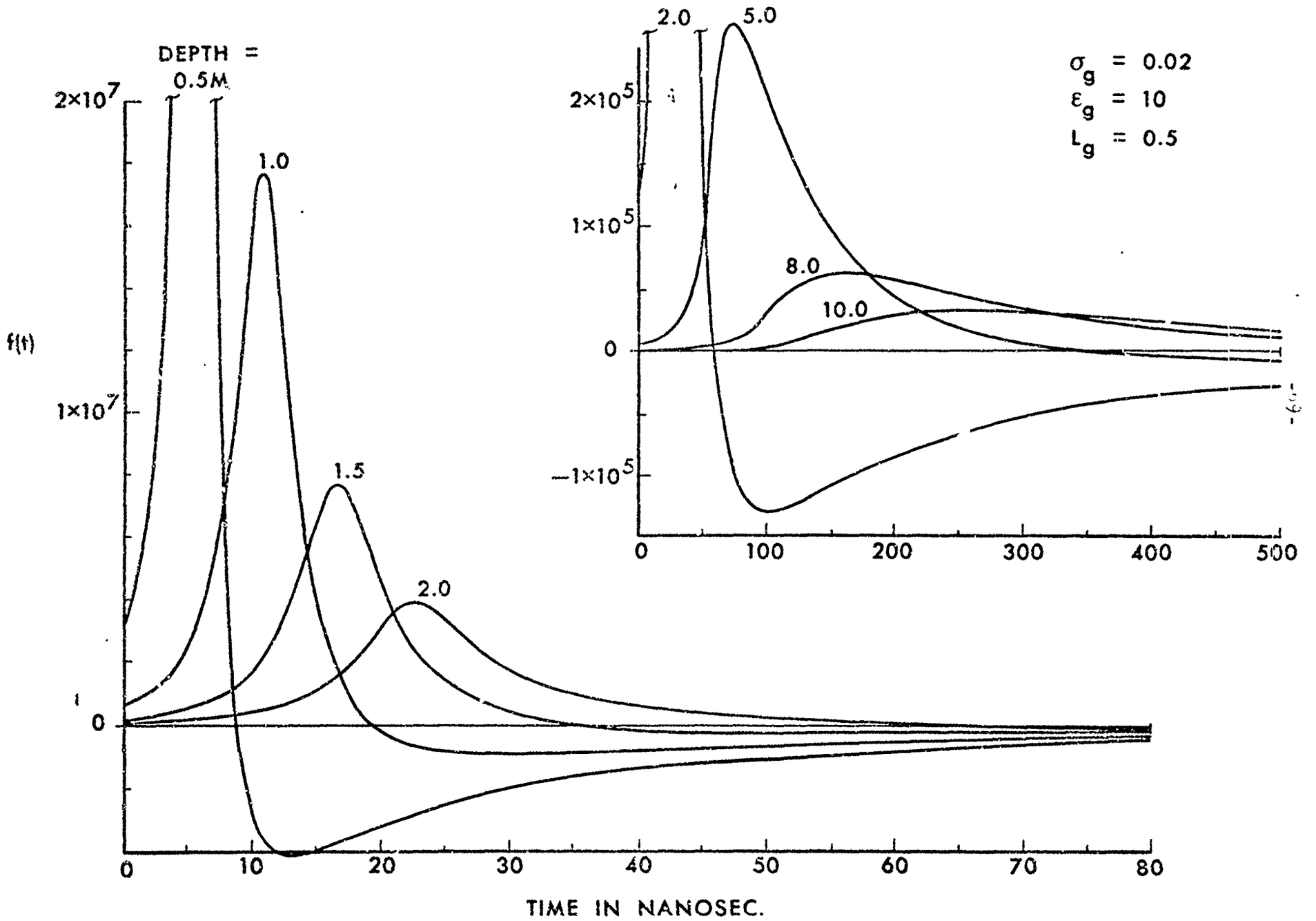

PERFORMANCE OF VALLEY SPANNING VLF ANTENNAS BASED ON ELECTROMAGNETIC MODELLING

A. N. Smith and E. J. Jackson
Westinghouse Georesearch Laboratories
Boulder, Colorado

Passive electrical characteristics of numerous transmitting antenna configurations, similar to valley-spanning prototypes of interest for moderate power application in the OMEGA Navigation System, were measured for models on alterable valleys. Resulting parametric curves and modelled near-zone field distributions plus soil conductivities of candidate sites enable accurate prediction of power and bandwidth capability for cost studies.

The communicator/navigator generally hands his problem to the communications systems engineer in the form of a desired reliability (availability in some noise environment) in a coverage area for some signal format yielding a specified information rate. These requirements filter down to the antenna system designer as a minimum radiated power (P_r) at some frequency (f) or range thereof in some specified minimum bandwidth (B_{as}). Present-day technology supplies an upper limit on operating voltage, V_i, and previous generalized studies give a range of desirable efficiency η_{as} (and hence input power P_{as}) functionally related to radiated power level so that costs will probably be near a minimum. For the OMEGA System, the respective values have been established as $P_r \geq 10$ kW, $10.2 \leq f \leq 13.6$ kHz, $B_{as} \geq 10$ Hz @ 10.2 kHz; $V_i \leq 250$ kV, $P_{as} \leq 150$ kW; $\eta_{as} \geq 6.7\%$.

At VLF, where transmitting antennas are almost unavoidably electrically short, these six variables and four others are related by the four equations given below (applicable in general to any simple tuned circuit of lumped parameters and specifically to the one illustrated):

$$P_r = 6.95 \times 10^{-13} C_0^2 h_e^2 V_t^2 f^4 \equiv I_a^2 R_r$$

$$B_{as} = 1.108 \times 10^{-13} C_0 h_e^2 \eta_{as}^{-1} f^4 \equiv f/Q_{as}$$

$$P_{as} = P_r/\eta_{as} \qquad \text{(MKSQ units)}$$

$$V_t = [\,1 - F(f/f_0)^2\,]\, V_i \quad (f_0 = (2\pi \sqrt{L_a C_0})^{-1})$$

The remaining four quantities C_0 (electrostatic capacity), f_0 (self-resonant frequency), V_t (mean toploaad voltage) and h_e (effective height) are thus determined if the original six are fixed; this is usually not the case, but certain ones are allowed to take on values below well-defined upper limits, so that cost- and performance-trade comparisons can be carried out for several candidate sites as well as for several configurations in final single selection. A significant

aspect of the trade to minimize cost is the balancing of various possibilities for tuning helix resistance R_h against ground system resistance R_g, which are the two major loss components, always in regard to the condition of antenna system efficiency. In performance trading, one finds besides that specification of both power and bandwidth at more than one frequency in the operating band overdetermines the system. Thus one specifies minimum acceptable for each at that frequency it is hardest to attain; e.g., for OMEGA P_r at 10.2 kHz, and B_{as} (under an earlier concept) at 13.6, but not both at both frequencies. V_i must be corona free.

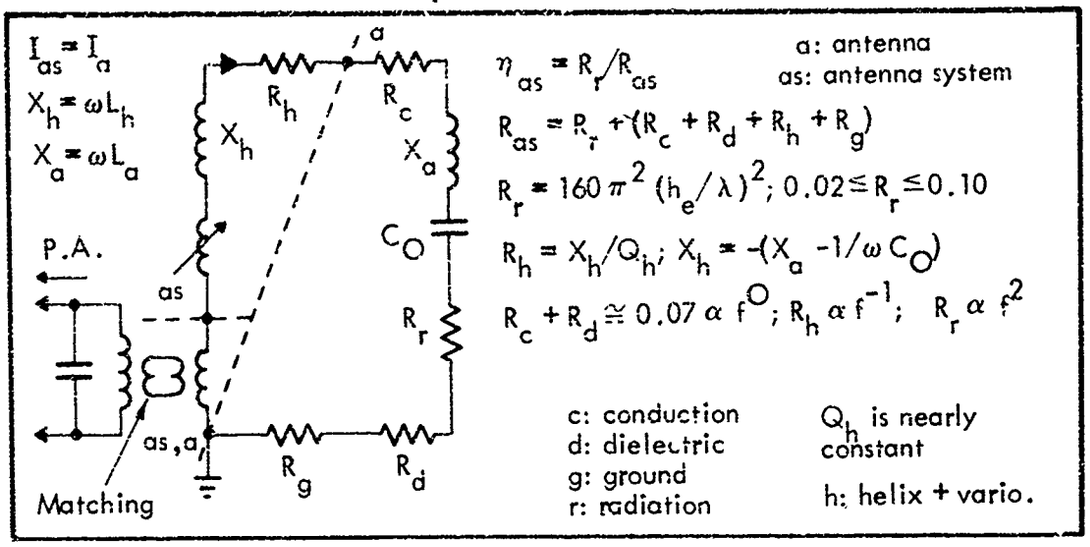

The environment is significant to performance determination in two respects: geometrical, relating to C_0, h_e (capacity centroid), and f_0 (distance relative to wavelength over which charge must be carried to components of C_0); and electrical, relating to the nature of the impedance plane, losses in which must be controlled by design of some ground system so as to simultaneously permit attainment of P_r and B_{as}. Since the cost optimization process must consider both fixed (installed) as well as operating (capitalized over stated period of years), some latitude is offered to charge against site modification for efficiency (such as elevating spans on towers) versus more transmitter and prime power.

The power, bandwidth, voltage, and efficiency figures given above imply, through the fundamental equations, that we look for sites yielding effective heights for OMEGA applications, from 100 to 200 meters and capacity from 0.050 to 0.030 μfds; the inverse relationship of capacity and inductance usually results in f_0 between 25 and 40 kHz, so that V_t is within 10% of V_i at the low end of the band. Reactances to tune are then such as to require helix Q's between 1500 and 3000 in order to hold R_h to values such that the residual ground system loss R_g can be obtained with reasonable installation.

The valley-spanning approach to obtain these figures is advantageous only because of the relatively modest power and efficiency necessary in the OMEGA system, since the very presence of the ridges used as

supports for the spans precludes economic installation of an extremely elaborate ground system and also results in high field (both H- and E- fields) concentrations in locations difficult to reach with a wire grid. A high power, high efficiency installation requires the span supports to be such as not to get in the way. Displaying the loss budget computation for the ground system in the form

$$R_g = (R_H + R_E)_{inside} + (R_H + R_E)_{outside} + R_{wires} + R_{termination}$$

in which

$$R_H + R_E = \mathrm{Re}\,(1/I_a^2) \int [\eta\,(H_0)^2 + \frac{h}{\sigma}\,\omega^2 \epsilon_0^2\, E_z^2]\, dA \qquad \begin{matrix} \text{inside: } a_i \text{ to } a_o \\ \text{outside: } a_o \text{ to } 1/\beta_0 \end{matrix}$$

shows the critical role that field distributions play in making performance predictions have to do with loss budget. The most convenient way to arrive at these is through scale modelling.

Capacity can be calculated rather easily to a fair degree of accuracy, because its logarithmic dependence on the ratio h/a makes this rather insensitive to inaccuracies in knowledge of height; not so with effective height, since it is a summation of production of local height with capacity. Thus again modelling by analogue methods is of great aid in accurate performance predictions.

Some 60 configurations for valley-spanning antennas for the OMEGA application have been modelled at WGL, at 480/1 scale in air. 26 more were done for one of the high-power communication stations. Another 1100 variants were studied in an electrolytic tank. The results generally show that the required C_0 and h_e for OMEGA power and efficiency can be obtained with from 6 to 4 spans over valleys 7,000 or more feet wide, with aspect ratio 4/1, without use of support towers, and with ground systems of the order of 2,000 foot radius if the conductivity is 10^{-3} mhos per meter or higher. Extremely high soil conductivity is not advantageous if there is a large seasonal decrease in effective conductivity (e.g. snow) for which provision must be made in ground system design to meet radiated power requirement because danger exists that during high-conductivity portion of the year bandwidth cannot be met without artifically supplying extra loss. From field strength pattern measurements, no evidence exists that valley-span antennas of the proportions studied exhibit any characteristics of slots, as was one time discussed.

Work performed under sponsorship of OMEGA Project Office, PM-9, through Chesapeake Division, Bureau of Yards & Docks, U. S. Navy, under Contract N62477-68-C-0940.

SURFACE WAVE CONTRIBUTIONS TO THE BACKSCATTERING FROM LARGE, HIGH-DENSITY DIELECTRIC SPHERES.

BY

M. A. PLONUS AND H. INADA
DEPARTMENT OF ELECTRICAL ENGINEERING
NORTHWESTERN UNIVERSITY
EVANSTON, ILLINOIS

An application of the Watson transformation to the Mie series divides this solution in geometric optics and diffracted fields. It will be shown that the geometric optics fields are smaller than heretofore assumed. The diffracted field comes from two types of surface waves. One of these is the dominant contributor to the backscatter. Numerical results for values of ka from 5 to 20 will be presented.

The following figure shows the backscattering from a dielectric sphere as calculated from the Mie series. The top continuous curve shows the results which are obtained when the geometrical optics method is applied to the sphere [Atlas and Glover, 1962]. There is little agreement with the exact results. After an application of the Watson transformation to the Mie series an integral can be split off which can be identified with the geometric optics contribution since it comes from the lit region of the sphere [Inada and Plonus, 1969]. The lower curve in Fig. 1 shows the results which were obtained from this contribution. The geometric optics contribution for this particular range of ka clearly cannot account for the major backscatter.

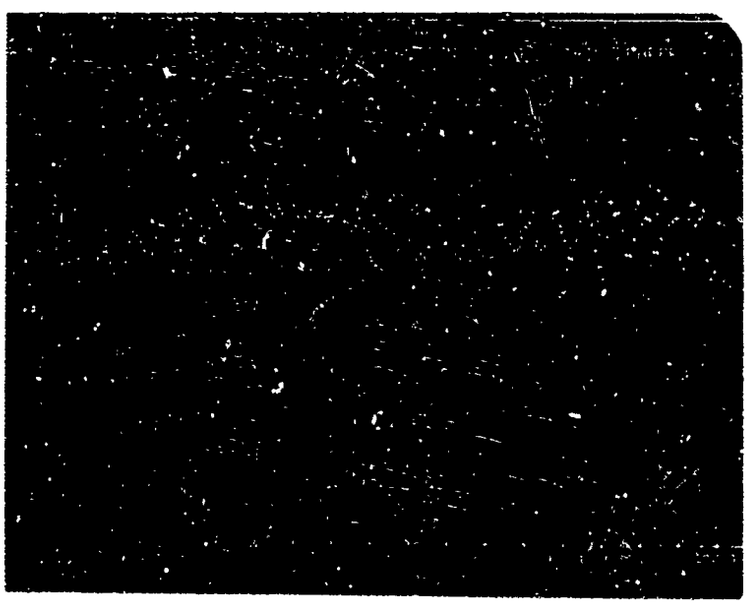

Fig. 1. Backscattering Cross section curves from the Mie Series and from Geometric Optics.

The Watson transformation yields other terms which are residue contributions and can be identified with surface waves. These waves can travel about the sphere many times. Fig. 2 shows the residue contribution of one pole (mode 1). N=1 is a wave that has travelled around the back of the sphere once, N=2 is a wave that has travelled twice, etc.

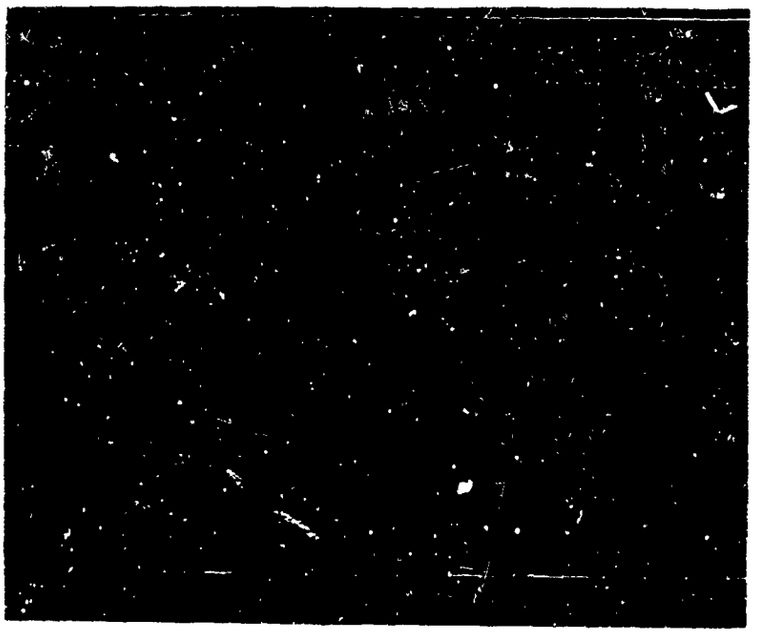

Fig. 2. Surface Wave Contribution to Backscattering (dominant pole only).

Once the existence of the surface waves has been established, it is not difficult to see that interference between waves which travelled around once, twice, etc. can exist.

The next figure shows the interference curves for all N for three separate poles (l=1,2,3). Let us examine the resultant curve due to the first pole. Up to ka=7 we have a simple periodic curve which when we re-examine Fig. 2 could be the interference between N=1 and N=2. For ka > 7, the l=1 curve becomes doubly periodic which means N=3 is coming into play. Similar observations can be made for the other pole contributions. Notice that for higher l's the corresponding residue contribution has a smaller peak which occurs at larger ka.

Fig. 3 Surface Wave Contribution to Backscattering showing interference between surface waves of N=1,2,3.

The next figure shows that the surface waves are the major contributors to the backscattering. The small periodicity of $ka \approx .7$ can be explained as being due to interference between surface waves which have gone around the sphere a number of times, whereas the large periodicity of $ka \approx 10$ seems to be due to the contribution of the different poles ($l=1,2,\cdots$) which peak at different values of ka.

Fig. 4. Backscattering Curves showing that the surface waves are the dominant contributors to the total backscatter.

H. Inada and M. A. Plonus (1969), "Numerical Results for Backscattering from Large, High-Density Dielectric Spheres", Proc. IEEE, 57, No. 6, 1192-1193.

D. Atlas and K. M. Glover (1962), "Backscatter by Dielectric Spheres with and without Metal Caps", Proc. Inter-Disciplinary Conf. Electromagnetic Scattering (Pergamon Press, New York), 213-236.

MICROWAVE TRANSMISSION MEASUREMENTS THROUGH RADIANTLY HEATED ANTENNA WINDOWS

A. C. Lind, J. F. Fox
McDonnell Douglas Astronautics Company - Eastern Division

and

D. Q. Durant
McDonnell Aircraft Company
St. Louis, Missouri

A new technique has been developed which allows continuous microwave transmission measurements to be made through reentry vehicle antenna windows while they are subjected to high heat fluxes. The antenna window specimen is radiantly heated by a cylindrical graphite heating element which produces a heat flux of approximately 280 Btu/ft^2-sec. Unique data is shown on the degrading effect of moisture absorption in slip-cast fused silica.

1. Introduction - During reentry, the antenna window of a missile is subjected to very high heat fluxes. Communication system performance is degraded, not only by the plasma that forms around the vehicle, but also by losses induced in the window material as a result of the severe heating. Dielectric constant and loss tangent data is generally not available in the temperature region of interest, that is, greater than 3,000°F. As a result, others (Mead, 1967; Cetaruk, 1968) have performed microwave transmission measurements through antenna window samples that have been heated with a plasma jet. This type of measurement provides a qualitative estimate of antenna window performance during reentry. In the plasma jet test, the transmission measurement is possible only after plasma jet shutdown because of the interference effects of the plasma during the heating cycle. The interpretation of such results can be misleading if transient material effects are important or if the window cools significantly in the finite time required to shut down the plasma jet. The facility described in this paper employs radiant heat and is designed so that the heating element does not interfere with the microwave measurement. Continuous microwave data is obtained during the entire heating and cooling cycles.

2. Description of Facility - A schematic of the facility is shown in Figure 1. The antenna window specimen is supported in a water cooled, open-ended X-band waveguide that transmits to a receiving antenna located several feet away. The waveguide is located at the base of a tubular, electrically heated (45 kW), graphite element that is used to radiantly heat the window specimen. The system is purged with nitrogen to minimize burning of the graphite element which is at a temperature of approximately 5,000°F. A loose fit between the specimen and waveguide results in poor heat transfer and minimizes cooling of the window by the waveguide. The specimen also protrudes slightly out of the waveguide to insure a uniform surface temperature. The tubular heating element concept allows continuous microwave transmission during the heating cycle.

The waveguide assembly is interchangeable with an identical unit containing a water-cooled copper calorimeter to obtain heat flux calibrations. A typical heat flux profile is shown in Figure 2. A steady state heat flux near 280 Btu/ft^2-sec is reached after approximately 30 seconds. The test time is arbitrary, and for the data shown here was 2 minutes; this test time is sufficient to produce a significant melt layer on slip-cast fused silica window specimens.

3. Microwave Transmission Data - The received microwave signal is recorded on an X-Y recorder which is calibrated with a precision attenuator before each test in terms of db loss. Directional couplers are employed in the transmission leg to allow visual monitoring of the signal generator output and reflected power level during the test. Typical transmission data at a frequency of 10 GHz are shown in Figure 3 for slip-cast fused silica. The top trace was recorded with no window in the waveguide, and demonstrates the insignificant effect of the heating element on the microwave measurement. Two specimens taken from the same block of material were tested at the heating rate shown in Figure 2. One specimen was dried in a low temperature oven and then stored in a desiccator prior to testing. The other specimen contained a normal amount of moisture absorption. The dry specimen showed a gradual decrease in signal level reaching a steady state attenuation of 0.5 db. The specimen containing the moisture showed a sharp decrease in signal level corresponding to an attenuation of 7 db and then gradually returned to the attenuation level of the dry specimen. These test results demonstrate the importance of continuously monitoring transmission measurements during high temperature testing. No significant change in reflected power level was observed during either test. This is in contrast to the results of plasma jet tests where mechanical erosion of the window occurs, causing detuning changes that are difficult to take into account during data reduction.

4. Summary - The technique presented here is an improvement over other methods since it allows continuous microwave measurements during the entire heating cycle. The data presented for slip-cast fused silica demonstrates the importance of continuous measurements, and shows the degrading effect of moisture absorption during the initial heating of the material, which could affect communication system performance in a reentry situation. Also, this technique does not produce mechanical erosion of the window, so that the measurement of window material losses are not masked by detuning effects.

REFERENCES

K. E. Mead (1967), "Further Experimental Study on Transmission of Microwave Energy Through Dielectric Materials Exposed to a High Heat Environment," Sandia Laboratory Report SC-WD-67-236.

W. K. Cetaruk, T. J. O'Connor (1968), "Antenna Window Behavior in a Simulated Reentry Heating Environment," Proc. of the USAF Avionics Laboratory - Georgia Institute of Technology Symp. on Electromagnetic Windows, AFAL-TR-68-97, Vol. III.

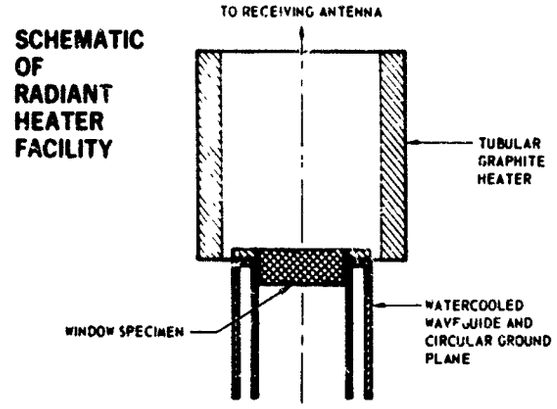

FIGURE 1

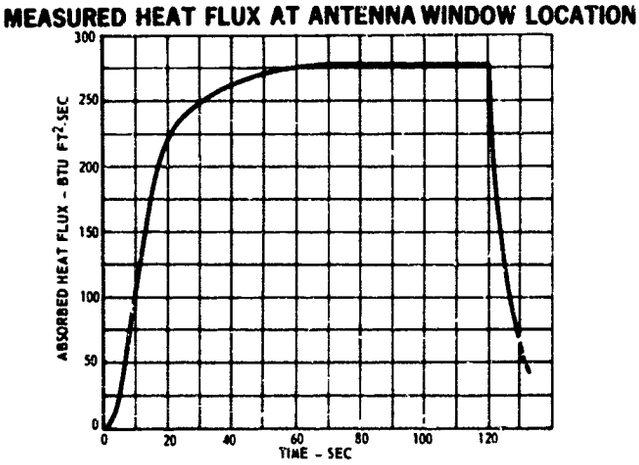

FIGURE 2

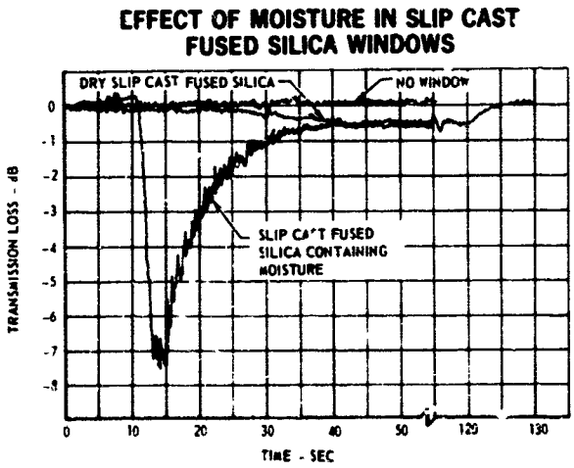

FIGURE 3

OPTIMUM FREQUENCY FOR A VLF TELECOMMUNICATION SYSTEM USING BURIED ANTENNAS

R. Gabillard, J. Fontaine, P. Degauque
University of Lille, France

Abstract

This paper is a study of the best choice of frequency for a VLF telecommunication system between buried receiving and transmitting antennas. The efficiency of such a system depends on numerous parameters. We show that there is an optimal direction of the embedded antennas which is different according to we use a frequency higher or lower than a critical one, f_c. We also show that the electric field E_r increases toward a maximum value at a frequency f_{opt}. We give the expressions of f_c and f_{opt}. The ratio of the electric field E_r at the optimal frequency to the electric field E_φ at ELF brings into evidence the interest of the choice of the optimal frequency to establish a VLF subsurface communication.

PROPAGATION BETWEEN PARALLEL IMPEDANCE SURFACES

R. B. Dybdal

The Aerospace Corporation, El Segundo, California

The modal structure of a parallel plate waveguide characterized by impedance boundary conditions is analyzed. A formal solution for both parallel and perpendicular modes may be obtained and impedance loci are given for the lossless equal impedance case.

The propagation between parallel impedance surfaces characterized by impedance boundary conditions is analyzed. This problem was first considered by Barlow and Cullen [1953] and later by Barlow [1965] and Wait [1967]. The geometry is depicted in figure 1. The modal structure

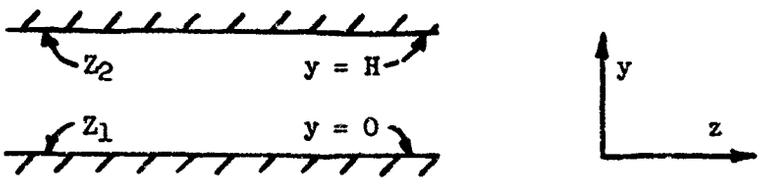

FIGURE 1. Geometry of Parallel Plate Configuration

may be formulated from Hertzian potentials [Collin, 1960] and a suitable potential function is

$$(1) \quad \psi_{H,E} = \left(e^{-p_o y} + R_{H,E}\, e^{-p_o(H - y)}\right) e^{-j(k^2 + p_o^2)^{\frac{1}{2}} z}$$

The subscript H goes with perpendicular polarized modes; the subscript E, with parallel polarized modes. Real values of p_o correspond to bound surface wave type modes; imaginary values, to plane wave components bouncing between the surfaces.

The solution for the parameters p_o and $R_{H,E}$ for arbitrary impedance values has been obtained and the orthogonality relations reveal modal energies are coupled in the lossy case [Dybdal, 1968]. For equal value impedances, R_E and R_H reduce to ± 1 simplifying the modal solution. The properties of this case are summarized in table 1. Impedance loci may be developed for the lossless case. Note that losses make p_o complex. The impedance loci are depicted in figures 2 and 3 and p_o is obtained from the intersection of the loci and a horizontal line drawn at the surface impedance value. The usual impedance requirement for bound surface wave modes is demonstrated here; i.e. inductive impedance is required for bound perpendicular modes; capacitive, for bound parallel modes. The cutoff condition for bounce modes is $|p_o| = k$ and is shown in the loci for a waveguide 1.3 wavelengths in height.

TABLE 1. Mode Characteristics for the Equal Impedance, Lossless Case

Mode	$R_{E,H}$	Nature of p_o	Impedance Value	Nature of Impedance
			Perpendicular Modes	
A	+1	real	$j\frac{\lvert p_o\rvert}{\omega\epsilon}\tanh\frac{\lvert p_o\rvert H}{2}$	inductive
B	+1	imaginary	$-j\frac{\lvert p_o\rvert}{\omega\epsilon}\tan\frac{\lvert p_o\rvert H}{2}$	capacitive-inductive
C	-1	real	$j\frac{\lvert p_o\rvert}{\omega\epsilon}\coth\frac{\lvert p_o\rvert H}{2}$	inductive
D	-1	imaginary	$j\frac{\lvert p_o\rvert}{\omega\epsilon}\cot\frac{\lvert p_o\rvert H}{2}$	inductive-capacitive
			Parallel Modes	
E	+1	real	$-j\frac{\omega\mu}{\lvert p_o\rvert}\coth\frac{\lvert p_o\rvert H}{2}$	capacitive
F	+1	imaginary	$j\frac{\omega\mu}{\lvert p_o\rvert}\cot\frac{\lvert p_o\rvert H}{2}$	inductive-capacitive
G	-1	real	$-j\frac{\omega\mu}{\lvert p_o\rvert}\tanh\frac{\lvert p_o\rvert H}{2}$	capacitive
H	-1	imaginary	$-j\frac{\omega\mu}{\lvert p_o\rvert}\tan\frac{\lvert p_o\rvert H}{2}$	capacitive-inductive

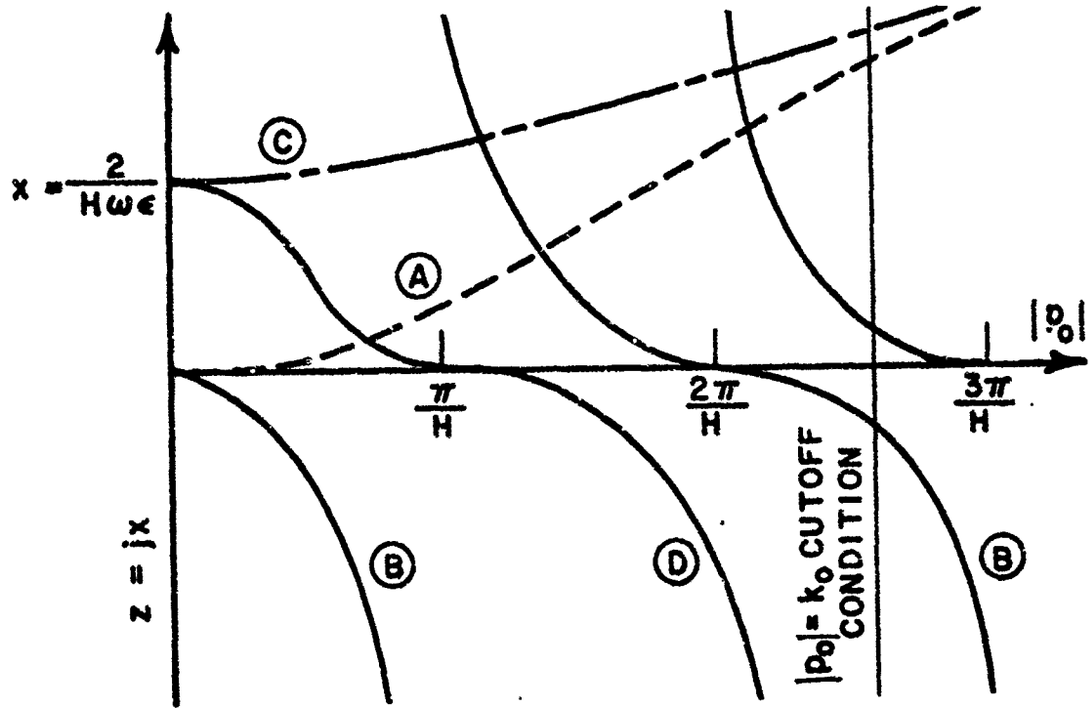

FIGURE 2. Impedance Loci for Perpendicular Modes

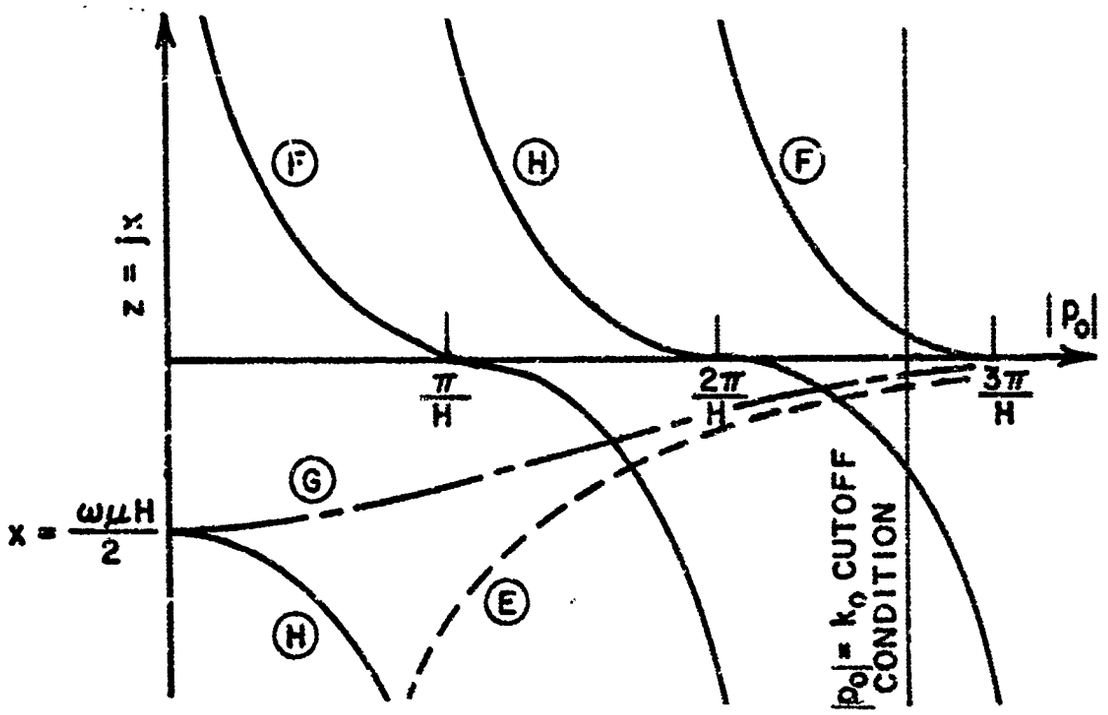

FIGURE 3. Impedance Loci for Parallel Modes

This work was performed while the author attended The Ohio State University and was supported in part by a sub-contract between The Andrew Corporation and The Ohio State University Research Foundation.

References

Barlow, H.M. and Cullen, A.L. (1953), Surface Waves, Proc. IEE, Part 3, 100, 329-341.

Barlow, H.M. (1965), Screened Surface Waves and Some Possible Applications, Proc. IEE 112, No. 3, 477-481.

Collin, R.E. (1960), Field Theory of Guided Waves, pp. 22-27, (McGraw-Hill Book Co., Inc., New York, N.Y.).

Dybdal, R.B. (1968), Waveguide Applications of Impedance Surfaces, Ph.D. dissertation, The Ohio State University, Columbus, Ohio.

Wait, J.R. (1967), On the Theory of Shielded Surface Waves, IEEE Trans. MTT MTT-15, No. 7, 410-414.

IMPEDANCE OF A DIPOLE IN A LARGE LABORATORY MAGNETOPLASMA

S.Y.K. Tam

Plasma and Space Physics Laboratory
RCA Limited
Montreal, Canada

Impedance of a 9.2 GHz $\frac{\lambda_0}{2}$-dipole in a large dc magnetoplasma (diameter $\approx 7\lambda_0$) have been measured for various electron densities, $0 \leq X = \left(\frac{\omega_{pe}}{\omega}\right)^2 \leq 2$, and magnetic fields, $0 \leq Y = \left(\frac{\omega_{ce}}{\omega}\right)^2 \leq 1.3$, λ_0 being the free-space wavelength, ω, ω_{pe}, and ω_{ce} the signal, plasma and electron cyclotron frequencies respectively. Results have been consistent with the theory.

INTEGRAL EQUATION APPROACH TO THE RADIATION FROM A VERTICAL MONOPOLE OVER AN INHOMOGENEOUS GROUND PLANE

(To appear in January 1970 issue of Radio Science)

J. R. Wait and K. P. Spies
ESSA Research Laboratories, Boulder, Colorado 80302

The possibility that HF antenna radiation can be enhanced at low angles, by a tapered ground system is explored. The model consists of a vertical linear antenna erected over a radially inhomogeneous ground system. The surface impedance is chosen to be a smooth monotonic function of the distance from the base of the antenna. In a practical scheme, this can be achieved by locating a radial wire system in a symmetrical fashion beneath the monopole. The combination of the equivalent wire grid impedance and the ground impedance is computable from previously developed theory.

It is first shown that the tangential magnetic field satisfies an integral equation of the Volterra type. Allowing the effective surface impedance to vary in an exponential fashion, a power series solution for the tangential magnetic field is then obtained. This involves integral and half-integral powers of the distance from the base of the antenna to a point on the ground surface. As a check for the homogeneous ground (i.e., no wire grid system), it reduces to the appropriate series expansions for the Sommerfeld attenuation function. The power series solution, so obtained, is supplemented by a numerical evaluation of the integral equation.

Using the solutions obtained above for the tangential fields, the radiation pattern of the antenna is calculated for several inhomogeneous ground models. Some earlier results using simplified assumptions are confirmed.† It is shown that a tapered ground screen model is much better than an abruptly truncated system. Some consideration is also given to intentional azimuthal variation of the ground system.

---

† J. R. Wait (1967), Pattern of a linear antenna erected over a tapered ground screen, Can. J. Phys. 45 (9), 3091-3101.

MICROWAVE (4.75GHz) SURFACE IMPEDANCE MEASUREMENTS OF A 1° DIELECTRIC WEDGE ON A PERFECT CONDUCTOR

R.J. King and C.H. Hustig

University of Wisconsin, Madison, 53706

Abstract:

When propagating in the direction of increasing depth, the results near the wedge apex compare best with calculations based upon simple parallel stratified media theory. When propagating in the direction of decreasing wedge depth, the results compare reasonably well with the theory given in 1967 by Schlak and Wait. However, the nature of the surface impedance is decidedly different for the two cases, being inductive near the wedge apex for the first case, and capacitive with a negative real part for the second case.

SESSION VIII, 1:30 p.m., Thursday, July 17, 1969

Round Table Discussion on:

DESIGN TECHNIQUES FOR PATTERN CONTROL BY GROUND SCREENS

SYNOPSIS by R. V. Row, Sylvania, Waltham, Mass.

The moderator (R. V. Row) introduced the two others sitting at the table with him: Dr. J. R. Wait (ITS/ESSA Boulder, Colo.), and R. D. Wengenroth (General Electric HMES, Syracuse, N.Y.), and proceeded to invite the participants to range further afield in their discussions than the advertised title of the round table would indicate and to consider terrain, fences and other obstacles within the scope of the meeting.

The discussions were then opened by J. R. Wait who discoursed on the proper use of transfer impedance and input impedance between antennas. He pointed out that most radio propagation work in the literature deals only with the transfer impedance and when terms like transmission loss or system loss are used by an author care must be taken by the reader to ascertain how the input power was calculated. Frequently input power is calculated on the basis of a dipole in free space. The speaker then proceeded to sketch briefly how a perturbation technique, often known as the compensation theorem, has been used to compute both input impedance and transfer impedance. For input impedance of an antenna and ground screen one need only be concerned with fields close in to the antenna, whereas the fields over the entire ground surface lying between the antennas contribute to the mutual impedance. He commented on the wide utility of the method and the fact that it has variational stationary properties which reduce the relative error in the perturbed quantity being calculated, to a lower order than the error in the assumed tangential E or H fields.

The moderator invited E. W. Seeley (U.S. Naval Weapons Center, Corona, Calif.) to comment on his calculation of the radiation efficiency of a long horizontal above ground wire antenna. (See pp. 174-178 of Vol. I of EFAP Proceedings.)

It was stated by Seeley that his expression for radiation efficiency is based on the actual input power to the antenna. The moderator attempted to restate this in terms of the E field maintained at a point in space by the actual antenna and a reference dipole each with the same input power. Seeley stated that it is more useful at VLF to consider power density radiated in a certain limited range of angles (10-15 degrees) above the horizon, rather than total power radiated, since this is the power that maintains the field at a distance via ionospheric reflection.

The moderator invited W. L. Curtis (Boeing Co., Seattle, Wash.) to comment on the experimental and interpretive theoretical work done by he and Coe [1964] on antennas on large ground screens over lossy earth. He pointed out that both the experimental work and a subsequent theoretical study [Curtis 1964] using the compensation theorem showed that for engineering purposes the radiation pattern of any low profile antenna on a finite size ground plane on a flat earth can be easily obtained from a free-space pattern of the antenna and ground plane. This means that modeling or other free-space antenna design techniques can be used, even if the antenna is to be placed over flat ground. To first order one earth loss correction curve can be used for all frequencies above the HF band and all ground planes greater than $\lambda/2$ in radius. The small change in this 'universal' correction due to ground screen size can be taken into account using the curves in Curtis [1964]. In the HF band and at lower frequencies where the ground refractive index is frequency dependent different correction curves would need to be prepared.

Professor L. B. Felsen (Brooklyn Polytechnic Institute) then suggested that there is another way of looking at antennas and ground screens, namely ray optics which provides useful insight not only for the input impedance but also for the radiation field. He illustrated his remarks by the example of a radiator over the center of a circular screen. In this case all the edge scattered rays travel in radial directions, and the scattering properties of an edge are well known and available in the literature. This way of looking at the problem also provides insight into the effect of non-circular screens, for example an elliptical screen,

where only four rays are scattered back to the center.

T. Kaliszewski (General Electric HMED, Syracuse, N.Y.) pointed out that diffraction and ray optics concepts were combined by Senior [1956] in studying ground wave propagation across edges. Krause [1967] has developed similar ideas for looking at sloping perfectly conducting screens and non-planar screens. Apparently the method is not readily adapted to imperfectly conducting screens, which is the situation of greatest practical interest.

Professor Felsen suggested the the surface impedance concept could be used with imperfectly conducting screens.

V. Arens (Sylvania Electronic Systems, Mountain View, Calif.) commented that he had adopted this point of view and used the plane wave reflection coefficient appropriate to the specular point in question to calculate the radiation pattern from a finite vertical dipole over an imperfect ground screen. Edge diffraction was not considered and is believed to be a second order effect [reported at the ARPA sponsored OHD symposium, Boulder, Colo 1966]. Comparison was excellent between predictions m .e this way and measurements made on a large circular array in the HF band.

J. R. Wait stated that indeed the ray approach gives insight into the pattern effects of ground screens. He proceeded to explain an approach he used to study the pattern of an array of slot antennas in a semi-infinite ground plane above a lossy half space. Employing the reciprocity principle he considered the incident wave (vertically polarized) from above, removed the lower dielectric half space and replaced its effect by an image plane wave incident from below. This procedure satisfies the boundary conditions except in a region close to the edge of the half-screen along the dielectric interface and indeed the results agree with those found by Clemmow [1953] who used a somewhat similar plane wave spectrum approach. The results also agree with those found from the compensation theorem. [These results were presented at the Congres International Circuits et Antennes Hyperfrequences, Paris, October 1957.† Experimental results dealing with this same problem were reported at this same

† J. R. Wait, L'Onde Électrique, 38e Année, No. 376 bis, Supplement Special, vol. 1, pp. 21-29, 1957.

congress by Robieux and Simon.] The speaker then went on to formulate an exact two dimensional integral equation for inhomogeneous ground problems and cast in the form of attenuation functions. He also suggested that the ray optics approach is not easy to justify in many practical cases where only modest or even small size ground screens are being considered.

W. L. Curtis commented that the ray theory shows that for a truncated ground plane the radiation pattern has small oscillatory lobes just where measurement and the compensation theory say they are, and that this kind of 'prediction' works even on planes as small as a half wavelength in radius.

The moderator then invited E. A. Thowless (U.S. Naval Electronics Laboratory Center, San Diego, Calif.) to review the work they have done on ground screens. Thowless briefly reviewed the contents of four NEL reports as follows:

NEL Report 1346 - "Ground System Effect on High-frequency Antenna Propagation," by W. E. Gustavson, W. M. Chase and N. H. Balli, 4 January 1966. Based on model measurements it shows that there is significant improvement (5 to 7 dB) in radiation pattern at angles below 20 degrees due to ground screens of radius 2 1/2 to 7 1/2 wavelengths and moderately conducting ground at frequencies of 10 to 30 MHz. It was deduced that mesh sizes of 1 or 2 feet would be adequate for screens used in the HF band.

NEL Report 1359 - "HF Extended Ground Systems: Results of a Numerical Analysis," by G. D. Bernard, W. E. Gustavson and W. M. Chase, 24 February 1966. Based on theoretical work of Wait and Walters [1963] on circular sector ground screens. Computations are presented concerning circular screens for frequencies of 4, 8, 16, 32 MHz, ground screen radii of 2, 4, 8, 16, 32, 64, 128 wavelengths, grid spacing of 6, 12, 24, 48 inches and ground parameters of $\epsilon = 4$, $\sigma = .003$ mho/m. $\epsilon = 10$, $\sigma = 0.01$, $\epsilon = 20$, $\sigma = .03$ and $\epsilon = 30$, $\sigma = .1$ and elevation angles of 2, 5, 10, 15, 20, 25 degrees. In general an improvement of 3 to 9 dB is attainable over

poor soil with a ground screen of 250 foot radius. The report contains a FORTRAN computer program listing.

NEL Report 1430 - "A Numerical Analysis of HF Sector Ground Screen Systems," by J. M. Horn, 11 January 1967. Presents further numerical computations based on Wait and Walters [1963], this time for sector screens (made up of radial wires) up to 128 wavelengths radius. Frequency 10 MHz. $\epsilon = 10$, $\sigma = .01$, 1λ circular impedance disc of 12 inch square mesh of No. 10 AWG wire for various sector angles in 10 degree increments and observing directions both on the symmetry axis of a sector screen and at 10 degree increments away from this axis. It was found that if one stays at least 10 degrees away from the edge of a sector then the 'gain' at any elevation angle remains within 1 decibel of its value over a circular screen of the same radius. It was pointed out that the number of radial wires in a sector was doubled every time the screen radius was doubled. The use of such a radial wire screen can reduce the wire requirements 20 to 40 percent below a square mesh screen having the same performance. The report contains a FORTRAN computer program listing.

NEL Report 1567 - "Vertical Plane Patterns of High-frequency Monopoles and of Elevated Vertical Dipoles with and without Extended Ground Planes," by J. M. Horn, (Fall 1968). Discusses two methods of enhancing gain at low elevation angles. One considers the effect of long ground screens on a vertical $\lambda/4$ monopole antenna and the other an elevated $\lambda/2$ vertical dipole both with and without extended ground planes. Frequency 10 MHz (and a 2 to 1 frequency range above and below 10 MHz); ground constants same as in NEL report 1359. Four fixed heights of the elevated dipole and ground screens of 4 and 8 wavelengths. It is shown that an elevated vertical dipole at a height of $\lambda/2$ with no ground plane will have the same low angle gain as a $\lambda/4$ monopole over a 4 to 8λ ground screen. Apparently more gain improvement is achieved by elevating a dipole than by constructing a ground screen, at least for the ground constants examined here. The improvement is greater the greater the height of the element. A computer program listing is available for this report.

The moderator invited R. G. FitzGerrell (ITS/ESSA, Boulder, Colo.) to comment on a method for measuring the absolute gain of vertically polarized HF band antennas. FitzGerrell then reviewed his paper [1967] where he discussed a method of using a horizontally polarized reference antenna as a gain standard, combined with an airborne platform having an antenna whose polarization can be switched between vertical and horizontal. Up to angles of about 30 degrees the 'gain' of the horizontal standard is relatively insensitive ($\pm$ 1 dB) to the assumed ground dielectric constants and conductivity in the frequency range 10 to 1000 MHz. The results of some model measurements at 400 MHz were presented. J. R. Wait asked if the formula and graphs presented included the effect of ground on the input impedance of the $\lambda/2$ horizontal dipole. The speaker replied in the affirmative and that his result agrees with the calculation by Surtees [Ph.D. thesis at University of Toronto, 1952].

V. Arens suggested that on the airplane shown by FitzGerrell the close coupling of the loops would affect the actual radiated power when one was rotated from a nominal vertical to a nominal horizontal polarization. R. FitzGerrell replied that this effect† was corrected for experimentally in the data reduction of the flight test measurements. There was some further discussion among V. Arens, R. FitzGerrell and H. Cottony (ITS/ESSA, Boulder, Colo.) concerning impedance variations on the aircraft antenna.

The moderator then drew attention to the work done by A. C. Wilson [1961] at CRPL on measuring the effect of a ground screen of radial wires on the radiation pattern of a vertical monopole.

The moderator suggested that Professor S. W. Maley (University of Colorado, Boulder, Colo.) might like to comment on his work comparing measurements and the compensation theorem theory of ground screens.

Professor Maley referred to his talk of the previous day in answer to this suggestion and invited J. R. Wait to make any additional comments. J. R. Wait expressed the hope that

---

† The actual effect referred to is the coupling of the antennas to the aircraft structure (Ed.).

the idea of a fast wave screen or screen which would exhibit negative wave tilt might (mentioned by S. Maley in Session IV) lead to some interesting new developments.

W. Henry (U.S. Coast Guard, Washington, D. C.) asked how one can justify (in applying the compensation theorem) keeping the tangential H fields the same in the unperturbed and perturbed conditions. J. R. Wait stated that in fact these fields aren't identical but that due to the variational (stationary) properties of the compensation theorem only second order errors are made in the perturbed quantity being calculated. If one wishes, the compensation theorem can be used to verify that the perturbed tangential H field is only very slightly changed from its unperturbed value. The moderator ventured the opinion that this stationary property of the compensation theorem was not sufficiently emphasized by its users.

T. Kaliszewski observed that J. B. Andersen [Teleteknik, Copenhagen, 1965] measured the effects of an extended ground screen system on a log-periodic HF band antenna and obtained excellent agreement with the predictions of the compensation theorem.* This agreement should do much to convince those in doubt about the credibility of the compensation theorem approach. J. R. Wait by way of reply suggested that it is really not necessary to rely on experiment to provide convincing evidence. In connection with a study of mode conversion of VLF waves at a land-sea boundary he showed [Wait, 1969] that a rigorous mode matching technique and the compensation theorem approach yield the same first order results, provided the reflected modes are neglected in estimating the fields on the earth's surface in the later method.

Professor R. J. King (University of Wisconsin, Madison, Wis.) commented that the tangential E field is often more sensitive to boundary perturbations than the H field and hence estimates of the H field are likely to be more accurate than those of the E field which is frequently discontinuous at boundaries. He then addressed some remarks to the subject of variable surface impedance screens, and expressed hope that some progress will be made on the inverse problem of

---

* J. B. Andersen, Teleteknik 9, No. 2, 33-40, 1965.

determining from a specification of the desired radiation pattern what the required variable surface impedance must be. J. R. Wait then spoke briefly on some of the effects on the radiation pattern when a tapered impedance screen is used. This way it is possible to reduce the high angle lobing evident with abruptly terminated large screens, at the expense of gain at low angles. The compensation theorem can be used to formulate an integral equation for the impedance contrast.

R. J. King stated that the solutions to such a problem turn out to be non-reciprocal and that this difficulty probably lies in the effect of the local ground on the impedance of the antennas which must be somehow properly handled in the formulation. (JRW's solutions referred to above were reciprocal., Ed.)

W. L. Curtis suggested that the abrupt change of impedance at the edge of a screen is necessary to the attainment of low angle gain.

R. D. Wengenroth was then invited to comment on some of the practical problems of measuring antenna system performance with or without ground screens. He suggested that even though we may some day be able to solve the synthesis problem, it will be too difficult to realize the solution in practical terms because of lack of control of the environment over a great enough distance. Another difficulty is the lack of sufficiently detailed knowledge about the characteristics of probing antennas (in their environment) used to measure performance of ground based arrays. For HF communication systems needs the kind of results currently available on measured patterns and gain are usually adequate. In some cases however better quality data is needed and then the environmental influences on the probing antenna seriously limit the ability to make absolute gain measurements, but not relative gain measurements. He discussed the need in many cases to make measurements at very long distances from the nominal 'antenna' installation to take proper account of hills and other terrain features extending many miles away from a rough terrain antenna site. In such instances a large high performance high altitude aircraft like the KC-135 is needed. The theoretical work to

determine what features of terrain are influential is a necessary concomitant to the experimental work.

The moderator pointed out for the benefit of those who did not attend the tutorial sessions that R. H. Ott (ITS/ESSA, Boulder, Colo.) has developed a theoretically based computer executed method for predicting the pattern over irregular terrain, and R. Row (Sylvania, Waltham, Mass.) described a somewhat different approach to calculating the field over two dimensional irregular terrain.

V. Arens asked R. D. Wengenroth about the influence of the airborne loop antenna on cross polarization measurements. R. D. Wengenroth replied that some test results with both vertical and horizontal dipoles showed the loop to have 'good' (20-30 dB) rejection of the cross-polarized component, so that cross polarization effects shouldn't have corrupted the normal measurements.

The moderator thanked the panel contributors and the audience in general for their thoughtful and stimulating discussions and called the session to a close at 3:45 p.m.

REFERENCES

Coe, R. J. and W. L. Curtis, Effect of Lossy Earth on Antenna Gain, Radio Science 68D (2), 251-255, Feb. 1964.

Curtis, W. L., Effect of Lossy Earth on Antenna Gain, Part II, Radio Science 68D (7), 813-818, July 1964.

Senior, T. B. A., Radio Propagation over a Discontinuity in the Earth's Electrical Properties. Monograph 192R, 1-11, Inst. Elect. Engrs. (London) August 1956.

Krause, L. O., Enhancing HF Received Fields with Large Planar and Cylindrical Ground Screens. IEEE Trans. Ant. and Propagation, AP-15 (6), 785-795, November 1967.

Clemmow, P. C., Radio Propagation over a Flat Earth across a Boundary Separating Two Different Media. Trans. Roy. Soc., London 246, 1, 1953.

Wait, J. R. and L. C. Walters, Influence of a Sector Ground Screen on the Field of a Vertical Antenna, National Bureau of Standards Monograph 60, 15 April 1963.

FitzGerrell, R. G., Gain Measurements of Vertically Polarized Antennas over Imperfect Ground, IEEE Trans. Ant. Prop. AP-15 (2), 211-216, March 1967.

Wilson, A. C., Measurements of Low-Angle Radiation from a Monopole, J. Res. Natl. Bur. Std., Vol. 65D (6), 641-645, Nov.-Dec. 1961.

Wait, J. R., On Mode Conversion of VLF Radio Waves at a Land-sea Boundary, IEEE Trans. Ant. Prop. AP-17 (2), 216-220, March 1969.

Additional Reference

Wait, J.R., Characteristics of antennas over lossy earth, Chap. 23 in Antenna Theory, Pt. 2 (edited by R.E. Collin and F. J. Zucker), McGraw-Hill, New York, 1969.

ADDED MATERIAL (Ed.)

Professor S. W. Maley suggested during the round table discussions that laboratory models be used to study the effect of a "fast-wave" ground system on the radiation pattern (with reference to his paper on pg. I-196). However, it was not clear how such a "fast-wave" impedance boundary is to be fabricated.

There was also some discussion concerning the tangential field approximations used in applying the compensation theorem formulation to the self-impedance calculation of a monopole. As indicated elsewhere in the summarized discussions, the stationary property permits a crude approximation to the tangential magnetic field to yield relatively good self-impedance estimates. Professor R. J. King then pointed out formulations involving tangential magnetic fields are less influenced by local inhomogeneities than are representations involving the tangential electric fields. This point was attributed to earlier work by K. A. Norton (1942) on related subjects.

Professor R. J. King then suggested that, in the future, effort be directed toward the synthesis of antenna ground systems. He hoped to be able to synthesize the system to meet the objectives, e.g., specify a variable surface impedance over the ground surface, and/or possibly the ground screen shape and size.

Reference

Norton, K. A. (1942), The polarization of downcoming ionospheric radio waves, FCC and NBS Rept. No. 60047, pp. 58-61 (Available through ESSA Library, Boulder, Colorado).

SUMMARY OF DISCUSSIONS AND POINTS OF VIEW RAISED DURING REGULAR SESSIONS

After nearly every paper, questions from the floor were raised. Many of these were in the nature of comments about details of the presented material and need not be recorded here for posterity. Furthermore, many of the points raised, concerning the effects of finite ground plane and related environmental effects, were discussed in the "round table" session on "Pattern Control by Ground Screens." The discussions and discourses at this session have been admirably summarized by the moderator Dr. R. V. Row. His summary appears on page 86 in this present volume.

It was apparent that many authors described the results of complicated numerical calculations which arose from integral equation or related point-matching techniques. Since an analytical view of the environmental influence on antenna radiation leads to a boundary-value problem, it is not really surprising that various numerical techniques are resorted to. This trend in applied electromagnetic theory has been criticized by a number of prominent researchers from academia. Their viewpoint was elegantly put forward by Professor L. B. Felsen in a written communication following the conference. I am taking the liberty to quote from his letter as follows:

> "If I may voice again a personal concern which has to do not only with my session but with papers in general, there is now with the availability of computers the temptation to furnish detailed numerical results for special boundary value problems involving oddly shaped scatterers, propagation through a special environment, etc. Such work is justifiable if the numbers are required for a special, particular application. However, unless such work is related to, and interpreted quantitatively via, approximate analytical techniques which grant an insight into the radiation and scattering mechanism, it does little to advance our understanding; in fact, failure to make such critical comparisons is to exploit inadequately the contribution that judiciously chosen accurate solutions can provide. Continued and excessive emphasis on numerical results without adequate theoretical perspective will tend to negate advances made through the years in propagation and diffraction theory. I have often shuddered to think of the day when orientation toward numerical computation will be carried so far as to remove motivation for devices such as the Watson transformation, which not only do an inefficient job much more efficiently but also add invaluable insight into physical phenomena."

The points raised by Professor Felsen should be carefully considered by those involved in computer-oriented approaches to electromagnetics. I personally share his misgivings that computer printouts themselves give little physical insight. On the other hand, iterative solutions of integral equation formulations lead to a quantitative understanding of the relevant phenomena. In particular, if the variational property of the compensation theorem formulation is utilized, an economical and accurate solution to a wide class of problems can be obtained with ease. After all, "insight" means different things to different people. If all the properties of a given electromagnetic environmental problem can be obtained in a compact graphical chart or nomograph, then who can say this gives less insight than an asymptotic result which has an uncertain region of validity (e.g., it may be only valid if the range r tends to infinity -- but one would like to know if ∞ is 1 meter or 1 megameter).

Detailed Comments†

Session I: Professor L. B. Felsen suggested that D. A. Hill (author of paper No. 2, pg. I-10) consider the method of Louis Cagniard in treating electromagnetic transient problems. (See A. T. deHoop, Appl. Sci. Res. Sec. B, vol. 8, 349-356, 1961.)

Session II: Dr. J. R. Wait wondered whether R. J. Lytle's solutions (in paper No. 1, pg. II-8) for the prolate spheroid could not be obtained by applying the reciprocity theorem to the case of a uniformly excited circumferential gap. The solution of this scalar problem is well known.

Several individuals in the audience questioned the validity of Dr. Franceschetti's results (in paper No. 2, pg. I-33). It was concluded that the results were only valid for direct current or extremely low frequencies.

C. J. Sletten asked Mrs. Chatterjee (paper No. 3, pg. I-38) how the boundary condition at the tip of the conical structure was satisfied. Dr. Wait explained that the eigenvalues were determined from the condition that the tangential electric fields were zero on the perfectly conducting spherical tip. Several questions from the floor, concerning the convergence of the proposed solution, were left unanswered.

---

† The page number in Vol. I and Vol. II where papers appear, is indicated.

Several individuals in the audience questioned Professor H. Kurss (paper No. 4, pg. I-42) about the justification for his assumption of uniform current in the loop. Dr. Wait ventured the opinion that for loops near the ground, the loop circumference needed to be small compared with the skin depth in the earth. This is much more stringent than merely requiring that the loop dimensions be small compared with a free-space wavelength. Dr. R. J. Phillips indicated that he and his colleagues at Berkeley had used a similar formulation and the paper was published in a recent issue of the journal Geophysical Prospecting (full reference not available, Ed.).

The interesting paper by P.R. Bannister (paper No. 5, pg. I-45) provoked considerable discussion. The mathematical validity of the image concept was questioned out of context by some individual in the audience. It was stressed by the author that the results were valid only in the quasi-static sense, i.e., where distances were small compared with a free-space wavelength.

C. J. Sletten questioned Dr. D.B. Large (paper No. 6, pg. I-50) about the motivation for his finite wire calculations. The author replied that the results were used in interpreting geophysical data at ELF for his company.

Session III: Several in the audience asked for clarification of R. J. King's analyses (papers Nos. 2 and 3, pg. I-64, I-66) concerning wave propagation over an impedance boundary. Professor King confirmed that his results were valid even when the refractive index of the ground was not large. However, the transition to a refractive index of unity (i.e., free space) was not permitted. This appears to be a problem which has not yet been solved satisfactorily.

Dr. Wait provided a rebuttal (in support of Arnold Sommerfeld) concerning the severe criticisms of the "master" by Carson Tsao (paper No. 6, pg. I-77). In the rebuttal, it was pointed out that Sommerfeld's results were not intended to be used in the quasi-static region where the height of the dipole above the ground was small compared with the wavelength. Actually, a quasi-static evaluation of Sommerfeld's integrals (published in 1909!) leads to results fully consistent with electrostatic concepts.

Session IV: Many of the points raised here were covered in the round table discussions. However, there was a question raised by Drs. Row and Wait about the possibility of a cross-polarized radiation from the wire grid. It was concluded that the effect is small when dealing with a square mesh which is more or less isotropic in its reflecting properties. [With reference to paper No. 6, pg. I-103, by G. A. Otteni.]

Session V: In the papers (Nos. 2 and 3, pg. I-108, I-112) by K. K. Mei, et al., the rigidity boundary conditions were questioned. It was agreed that they are not realistic but they are convenient.

Several people asked Dr. Oya (paper No. 5, pp. II-39) how he managed to cope with the plasma boundary conditions on the antenna surface. It appears this question was avoided by assuming a current distribution.

Session VI: No specific comments were recorded nor did the session chairman volunteer any.

Session VII: Dr. R. V. Row questioned whether the anisotropic effects described by R. J. Phillips (paper No. 1, pg. I-169) would be present given the very low dc magnetic fields measured near the moon. Dr. Phillips assured him that in the frequency range from 10-20 kHz the media would be anisotropic.

E. W. Seeley (paper No. 2, pg. I-174) was criticized for using efficiency to characterize the antenna gain and antenna patterns in Figures 5 and 6. Comparison with established antenna definitions was urged.

In G. E. Webber's paper (No. 5, pg. II-50), Dr. Wait wondered about the appropriateness of calling the propagation mechanism a surface wave or a Zenneck wave. Perhaps a guided wave or trapped mode might be a more accurate and descriptive term.

Some post conference interest was expressed in the unique phase dispersion method described by P. Cornille (paper No. 7, pg. I-190). Actual data on a specified layered geology would be appreciated.

Session IX: V. R. Arens asked D. C. Chang (paper No. 2, pg. II-58) why so much effort was made to obtain closed form solutions rather than simply use a computer to evaluate the Fourier integral for all parameters of interest. This was answered by Dr. Chang with the comment that a closed form solution is preferable because of the greater insight into the solution which it provides and because of its greater utility in design. Dr. Wait (co-author) also commented later that the closed form solutions were needed in the numerical inversion of the integral equations for a finite linear antenna over a conducting half-space. Also, there is an economic aspect of the problem which is not negligible unless, of course, one has unlimited funds.

Comments on the physical realizability of the model used by Dr. Curtis (paper No. 3, pg. II-64) were made by Dr. Wait. He indicated that the postulated complex dielectric constant did not satisfy the Kramers-Kronig relations and thus apparent violations of causality

could be expected. Dr. Wait and Dr. Curtis agreed, however, that the violation was not practically very important.

A comment was made by Pitt Arnold after the session that, in his experimental investigations, he has never observed minima in the vertical radiation patterns like those shown by Dr. J. R. Wait (paper No. 10, pg. II-84). Mr. Arnold further commented that in experimenting with various types of terminations for radial wire ground systems the radiation pattern was negligibly affected. Professor S. W. Maley commented that differences were probably due to different ground and ground system parameters. Dr. Wait later commented that the calculated lobe structures for truncated ground systems have been verified by W. E. Gustafson and colleagues at the Navy Electronics Laboratory and W. L. Curtis and colleagues at Boeing Laboratories, Seattle. Of course, for a tapered system (including some radial wire systems), the lobe structure is less pronounced. Dr. D. B. Large asked how an approximate solution having no mathematical basis can be verified as meaningful. Dr. Wait answered that certain aspects of a solution such as boundary behavior or asymptotic behavior can be examined for correctness or approximate correctness. Also mathematical means are available for verifying that an approximate solution is nearly equal to the exact solution of the equation in question.

A question concerning R. J. King's paper (No. 11, pg. II-85) was raised about the measurement technique for the electric field over the dielectric wedge. Professor King explained that measurements were made by a scattering dipole technique and that great difficulty was experienced in synthesizing a low reflection termination at the edges of the dielectric wedge material.

Mrs. G. B. Goe of ITS/ESSA made an unscheduled presentation on Noise and Cerenkov Radiation. (See pg. II-114)

I have prepared this summary of the discussions with the help of written comments supplied to me from C. J. Sletten and S. W. Maley for sessions which they chaired. All the other comments, except for the quoted gem from Professor Felsen are based on my own (incomplete) recollections of the events. I accept the blame for any baises that the reader may detect. Certainly, they do not reflect the official (or unofficial) policy of the federal agencies of the U. S. Government which have sponsored this meeting.

James R. Wait

4 August 1969

CORRECTIONS TO VOLUME I

Finite tubular antenna above a conducting half space (Paper No. 1 in Session III, pp. 59-63) by D. C. Chang

Because of errors involved in numerical computation, the scale factor on the abscissae in Figs. 2 and 3 should be modified by about a factor of 2. However, the discussion following these figures is still valid. The correct input conductance (in milli-mhos) of a tubular antenna of radius $a = 0.007\lambda_0$ and $h = 0.25\lambda_0$ is tabulated in the following:

$\frac{d}{\lambda_0}$	0.27	0.3	0.5	1.0	2.0	4.0
Sea-water ($\sigma = 4$ ohm/m, $\epsilon_r = 80$ at 600 MHz)	7.14	8.32	9.09	8.88	8.84	8.84
Wet-earth ($\sigma = 10 \times 10^{-3}$ mho/m, $\epsilon_r = 10$ at 100 MHz)	7.66	8.63	8.97	8.86	8.84	8.84

When the antenna is located several wavelengths above the ground, the theoretical results compare favorably with experimental measurement of a single antenna in the free-space† (8.90 milli-mhos). For a more detailed discussion, the reader is referred to a paper by Chang and Wait (1969) listed in the references.

† R. B. Mack, "A study of Circular Arrays," Tech. Rept. No. 382, Crufts Lab., Harvard Univ., Cambridge, Mass., May 1, 1963.

- - - - - - - - - - -

Reflection of waves of arbitrary polarization from a rectangular mesh ground screen (Paper No. 6 in Session IV, pp. 103-107) by G. A. Otteni

On page 104, the last paragraph should read: It is assumed that..... as $E = Z_i I$, (Z_i is the internal impedance of the wire and is approximately $Z_m/2\pi r$) .... for an axial current I....with surface impedance Z_m. In addition.....

On page 107, for the sample calculations in the second paragraph, the grid wire spacing $a = \infty$ and b = 2 m. for parallel wires.

- - - - - - - - - - -

Numerical solution of dipole radiation in a compressible plasma with a vacuum sheath surrounding the antenna (Paper No. 3 in Session V, pp. 112-116 by S. H. Lin and K. K. Mei

The second sentence of the last paragraph on page 114 should have read: This behavior of input reactance near ω_p is in contrast with that for infinitely long cylindrical antenna found by Miller (1968).

Phase measurements of electromagnetic field components (Paper No. 7 in Session VII, pp. 190-195) by P. Cornille

The corrected version of Fig. 4 is given below:

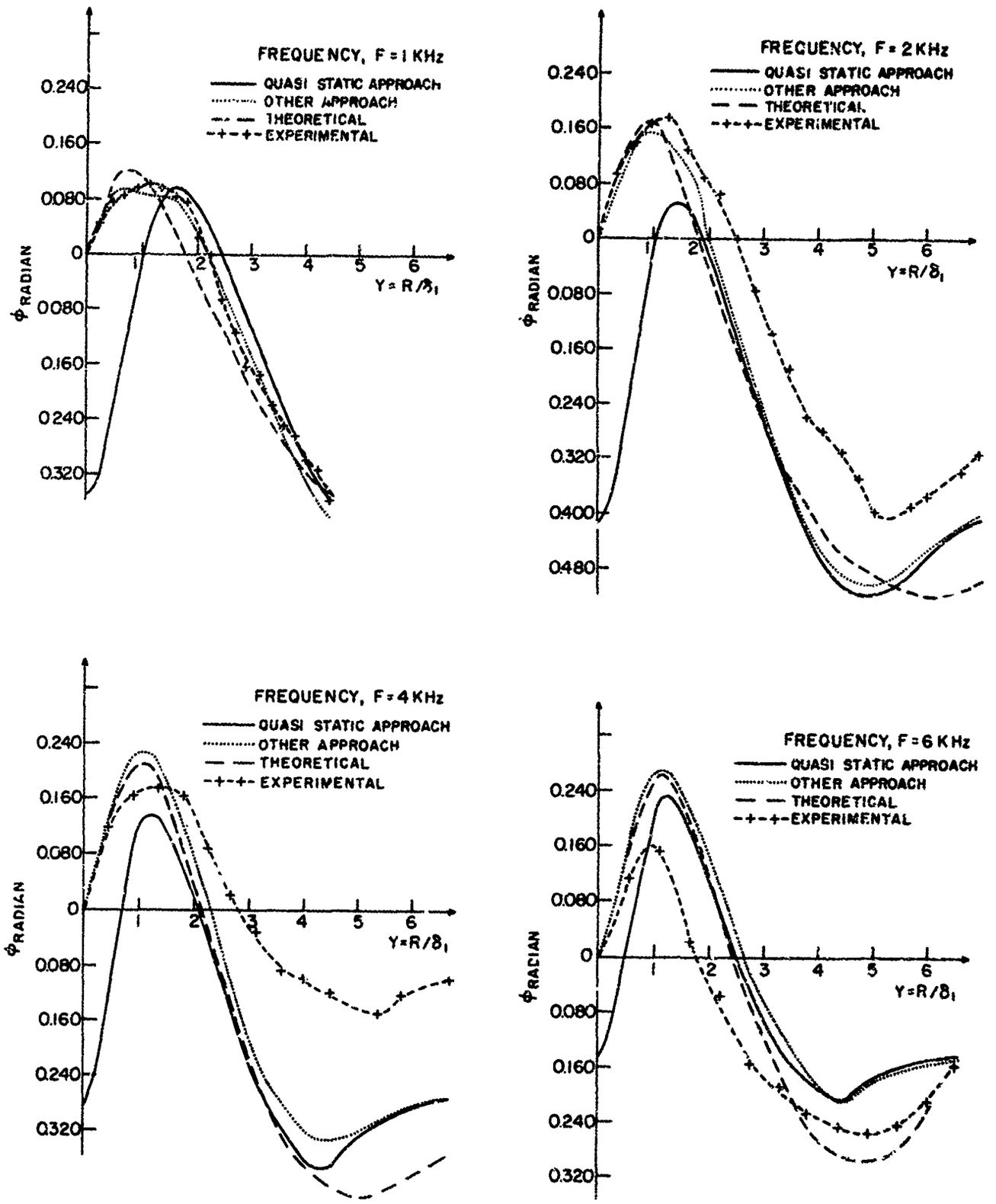

Radiation from a parallel-plate waveguide into an inhomogeneously filled space (Paper No. 6 in Session I, pp. 28-31) by R. J. Kostelnicek and R. Mittra - revised pg. 29

for the canonical problem. The first step involves expressing the fields in region B in terms of waveguide modes and in region E in terms of a continuous spectrum (Fourier integral) representation. Similar transform representations are employed in regions A, D, and C. Typical representations for the magnetic intensity in regions B and E for a TM_{po} incident mode of unit amplitude are given by

$$(Hy)_B = \cos\left(\frac{p\pi x}{b}\right) e^{-\beta_o z} + \sum_{s=0}^{\infty} B_s \cos\left(\frac{s\pi x}{b}\right) e^{\beta_s z} \tag{1}$$

and

$$(Hy)_E = \int_0^{\infty} E(\alpha) e^{-\xi(z-\ell-2t)} \cos(\alpha x)\, d\alpha \tag{2}$$

The longitudinal wave numbers are given by $\beta_s = \sqrt{(s\pi/b)^2 - k_o^2}$ in region B, $\xi = \sqrt{\alpha^2 - k_o^2}$ in E, and $\eta = \sqrt{\gamma^2 - k_o^2}$ in C. The mode coefficients and spectral weight functions are B_s, $D(\alpha)$, $E(\alpha)$, $C(\gamma)$, and $A(\alpha)$.

The next step is to solve for the various mode and weight coefficients by matching the transverse field components at $z = \ell$ and $z = \ell + 2t$, thereby obtaining $D(\alpha)$ and $A(\alpha)$ in terms of $E(\alpha)$. Field matching is once more carried out at the $z = 0$ interface for $|x| \geq b$ and subsequently for $|x| \leq b$. The resulting four equations are Fourier transformed and combined to yield the following relationships:

$$b(1+\delta_p^o)\delta_s^o = \pi E\left|\frac{s\pi}{b}\right| R'\left(\frac{s\pi}{b}\right) \tag{3}$$

$$\cos(\gamma b)\pi\eta E(\gamma) R'(\gamma) = P.V. \int_0^{\infty} E'(\alpha)\left[\frac{R'(\alpha)}{\xi - \eta} - \frac{Q'(\alpha)}{\xi + \eta}\right] d\alpha, \tag{4}$$

together with two companion relationships giving the coefficients B_s and weight function $C(\gamma)$ in terms of an integral relationship involving $E(\alpha)$. In equations (2) and (3) we have written $E'(\alpha) = \alpha \sin(\alpha b)\, E(\alpha)$, $R'(\alpha) = R(\alpha) \exp(\xi\ell)$ and $Q'(\alpha) = Q(\alpha) \exp(-\xi\ell)$. The quotients $1/R(\alpha)$ and $Q(\alpha)/R(\alpha)$ are respectively the transmission and reflection coefficients for a uniform plane wave incident onto the dielectric or plasma slab at an angle given by $\theta = \sin^{-1}(\alpha/k_o)$. Equations (3) and (4) represent a homogeneous integral equation for $E(\alpha)$ and a requirement that $E(\alpha)$ take on certain specified values at $\alpha = s\pi/b$ ($s = 0, 1, 2, \ldots$).

Revised pg. 30

The above formulation is exact, and for the limiting case when $\kappa = 1$, an exact solution for $E(\alpha)$ can be constructed using the function-theoretic technique.

Modified Method of Solution

The solution of (3) and (4) for $E(\alpha)$ by the modified function-theoretic technique is accomplished by the construction of a sectionally holomorphic function $F(\omega)$ of a complex variable ω, which has a certain pole-zero configuration, and specified branch singularities. Integrations in the complex plane yield results which, when compared with (3) and (4) and the compaion relations for B_s and $C(\gamma)$, give the required solutions and the normalization condition. These are:

$$F(-\beta_s) = -b(-1)^s \beta_s (1+\delta_s^o) B_s \tag{5}$$

$$F(\xi) = \pi \xi R'(\alpha) e^{j\alpha b} E(\alpha) \tag{6}$$

$$F(\eta) \frac{Q'(\gamma)}{R(\gamma)} + F(-\eta) = \pi \eta C(\gamma) \tag{7}$$

and

$$F(\beta_p) = b(-1)^p \beta_p (1+\delta_p^o) \tag{8}$$

The function $F(\omega)$ may be factored into the form $F(\omega) = F_1(\omega)\ T(\omega)$, where $F_1(\omega)$ represents that function employed in the solution of the canonical problem (Mittra and Bates, 1965), and $T(\omega)$ represents the departure from the canonical function due to the presence of the slab. The preceeding integrations and comparisons together with the factored form of $F(\omega)$ yield an auxiliary integral relationship

$$T(\omega) = \frac{1}{\omega - \beta_p} + \int_\sigma \frac{\lambda(z)\ T(z)}{\omega + z}\, dz\ . \tag{9}$$

Equation (9) is not very convenient for numerical methods of solution when ω is on the path σ due to the singular nature of the partial kernel $\lambda(z)$, which has poles on σ due to the surface modes excited within the dielectric slab. However, the path σ may be deformed to say σ' on which the integrand of (9) is wholly analytic. Numerical methods are now employed together with a process of analytic continuation, and the required values $T(\omega)$ and $T(-\omega)$ obtained.

The near fields may be obtained from the modal expansion in region B and from the Fourier transforms in the open regions. The radiation fields are obtained directly from the spectral weight coefficients by employing the method of saddle-point integration (Collin, 1960). The surface modes may be obtained from the residues of the integrand in the transform representation in region A.

AUTHOR INDEX

(For both Vols. I and II)

List of Attendees

Adams, Gene W.
ITS/ESSA

Arens, V. R.
Sylvania Electronic Systems
Mountain View, California

Arnold, P. W.
ITS/ESSA

Bachynski, M. P.
RCA
Montreal, Canada

Bahar, E.
University of Nebraska
Lincoln, Nebraska

Balmain, K. G.
University of Toronto
Toronto, Canada

Bannister, P. R.
U. S. Navy Underwater Sound Laboratory
New London, Connecticut

Bertoni, H. L.
Polytechnic Institute of Brooklyn
Farmingdale, N. Y.

Bishop, R. H.
Upper Air Research Center
Salt Lake City, Utah

Blacksmith, Philipp
AFCRL
Bedford, Mass.

Bonkowski, R. R.
Aerospace Corporation
San Bernardino, California

Bruscaglioni, P.
University of Florence
Florence, Italy

Brown, Russell
U. S. Navy Research Laboratory
Washington, D. C.

Bussey, H. E.
National Bureau of Standards
Boulder, Colorado

Carey, R. B.
Federal Communications Commission
Washington, D. C.

Carress, F. S.
U. S. Naval Avionics Facility
Indianapolis, Indiana

Chambers, B.
University of British Columbia
Vancouver, B. C., Canada

Chang, D. C.
University of Colorado
Boulder, Colorado

Chatterjee, Mrs. Rajeswari
Indian Institute of Science
Bangalore, India

Cohen, Robert
ITS/ESSA

Cloonan, Clifford
California State Polytechnic College
San Luis Obispo, California

Compton, R. E.
Martin-Marietta Company
Denver, Colorado

Cook, K. R.
Colorado State University
Ft. Collins, Colorado

Cooper, W. W.
Mass. Institute of Technology
Cambridge, Massachusetts

Curtis, W. L.
Boeing Airplane Company
Seattle, Washington

Cornille, P.
University of Lille, France
and
University of California
Berkeley, California

Cottony, H. V.
ITS/ESSA

DeVore, R. V.
Ohio State University
Columbus, Ohio

Dougherty, H. T.
WPL/ESSA

Dybdal, R. B.
Aerospace Corporation
El Segundo, California

Eckstein, Arthur
U. S. Army Electronics
Command
Fort Monmouth, N. J.

Felsen, L. B.
Polytechnic Institute of Brooklyn
Farmingdale, N. Y.

Fiala, Vladimir
Ionospheric Research Group
C. N. E. T.
Saint-Maur, France

Fikioris, J. G.
University of Toledo
Toledo, Ohio

FitzGerrell, R. G.
ITS/ESSA

Fox, J. F.
McDonnell-Douglas
Astronautics Company
St. Louis, Missouri

Franceschetti, Giorgio
University of Naples
Naples, Italy

Franklin, S. B.
U. S. Air Force Academy
Colorado Springs, Colorado

Gabillard, R.
University of Lille
Lille, France

Galejs, J.
Sylvania Electronic Systems
Waltham, Massachusetts

Gallet, R. M.
ESSA

GiaRusso, D. P.
Boeing Airplane Company
Seattle, Washington

Goe, Mrs. G. B.
ESSA

Goldan, P. D.
ITS/ESSA

Golden, K. E.
Aerospace Corporation
Los Angeles, California

Graf, C. R.
U. S. Air Force Security Service
San Antonio, Texas

Graff, P.
C. N. E. T.
Paris, France

Guarini, J. F.
U. S. Navy
Johnsville, Pennsylvania

Habicht, William
U. S. Navy Research Laboratories
Washington, D. C.

Hall, C. J.
U. K. Atomic Energy Authority
Aldermaston, England

Harvey, Don
U. S. Air Force
Rome Air Dev. Center
Rome, N. Y.

Hayes, Dallas
AFCRL
Bedford, Massachusetts

Heidig, W. R.
U. S. Naval Electronic Systems Command
Washington, D. C.

Henry, Dennis
New Mexico State University
Las Cruces, New Mexico

Henry, W. O.
U. S. Coast Guard
Washington, D. C.

Hill, D. A.
Ohio State University
Columbus, Ohio

Hochstim, Adolf
Wayne State University
Detroit, Michigan

Howe, Donald F.
Hq - USA Stratcom
Fort Huachuca, Arizona

Hunsucker, R. D.
ITS/ESSA

Kaliszewski, T.
General Electric Company
Syracuse, N. Y.

King, R. J.
University of Wisconsin
Madison, Wisconsin

Kirby, R. C.
ITS/ESSA

Kostelnicek, R. J.
University of Illinois
Urbana, Illinois

Kurss, H.
ITS/ESSA

Lambert, J. S.
Schellenger Research Laboratories
University of Texas - El Paso
El Paso, Texas

Large, D. B.
Westinghouse Electric Corporation
Boulder, Colorado

Leiphart, J. P.
U. S. Naval Research Laboratories
Washington, D C.

Lewis, R. L.
ITS/ESSA

Lin, S. H.
University of California
Berkeley, California

Livermore, Robert
U. S. Naval Research Laboratories
Washington, D. C.

Lu, H. S.
University of California
Berkeley, California

Lytle, R. J.
Lawrence Radiation Laboratory
Livermore, California

McCoy, D. R.
General Electric Company
Syracuse, N. Y.

McElvery, Richard
Sylvania Electronic Systems
Needham, Massachusetts

McInnis, P. A.
University of Sheffield
Sheffield, England

McIntosh, R. E.
University of Massachusetts
Amherst, Massachusetts

Ma, M. T.
ITS/ESSA

Maley, S. W.
University of Colorado
Boulder, Colorado

Mei, K. K.
University of California
Berkeley, California

Meltz, Gerald
Mitre Corporation
Bedford, Massachusetts

Miller, E. K.
MBAssociates
San Ramon, California

Moeller, A. W.
Bendix Communications Division
Towson, Maryland

Morgan, L. A.
Micronetics
San Diego, California

Nelson, Merle
U. S. Naval Oceanographic Office
Washington, D. C.

Olson, Irving
U. S. Navy Electronics Laboratory
San Dieg, California

Ott, R. H.
ITS/ESSA

Otteni, G. A.
General Electric Company
Syracuse, N. Y.

Oya, H.
NASA/Goddard Space Flight Center
Greenbelt, Maryland

Papa, R. J.
AFCRL
Bedford, Massachusetts

Partch, J. E.
ITS/ESSA

Patton, W. T.
RCA
Moorestown, N. J.

Peele, W. D.
U. S. Air Force Academy
Colorado Springs, Colorado

Perle, R. C.
U. S. Army SATCOM Agency
Fort Monmouth, N. J.

Phillips, R. J.
Jet Propulsion Laboratory
California Institute of Technology
Pasadena, California

Plonus, M. A.
Northwestern University
Evanston, Illinois

Plugge, R. J.
Atlantic Research
Costa Mesa, California

Potenza, J. E.
Hq - USA STRATCOM
Fort Huachuca, Arizona

Potter, D S.
Air Force Institute of Technology
Wright-Patterson AFB, Dayton, Ohio

Rawhouser, Robert
Air Force Avionics Laboratory
Dayton, Ohio

Rosich, R. K.
ITS/ESSA

Ross, D. B.
Communications Research Center
Ottawa, Canada

Row, R. V.
Sylvania Electronic Systems
Waltham, Massachusetts

Russo, A. J.
Sandia Corporation
Albuquerque, New Mexico

Rybak, J. P.
Colorado State University
Ft. Collins, Colorado

Seeley, E. E.
Naval Weapons Laboratories
Corona, California

Sletten, C. J.
AFCRL
Bedford, Massachusetts

Smith, A. N.
Westinghouse Electric Corporation
Boulder, Colorado

Stewart, Gordon
Aerospace Corporation
Los Angeles, California

Sugai, Iwao
Communications and Systems, Inc.
Falls Church, Virginia

Surtees, W. J.
Defence Research Board
Ottawa, Canada

Talekar, V. L.
Malaviya Regional Engineering College
Jaipur, India

Tam, S. Y. K.
RCA
Montreal, Canada

Taylor, W. C.
Stanford Research Institute
Menlo Park, California

Taylor, W. L.
ITS/ESSA

Thiele, G. A.
Ohio State University
Columbus, Ohio

Thompson, Alex
Wayne State University
Detroit, Michigan

Thowless, Eric
U. S. Naval Electronics Laboratories
San Diego, California

Tsao, C. K. H.
Raytheon Company
Norwood, Massachusetts

Utlaut, W. F.
ITS/ESSA

Wait, J. R.
ESSA

Wang, T. N. C.
RadioScience Laboratory
Stanford University
Stanford, California

Webber, G. E.
University of Washington
Seattle, Washington

Weisbrod, Steven
Micronetics
San Diego, California

Weider, Bernard
ITS/ESSA

Wengenroth, R. D.
General Electric Company
Syracuse, N. Y.

Wierman, Edward
Honeywell-Minneapolis Company
Minneapolis, Minnesota

Wong, W. H.
Utah State University
Logan, Utah

Woo, Richard
Jet Propulsion Laboratory
Pasadena, California

Ziolkowski, F. P.
Raytheon Company
Norwood, Massachusetts

Zuran, Joseph
General Dynamics
Rochester, N. Y.

Post Deadline Paper

NOISE AND CERENKOV RADIATION

G. B. Goe

Institute for Telecommunication Sciences
Environmental Science Services Administration
Boulder, Colorado 80302

Abstract

Radiation generated by a moving electron is suggested as a source of noise in the ionosphere. The moving electron travels with a velocity which exceeds both the thermal velocity of the electrons in the ambient (homogeneous) plasma and the phase velocity of light in the medium in order to fulfill the Cerenkov condition.

Introduction

It has been convincingly demonstrated by using automatic gain control (AGC) records that the principal plasma resonances observed by the Alouette I topside sounder do not occur naturally but are instead excited by the sounder transmitter. A "noise" background is recorded, however, even when the transmitter is turned off. Theoretical results suggest that the Cerenkov mechanism is useful to interpret the presence of the background noise and subsequent noise cut-off when the transmitter is turned off or the appearance of a resonance spike when the transmitter is turned on and the antenna is providing energy to the electrons.

Theory

Dispersion relations are derived using kinetic theory. The Cerenkov coherency condition is formally introduced into newly derived plasma dispersion relations in order to arrive at algebraic expressions for the dispersion relationships of a fully ionized warm, magneto-active plasma in the presence of a moving charge.

Comments

The particular restriction that the moving electron be constrained to travel parallel to the earth's magnetic field gives rise to a well-defined cut-off for the Cerenkov zone at the upper hybrid frequency $(f_N^2 + f_H^2)^{\frac{1}{2}}$ where f_N is the plasma frequency and f_H is the cyclotron frequency of the electrons. Under the same circumstances, the conditions near the plasma frequency are ill defined and, among other things, temperature dependent.

This theoretical work was published in detail in a research report: Goe, G. B., "Plasma Resonance and Radiation in the Upper Ionosphere," School of Pharmacy, University of Colorado, 28 July 1967, and has been out of print for some time. Additional copies of the report are, however, now available from the Department of Electrical Engineering, University of Colorado, Boulder, Colorado.

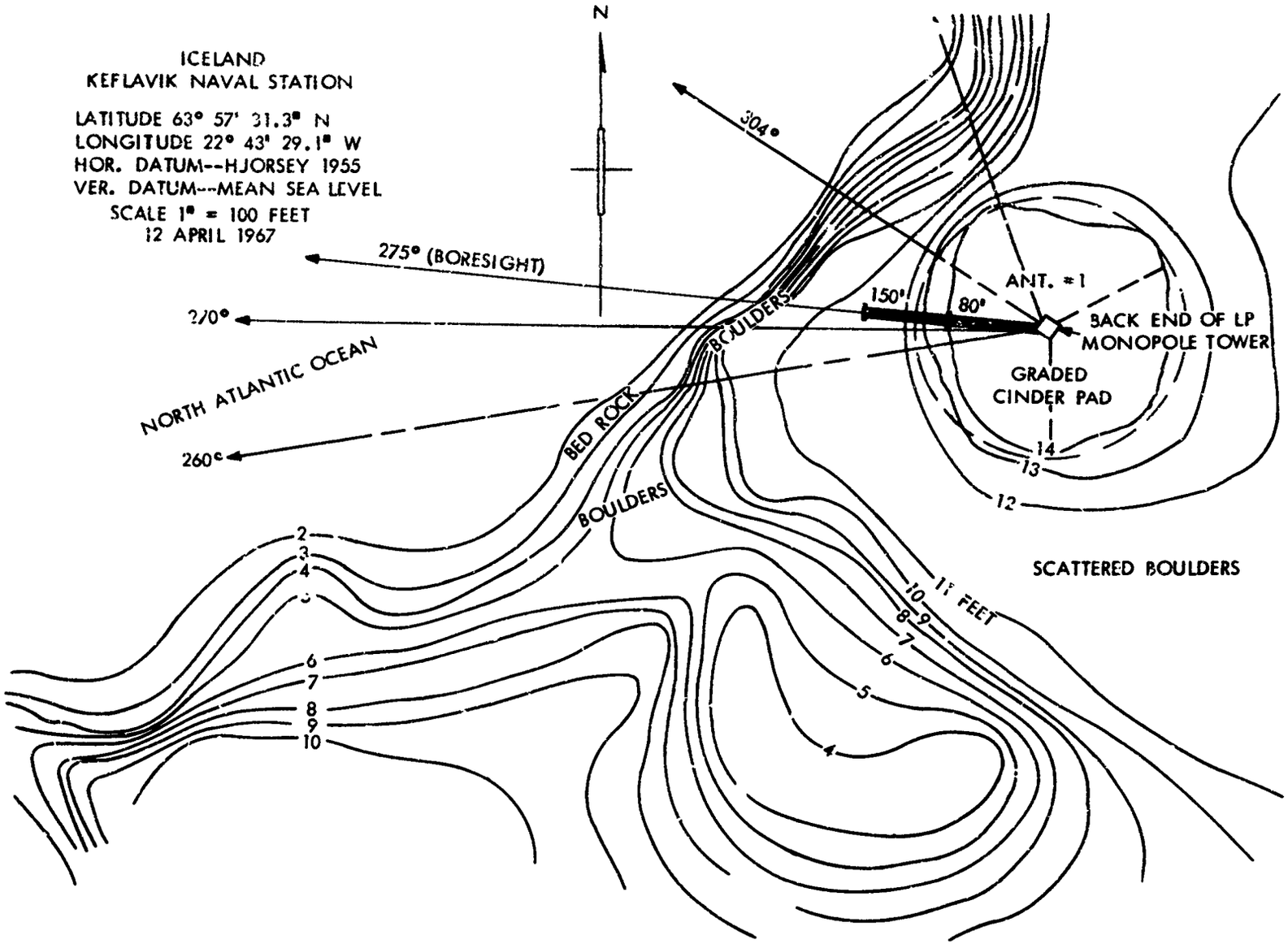
ICELAND
KEFLAVIK NAVAL STATION
LATITUDE 63° 57' 31.3" N
LONGITUDE 22° 43' 29.1" W
HOR. DATUM--HJORSEY 1955
VER. DATUM---MEAN SEA LEVEL
SCALE 1" = 100 FEET
12 APRIL 1967
N
304°
275° (BORESIGHT)
270°
260°
NORTH ATLANTIC OCEAN
BED ROCK
BOULDERS
BOULDERS
ANT. #1
150°
80°
BACK END OF LP
MONOPOLE TOWER
GRADED
CINDER PAD
SCATTERED BOULDERS
FEET
2
3
4
5
6
7
8
9
10
10
8-9
7
6
5
4
14
13
12